Thesis for the Degree of Doctor of Philosophy

Process Synthesis of Seaweed-Based Integrated Biorefineries via Biochemical Conversion Platform

by

Rofice Dickson

Department of Chemical Engineering

The Graduate School

Pukyong National University

August 2020

Process Synthesis of Seaweed-Based Integrated Biorefineries via Biochemical Conversion Platform

생화학적 전환 플랫폼을 이용한 해조류 기반 통합 바이오 리파이너리 공정 합성

Advisor: Prof. Jay Liu

by

Rofice Dickson

A thesis submitted in partial fulfillment of the requirement

for the degree of

Doctor of Philosophy

in Department of Chemical Engineering, Graduate School,

Pukyong National University

August 2020

Process Synthesis of Seaweed-Based Integrated Biorefineries via Biochemical Conversion Platform

A dissertation

by

Rofice Dickson

Approved by:

_____

(Chairman) Gyeongbeom Yi

_____

(Member) Min-Kyu Lee

_____

(Member) Manuel Pinelo

_____

(Member) Seyed Soheil Mansouri

_____

(Member) Jay Liu

August 2020

Table of Contents

ABSTRACT

Macroalgae are a valuable energy source that can be transformed into numerous products most notably fuels and chemicals due to their high content of carbohydrates, proteins, and vitamins. This study evaluates optimal designs for biofuels and biochemicals production from brown algae species *Saccharina japonica* via biochemical platform i.e. sugar platform and volatile fatty acid platform. Furthermore, this study investigates optimal designs for integrated biorefineries to compare their economics and environmental performance with standalone biorefinery designs. A superstructure-based process synthesis approach was used to develop optimization models that can investigate optimal design based on several objective functions such as net present value, yield, and CO_2 emissions. The developed models provide clear guidance on multi-criteria analysis consisting of technical (yields, operating conditions, and bottlenecks), economical (capital costs, energy consumption, minimum product selling price, maximum seaweed price), and environmental aspects (carbon dioxide emissions, water footprint, and cradle to gate life cycle assessment) of biorefinery.

Chapter one elaborates the motivation for this work. First, biorefinery concepts are explained to present an overview of possible raw

materials and conversion routes that can be used to produce biofuels and biochemicals. Social- and technical-challenges of producing biofuels from first- and second-generation biomass are then highlighted. The benefits of macroalgae, particularly of *Saccharina japonica* as a biorefinery feedstock are described. The main challenges of the seaweed-based biorefinery are then defined and role of process system engineering to address the major challenges and supporting the development of biorefinery are explained. Finally, literature review in the context of process synthesis and design of biorefinery is presented, therefore, highlighting literature gaps and the scope of the PhD thesis.

Chapter two explains the methodology used for synthesis and design of biorefinery. A superstructure-based optimization framework is presented by elaborating (1) different steps of framework, (2) objectives of each step, (3) input needed at each step to perform analysis, and (5) outputs from each step. The applied framework can perform optimization under deterministic and stochastic conditions. A strategy to quantify economic risk is discussed and the mathematical formulation of the optimization framework is outlined. Afterwards, techno-economic and environmental assessments methodologies are explained. Finally, input data used for techno-economic assessment including factors to determine total capital

investment and total cost of manufacturing, equipment cost, chemicals costs, and utility costs are detailed.

Chapter three presents the development of a mixed-integer linear programming model to provide decision support for investigating optimal design for integrated biorefinery producing bioethanol and proteins through the sugar platform. The developed superstructure and its mathematical formulation are outlined. Two objective functions were studied: maximization of yield and maximization of net present value. Minimum ethanol selling price and maximum seaweed price were determined to evaluate the economic viability of an optimal design. Sub-optimal process designs were also investigated, and sensitivity analysis was performed to identify major cost drivers for economic improvement. Finally, potential goals and research targets were proposed based on the results of sensitivity analysis for potential improvements to plant economics.

Chapter four demonstrates strategies to utilize all emissions from macroalgal biorefinery through sugar platform. Indeed, the presented superstructure is an extension of the one described in the previous chapter. The central idea of optimization in this chapter is (1) to improve overall process economics and environmental profile by utilizing waste streams

through process integration and (2) to compare the process economics- and environmental-indicators with standalone process design of biorefinery. The optimization model was formulated as a mixed-integer nonlinear programming model and solved for two different objective functions: maximization of net present value and minimization of CO_2 emissions. Process economic indicators were determined. A comprehensive sensitivity analysis model followed by a Monte Carlo simulation model was formulated to find the key drivers of biorefinery. Finally, economic risk assessment was performed to quantify economic risk based on minimum ethanol selling price.

Chapter five evaluates optimal designs, economics, and environmental performance of the mixed acids and mixed alcohols production through the volatile fatty acid platform. Seventeen designs alternatives were used to develop a superstructure. Mixed-integer nonlinear programming model was developed. Process integrations were incorporated into the model to maximize the sustainability of biorefinery. The effect of uncertainties on the process economics was investigated, and future targets were proposed for potential improvements to plant economics.

Chapter six presents a strategy of bio-succinic acid production through optimization of a superstructure that contains multiple biomass sources and technology alternatives. A mixed-integer linear programming model was developed that performs optimization under deterministic and stochastic conditions. Besides, the optimization model also performs economic risk assessment and cradle-to-gate life cycle assessment. The main reason for this chapter is to investigate optimal process design of bio-succinic acid that can be integrated with standalone bio-refineries to improve their economics. Besides, all three generations of biomass are studied to find optimal process design using the best feedstock.

Chapter seven provides a summary of this work and concludes with a comparison of all the process designs based on their economic and environmental merit.

개요

거대 조류는 탄수화물, 단백질 및 비타민의 함량이 높기 때문에 바이오 연료 및 화학 물질과 같은 여러 제품으로 전환될 수 있는 귀중한 자원이다. 이 연구는 생화학적 플랫폼, 즉 당 플랫폼 및 휘발성 지방산 플랫폼을 이용하여 갈조류인 다시마로부터 바이오 연료와 화학 물질을 생산하는 최적의 바이오 리파이너리 설계를 평가한다. 또한, 이 연구는 통합 바이오 리파이너리의 최적의 설계를 조사하여 경제성과 환경성 측면에서 독립형 바이오 리파이너리와 비교한다. 최적화 모델을 개발하는데 상부구조 공정 합성 접근법이 사용되었고, 최적설계를 조사하기 위해 순현재가치, 수율, 이산화탄소 배출 등의 몇가지 목적함수가 사용되었다. 개발된 모델은 바이오 리파이너리의 기술적, 경제적, 환경적 측면의 분석에 대한 분명한 가이드 라인을 제공한다.

1 장은 이 연구의 동기에 대해 자세히 설명한다. 우선 바이오 연료와 화학 물질 생산에 사용될 수 있는 원료와 전환 경로의 개요를 제시하기 위해 일반적인 바이오 리파이너리 개념이 설명된다. 이 때 1 세대 및 2 세대 바이오 연료 생산이 직면한 사회적 및 기술적 과제 또한 강조된다. 그리고 나서 바이오 리파이너리 공급 원료로서의 거대 조류, 특히 다시마의 이점이 기술되며, 주요 과제를 해결하고 바이오 리파이너리의 개발을 지원하는 공정 시스템 공학의 역할이 설명된다. 마지막으로 바이오 리파이너리의 공정 합성 및 설계와 관련한 문헌 검토를 통해 현행 연구의 간극이 확인되고 이 연구의 범위가 설명된다.

2 장은 이 연구에서 바이오 리파이너리의 합성 및 설계에 사용된 방법론을 서술한다. 상부 구조 기반 최적화 프레임 워크는 다음의 순서로 설명된다: (1) 서로 다른 프레임 워크 단계, (2) 각 단계의 목표, (3) 분석을 수행하기 위해 각 단계에서 필요한 입력, (4) 각 단계의

출력. 이 최적화 프레임 워크는 결정적 조건을 물론 확률적인 조건에서도 최적화를 수행할 수 있다. 경제적 위험을 정량화하는 전략이 논의되며 최적화 프레임 워크의 수학식 역시 요약되었다. 기술 경제 및 환경 평가 방법론의 설명엔 총 자본 투자 및 총 제조 비용, 장치 비용, 화학 물질 비용 및 유틸리티 비용을 결정하는 요소를 포함하여 기술 경제 평가에 사용되는 상세한 입력 데이터가 포함되어 있다.

3 장에서는 당 플랫폼을 이용하여 바이오 에탄올 및 단백질을 생산하는 통합 바이오 리파이너리의 최적 설계를 조사하고 의사 결정을 지원하기 혼합 정수 선형 계획법 모델이 제공된다. 이를 위해 개발된 공정의 상부구조와 수학식 또한 요약되었다. 수율 극대화와 순현재가치의 극대화라는 두 가지 목적 함수가 연구되었다. 최적의 디자인의 경제적 생존 가능성을 평가하는 척도로서 최소 에탄올 판매 가격과 최대 해조류 가격이 결정되었다. 이 연구에서는 차선의 공정

설계도 조사되었으며, 경제성 개선을 위해 주요 비용 변동인자를 파악하기 위한 감도 분석 또한 수행되었다. 마지막으로, 공장의 경제성을 개선시키는 잠재적 요인과 민감도 분석 결과를 바탕으로 향후의 개선방향이 제시되었다.

4 장은 3 장에서 제시된 상부 구조를 확장하여 거대 조류 바이오리파이너리에서 당 플랫폼을 통해 모든 배출물을 활용하는 전략을 설명한다. 이 장에서 최적화의 중심 아이디어는 (1) 공정 통합을 통해 모든 폐기물 흐름을 이용하여 전체 공정의 경제적, 환경적 프로파일을 개선하고, (2) 개선된 공정 경제적, 환경적 지표를 독립형 바이오 리파이너리와 비교하는 것이다. 최적화 모델은 혼합 정수 비선형 계획법 모델로 수식화되었으며, 순현재가치의 극대화와 CO2 배출의 최소화라는 두 가지 목적 함수가 사용되었다. 이 장에서는 공정의 경제적 지표가 결정되었고, 바이오 리파이너리 경제성의 주요 변동요인을 찾기 위해 Monte Carlo 모사 후 포괄적인 민감도 분석

모델 또한 개발되었다. 마지막으로, 공정의 경제적 위험을 정량화하기 위해 최소 에탄올 판매 가격을 기준으로 경제적 위험 평가가 수행되었다.

5 장은 휘발성 지방산 플랫폼을 이용해 혼합 유기산 및 혼합 알코올을 생산하는 최적 설계의 경제적 환경적 성능을 평가한다. 이를 위한 공정의 상부 구조를 개발하는데 총 17 개의 공정 설계 대안이 사용되었으며, 이를 토대로 혼합 정수 비선형 계획법 모델이 개발되었다. 이 때 바이오 리파이너리의 지속 가능성을 극대화하기 위해 공정 통합이 모델에 고려되었다. 이를 이용하여 공정 경제성에 대한 불확실성의 영향이 조사되었고, 공장 경제성의 잠재적 개선을 위한 미래의 목표 또한 제시되었다.

6 장에서는 여러 바이오 매스 원료와 기술적 대안이 포함된 상부 구조의 최적화를 이용하여 바이오 숙신산의 생산 전략을 제시한다. 이 장의 주요 목적은 경제성을 향상시키기 위해 독립형 바이오

리파이너리와 통합될 수 있는 바이오 숙신산 공정의 최적 설계를 조사하는 것이다. 이 때, 최적의 바이오 매스 원료를 사용하는 최적의 공정 설계를 찾기 위해 3 세대 바이오 매스 모두가 조사되었다. 이를 위해 결정적, 확률적 조건에서 최적화를 수행하는 혼합 정수 선형 프로그래밍 모델이 개발되었는데, 이 최적화 모델은 경제적 위험 평가 및 cradle-to gate 전과정 평가도 수행한다.

마지막으로 7 장은 이 논문의 주요 결과를 요약하고 경제적, 환경적 장점에 근거한 모든 공정 설계를 비교한 결론을 제시한다.

LIST OF TABLES

LIST OF FIGURES

LIST OF ACRONYMS

Acronym	Definition
IEA	International Energy Agency
CEs	Carbon dioxide emissions
SP	Sugar platform
VFAP	Volatile fatty acid platform
VFAs	Volatile fatty acids
SJ	*Saccharina japonica*
DDS	Dry distiller solids
SA	Succinic acid
NPV	Net present value
MPSP	Minimum product selling price
TCI	Total capital investment
TCOM	Total cost of manufacturing
PSE	Process system engineering
MILP	Mixed-integer linear program
MINLP	Mixed-integer non-linear program
GAMS	General Algebraic modelling systems
TEA	Techno-economic analysis
ISBL	Inside battery limits
TDC	Total direct costs
TIDC	Total indirect costs
FCI	Fixed capital investment
ADFF	Abiotic fossil fuel depletion potential
AP	Acidification potential
ADP	Abiotic depletion potential
EP	Eutrophication potential
GWP	Global warming potential 100 years
ODP	Ozone depletion potential
POCP	Photochemical oxidation potential
TEP	Terrestrial ecotoxicity potential
MAETP	Marine aquatic ecotoxicity potential
FWAETP	Freshwater aquatic ecotoxicity potential
HTP	Human toxicity potential
MSP	Maximum seaweed price
MDDS	Minimum dried distilled solid price
MESP	Minimum ethanol selling price
MSAP	Minimum succinic acid selling price
MMAP	Minimum microalgae price

1 INTRODUCTION

In order to attain the global 1.5 ˚C target, the World needs to achieve virtually zero greenhouse gas emissions by 2050 [1]. On the contrary, the energy and material need of human society are increasing. Besides, continued economic growth still leads to the development of activities that are highly energy-intensive and mainly dependent on petroleum derivatives. The International Energy Agency (IEA) has estimated that oil consumption will continue to increase by at least 50% in coming years; consequently, oil production from post-peak oil fields is expected to decline from 70 million barrels/day in 2007 to 27.1 million barrels/day by 2030 [2–4]. Based on the current energy consumption trends, it is expected that by 2030, carbon dioxide emissions (CEs) will increase by 25–90% from 9.7 Gt/yr in 2014 [5,6]. This is an alarming situation.

Several alternate energy sources including biomass, wind energy, solar energy, geothermal energy etc. can be utilized to produce green energy in order to reduce the detrimental effects of producing energy from burning fossil fuels. The development of biorefineries to produce biofuels and biochemicals from renewable sources such as biomass is emerging as a promising alternative to meet the growing energy and chemicals demand while producing less CEs [7]. This is because the global biomass

production has been estimated around 150 billion t/yr [7]. Only a meager amount (1.25%) of it is utilized for useful purposes (food, energy sectors), the rest is wasted or dumped [7]. Researchers suggest that such huge wastage be curtailed, and maximum useful utilization be made possible out of it. Less expensive chemicals and biofuels can potentially be obtained from biomass which is wasted every year. Therefore, in this study, the development of biorefineries was considered to reduce the high consumption of fossil fuel.

Despite the tremendous potential of biorefineries to meet the World's future energy and chemicals demands, to date, a limited number of commercial-scale biorefineries exist [8]. This is mainly due to the high cost of biofuels and biochemicals compared to conventional fuels and petrochemicals, respectively. The implementation of biorefineries can be possible only when renewable products are economically viable against existing competitors. To solve this challenge, energy-efficient and integrated biorefineries are crucially needed [9].

1.1 Biorefinery concept

A biorefinery is a facility that sustainably processes biomass to produce marketable products and energy [10]. **Figure 1** gives an overview of

possible raw materials that can be processed using different conversion routes in a biorefinery to produce value-added products [10].

The raw materials that can be utilized as a feedstock in a biorefinery include food crops and residues, food waste (bakery waste, waste cooking oil, and so on), lignocellulosic biomass, municipal solid waste, and aquatic biomass (microalgae and macroalgae) [10]. In general, these feedstocks can be classified into four sectors: agriculture, forestry, industries, and aquaculture [11].

Likewise, based on the conversion technologies the biorefinery concept can be classified into two major platforms (1) biochemical and (2) thermochemical [10].

1.1.1 Biochemical platform

This conversion platform consists of three conversion routes: sugar (fermentation), volatile fatty acid (partial anaerobic digestion), and methane (complete anaerobic digestion).

The sugar platform (SP) uses hexose and pentose sugars extracted or converted from the carbohydrate part of biomass to mainly produce bioethanol [12]. Depending on the biomass different pretreatment technologies can be used to break down the structure of feedstock [13]. Biomasses that are rich in lignin (e.g., second-generation biomass) usually

require harsh pretreatment techniques such as acid thermal hydrolysis, alkaline thermal hydrolysis, ammonia fiber explosion, hydrogen peroxide, deacetylation, and steam explosion [14]. On the contrary, biomasses that are lean in lignin (e.g., brown algae, which is third-generation biomass) require moderate pretreatments such as hot water wash or simple milling [15]. Enzymatic pretreatment is also a very common technique that can be used to convert carbohydrates of biomass into mono sugars using enzymes such as cellulase [12]. In general, a combination of thermochemical- and biochemical-pretreatments are used to increase the overall conversion of carbohydrates to simple sugars [12]. The former mainly converts hemicellulose carbohydrates (xylan, galactan, arabinan, mannan, etc.) in the feedstock to sugars while the later converts cellulose carbohydrates (glucan, laminarian etc.) in the feedstock to sugars. Once the feed is pretreated and simple sugars are produced, microorganisms are then used to convert sugars into alcohols. The choice of microorganisms and fermenter are extremely important parameters to achieve high titer, yield, and productivity [16].

In the volatile fatty acid platform (VFAP), volatile fatty acids (VFAs) consisting of acetic acid, propionic acid, and butyric acid are produced by the partial anaerobic digestion of biomass using a mixed culture bacterial

ecosystem [17]. Anaerobic digestion consists of four stages: hydrolysis, acidogenesis, acetogenesis, and methanogenesis. In the first stage, the complex structure of biomass including carbohydrates, proteins, and lipids are broken down by bacteria into simple sugars, amino acids, and fatty acids, respectively. Acidogenic bacteria then convert the simple sugars into volatile fatty acids, ammonia, carbon dioxide, and hydrogen sulfide. These resulting volatile fatty acids are then digested by acetogens to produce acetic acids along with additional ammonia, hydrogen, carbon dioxide, and other acids including propionic acid and butyric acid. Finally, methanogens convert products from the preceding stages into methane, carbon dioxide, and water. Methanogenesis must be prevented to produce VFAs as the final product of fermentation. This is accomplished using inhibitors such as iodoform or bromoform [18]. This conversion route can produce two types of products i.e. mixed acids or mixed alcohols [19]. The choice of the digester (batch vs. continuous), temperature (mesophilic vs, thermophilic), fermentation time, and solid loading (high vs. low) are important parameters to achieve high product yield [20–23].

Unlike the VFAP, the methane platform considers the complete anaerobic digestion of biomass to produce biogas, consisting of carbon dioxide, water, and methane [24]. The composition of biogas depends upon

the type of digester, operating temperature, and digestion time [24]. Biogas has many industrial and domestic applications including electricity generation via fuel cell [25], steam and power generation via turbogenerator [26], and as an alternative to natural gas after gas purification [10].

1.1.2 Thermochemical platform

This platform mainly comprises of four types of processes: gasification, pyrolysis, hydrothermal liquefaction, and direct combustion.

The process of gasification is a thermal decomposition of biomass at relatively high temperatures (600˚C-1000˚C) and residence times of 1-30 s. Here, the biomass is converted into the gaseous phase of the product called syngas, consisting mainly of hydrogen, carbon monoxide, carbon dioxide, and methane. The heat supply method and the gasifying agent are the main drivers affecting the syngas yield [27].

The main product from pyrolysis is bio-oil, carbon-rich solid (charcoal), and non-condensable gasses similar to syngas. Pyrolysis is generally achieved at temperature ranges of 300˚C to 600˚C (depending on the feedstock) and atmospheric pressure in low or no oxygen environment to avoid combustion [28]. The main objective of this conversion route is

maximizing the liquid phase product by optimizing parameters such as reactor type and temperature, residence time, and mineral contents.

Unlike other thermochemical pathways (gasification and pyrolysis) which need intense drying, hydrothermal liquefaction utilizes water as a raw material for the conversion of biomass to liquid fuel under moderate temperature and high pressure. In general, hydrothermal liquefaction operates between a range of 250-350˚C of temperature and operating pressures from 10-20 MPa based on the feedstock [29]. The efficiency of this conversion pathway significantly depends on operating temperature, residence time, and feed to solvent ratio.

In the direct combustion pathway, the feedstock is oxidized to produce heat and power.

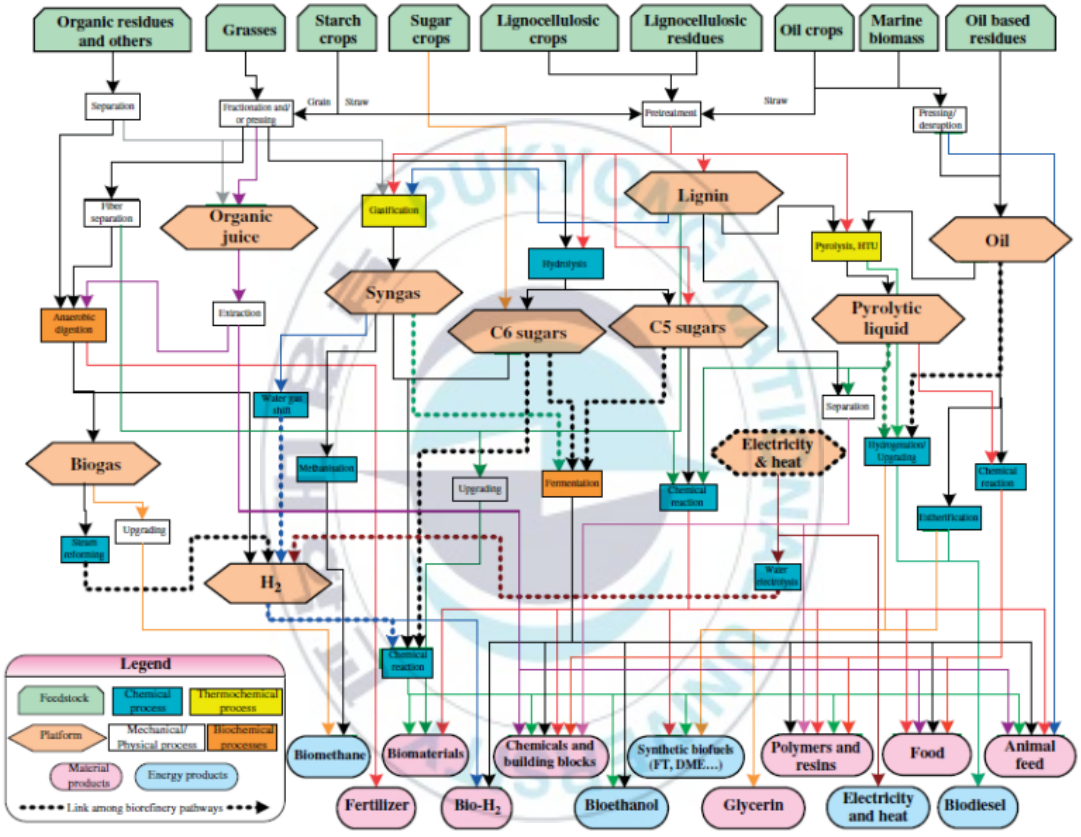

Figure 1. Overview of possible raw material, technological routes in potential biorefinery. Adapted from IEA Bioenergy [11].

1.2 Macroalgae as a biorefinery feedstock

As shown in **Figure 1**, biorefinery can process all kind of biomass including food crops, lignocellulosic, and/or aquatic biomass to produce biofuels, bioenergy, and biochemicals. However, all biomasses are not well-suited for large-scale biofuel production due to limited biomass availability or ethical issues. For example, biofuel production from food crops, which is 1st generation biomass, presents several social and environmental challenges such as the land, irrigation water, fertilizers, and most importantly market competition between first-generation biofuels and food [30]. Likewise, biofuel production from lignocellulosic biomass, which is 2nd generation biomass, offers a promising alternative of food vs fuel debate. However, 2nd generation feedstock poses technological challenges due to high lignin content and structural complexity, which require harsh pretreatment to break the structure before enzymatic hydrolysis and sugar liberation [31,32].

Aquatic biomass such as macroalgae and microalgae do not carry most of the aforementioned challenges and are thus promising candidates for edible crops and non-edible biomass [33]. Macroalgae, or seaweed, offer multiple advantages over terrestrial biomass including an extremely rapid growth rate and a CO_2 sequestration efficiency of 6–8%, which is higher

than that of terrestrial biomass, at 1.8–2.2% [34]. The advantage of seaweed for biofuel is that (1) it does not compete directly or indirectly for land that could otherwise be used for food, (2) it does not require irrigation water and fertilizers for cultivation, and (3) it improve the marine environment by capturing carbon dioxide, and dissolved nutrients that may otherwise cause eutrophication [35].

Macroalgae are phenotypically classified into brown, red, and green algae. To data 9000 species of macroalgae are known: 1200 species of green algae, 6000 species of red algae, and 2000 species of brown algae [35]. Brown algae represent the largest seaweed source, with a yearly production of 15.8 million wet tons in 2010, and can be used as an important precursor due to its high quantity of carbohydrates, proteins, and vitamins [36].

Unlike microalgae, macroalgae have low lipid content and are high in carbohydrates. Therefore, biofuel production from seaweed relies on the conversion of carbohydrates instead of lipids. The primary carbohydrates produced by brown algae include laminarin, cellulose, fucoidan, alginic acid, and mannitol [35]. The chemical composition of seaweed varies highly depending upon the species, growth conditions, and harvesting times [37]. Among brown alga species, *Saccharina japonica* (SJ) remained

the primary research focus [38]. This focus is probably due to the high carbohydrate content, lack of lignin, high levels bioactive compounds, simple pretreatment, easy carbohydrates processing, low levels of sugar degradation, and extensively available feedstock [39]. Global production of SJ increased from 5.1 Mt in 2010 to 8.2 Mt in 2016 [40]. This indicates SJ harvesting infrastructure is well developed and its market is growing rapidly.

Despite several advantages of brown algae and growing global market, most of the biorefinery concepts presented in **Section 1.1**, regarding this biomass, are still under development or at the demonstration (pilot) scale. Therefore, research and development efforts are required that should focus on giving clearer guidance based on multi-criteria analysis (technical, economic, and environmental). In a broader term, the objective of this PhD work is to investigate optimal process design for biofuel and biochemical production from brown algae—*Saccharina japonica*—and to evaluate its economic potential, opportunities, and challenges.

1.3 General seaweed-to-fuel refinery

In a typical seaweed biorefinery, as shown in **Figure 2**, seaweed can be processed using appropriate processing route (biochemical, thermochemical, chemical, or combustion) to produce a range of products

including biofuels (liquid, gaseous, and solids) and byproducts (dry distiller solids (DDS), succinic acid (SA), and microalgae). It can be seen that due to a large number of processing routes and products, the design of seaweed biorefinery is a challenging task.

The main challenges include:

1) to find optimal processing route and operating conditions of a biorefinery that is energy efficient, has a less environmental impact, and at the same time has reasonable capital investment cost, which is an important parameter from the point of the investors
2) to find optimal product and its production rate from the range of products keeping in view the fluctuating price of products with the price of petroleum
3) to find an optimal strategy for utilizing biorefinery waste streams (carbon dioxide, wastewater, and unreacted solids) into value-added chemicals to reduce the water- and carbon-footprint
4) to find a systematic way to analyze the impact of uncertainties on feedstock, biorefinery structure, product selection, and process economic indicators including net present value (NPV), minimum product selling price (MPSP), total capital investment (TCI), and total cost of manufacturing (TCOM).

These challenges can be addressed using the process design framework that allows to systematically analyze all biorefinery concept to find best route to reach the highest economic performance.

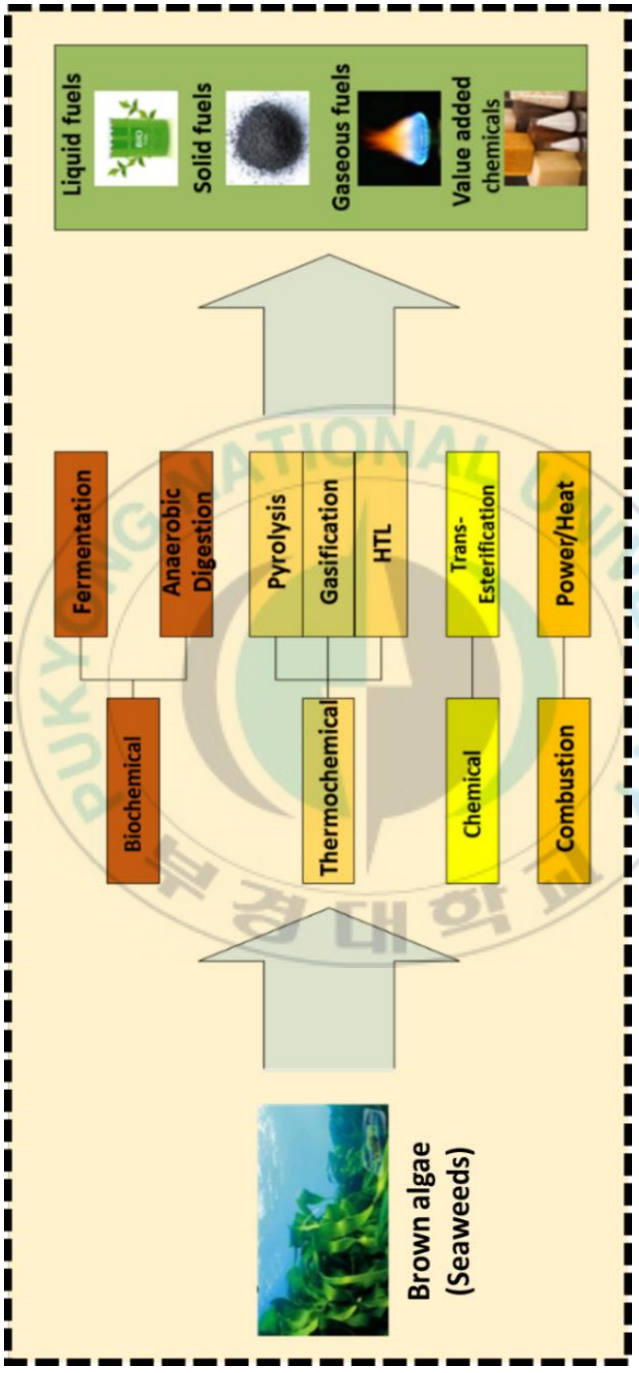

Figure 2. Roadmap of biofuel production from biomass.

1.4 Process design framework

Chemical process design is a complex and open problem that involves many activities at different levels. In other words, it is a multi-scale and multi-level decision-making problem that involves several activities such as process creation, development of basic concepts, experimental studies, the detailed design, etc. [41]. In general, the chemical process development life cycle consists of five distinct stages: concept stage, feasibility stage, development stage, manufacturing stage, and product introduction stage [42]. The outputs of each stage are the inputs to the following stage. At each stage, a decision is made to either (1) advance the design project to the next stage, (2) retain the design project at the current stage until pending critical issues are resolved, or (3) cancel the design project when a need is no longer recognized or when roadblocks have been encountered that render the project infeasible [43].

As the macroalgae based biorefinery is at its infancy, the decision-making process at the early stage level (*concept stage*) needs to be improved (1) to understand opportunities, challenges and limitations of seaweed biorefinery and (2) to support large and complex biorefinery design problems which consist of multi-disciplinary, limited, and uncertain data. This need can be fulfilled by the support from process system

engineering (PSE) which is one of the main research areas in chemical process development.

1.5 Role of PSE in the context of biorefinery concepts: introduction and classification

The main objective of PSE is to focus on how to design, integrate, and manage complex systems [44]. To achieve this objective, computer-aided tools—model-based tools and system engineering methods—are used that are considered the major backbone of PSE [45]. The most notable advantages of PSE include (1) study the behavior of the system without building it, (2) accelerate the product or process design-development life cycle, (3) save time, minimize human error, and get better designs, (4) help to find an un-expected phenomenon, the behavior of the system, (5) can be used for "what-if" scenarios, and (6) can be used to reduce the cost of changes required during the operation changes, and so on [45,46].

There are two primary paradigms in PSE: analysis and synthesis [47]. The *analysis problem* assumes that the process flowsheet, the equipment and operating conditions are known. The mathematical model pertaining to a specific task is then used to determine the process indicators or performance through simulation studies. Whereas in the *synthesis problem* process flowsheet and operating conditions are unknown, optimization

models and algorithms are then used to systematically determine the optimal flowsheet and operating conditions by a search in the space of the decision variables.

In process synthesis, there are two main methodologies—heuristic approach and mathematical programming approach—that a design engineer can consider to find the optimal process flowsheet and its operating condition [48]. The heuristic approach is based on the experience of an engineer, where he or she uses heuristic rules to find changes in flowsheet that may lead to an improved solution. The mathematical programming is an optimization-based approach that finds optimal flowsheet and its operating condition based on defined objective function such as maximization of profit. The mathematical programming strategy is divided into three steps (1) superstructure development (2) mathematical formulation, and (3) optimization-problem solution [49]. The *superstructure development* involves gathering all feedstocks, processing units, and products that can be potentially selected in the final flowsheet to perform a specific task. In addition, interconnections of different feedstocks, processing units, and products are defined in this stage. In the second step, the mathematical representation of superstructure is formulated that include equations pertaining to processing units and their

connectivity, logical constraints of processing and operating conditioning, and objective function. The *mathematical formulation* usually requires discrete variables to represent the choice of feedstock, processing units, and/or products, with which the optimization model become a mixed-integer linear programming (MILP) or mixed-integer non-linear programming (MINLP). The former (later) is the case when decision variables are liner (non-linear). Finally, the last step involves the extraction of an optimal solution by solving the formulated optimization problem.

Each of heuristic and mathematical programming methods has their own merits and demerits when compared to each other. Therefore, integrating these two methods has recently been developed and has resulted in the so-called hybrid method [50]. The main objective of this methodology is developing a systematic way to get optimal solutions by combining the merits of both the heuristic and mathematical programming approaches.

1.6 PSE contributions on process synthesis and design of a biorefinery

This section briefly overviews the advances in the area of PSE in the context of the biorefinery concepts.

Karuppiah et al. developed an MINLP model to optimize the topology and energy for the design of corn-based ethanol plants [51]. The superstructure was developed and solved in two stages. In the first stage, the optimal topology of biorefinery was determined by minimizing the total energy of the plant, while in the second stage heat integration was performed, where 40% reduction in steam consumption was achieved. Based on these results, Ahmetović et al. developed an MINLP model to reduce water consumption for the corn-based ethanol plants [52]. Voll and Marquardt et al. introduced a reaction flux network analysis as a novel and efficient tool for the systematic identification and screening of reaction pathways in the context of biorefinery using biochemical platform [53]. Zondervan et al. used a biochemical platform to develop superstructure [54]. The resulting formulation of the superstructure was an MINLP model that determines the optimal structure of biorefinery, which can produce multi-product including ethanol, butanol, succinic acid, gasoline and gasohol. Baliban et. al investigated the thermochemical conversion of biomass to liquid fuels using global optimization (branch-and-bound) algorithm to mathematically guarantee the solution obtained from an MINLP model [55]. The proposed superstructure and its mathematical model can optimize the topology and operating conditions of biorefinery,

and can simultaneously perform heat, power, and water integration. Kim et al. developed an optimization framework by combining processing alternatives from both biochemical and thermochemical platform to identify the best strategy for converting biomass to fuel [56]. Chen et al. investigated the optimal design and operation of flexible energy polygeneration systems to produce power, liquid fuels, and chemicals from coal and biomass [57]. The problem was solved to global optimality by a tailored duality- based decomposition method. Rizwan et al. proposed a two-stage stochastic optimization-based framework to determine the optimal topology and product portfolio for a microalgae-based biorefinery under techno-economic uncertainty [58]. Gong et al. developed models and algorithms for simultaneous technological integration, economic viability and environmental impact (global warming potential) of algal biorefinery process [59]. The tailored branch-and-refine algorithm based on successive piecewise linear approximation was used to globally optimize the resulting nonconvex solution. Posada et al. applied a quick screening method called early-stage sustainability assessment to identify the most promising bioethanol derivatives resulting from catalytic conversion [60]. The early-stage sustainability assessment consists of 5 main design criteria (economic, environmental impact from raw material

and process, safety and hazard) which are the important factors for designing a sustainable biorefinery. Gebreslassie et al. [61], and Zhang et al. [62] proposed multiobjective MINLP models for superstructure optimization of a hydrocarbon biorefinery via gasification and pyrolysis pathways.

The aforementioned developments in PSE are great contributions in their own right. But limited work has been done to systematically find the optimal process design for seaweed-based biorefinery. Besides, till to date, only a few biorefineries exist, more specifically seaweed biorefineries are not available at commercial scale. According to Kokossis et al., unless system engineers take breakthrough initiatives to develop advance tools and methodologies, that can simultaneously perform multi-level and multi-stage analysis, the concept of biorefinery will merely remain in scientific papers [63].

1.7 Scope of this study

Based on the presented arguments, the main objective of this PhD study is process synthesis of macroalgal biorefinery using superstructure-based optimization, where both the structure as well as the operating conditions of the biorefinery are determined by optimization. Based on the superstructures, optimization models were developed that can

systematically analyze biochemical pathways—sugar platform and volatile fatty acid platform—to find optimal processing pathways for biofuel and biochemical production from brown algae, *Saccharina japonica*. To determine the optimal biorefinery configuration we have applied the methodology that systematically (1) scan all alternatives, (2) perform ranking of the promising biorefinery configurations, (3) consider uncertainties to perform assessments under techno-economic and environmental uncertainties, (4) perform a risk assessment to present robust decision. The developed models can provide multicriteria analysis decision making support in a technical, economic, and environmental perspective.

2 METHODOLOGY

2.1 A systematic framework for sustainable biorefinery design

The overall framework used in this work is divided into five steps as shown in **Figure 3**. The framework uses superstructure-based optimization strategy to find optimal configurations of biorefinery under deterministic and stochastic conditions.

2.1.1 Problem statement definition

As shown in **Figure 3**, the framework starts with the problem statement definition, where the scope of the study is defined by selecting appropriate objective function(s) related to economic metrics (NPV, MPSP etc.), process performance (yield, resource utilization etc.), and life cycle assessment (global warming potential, human toxicity potential etc.).

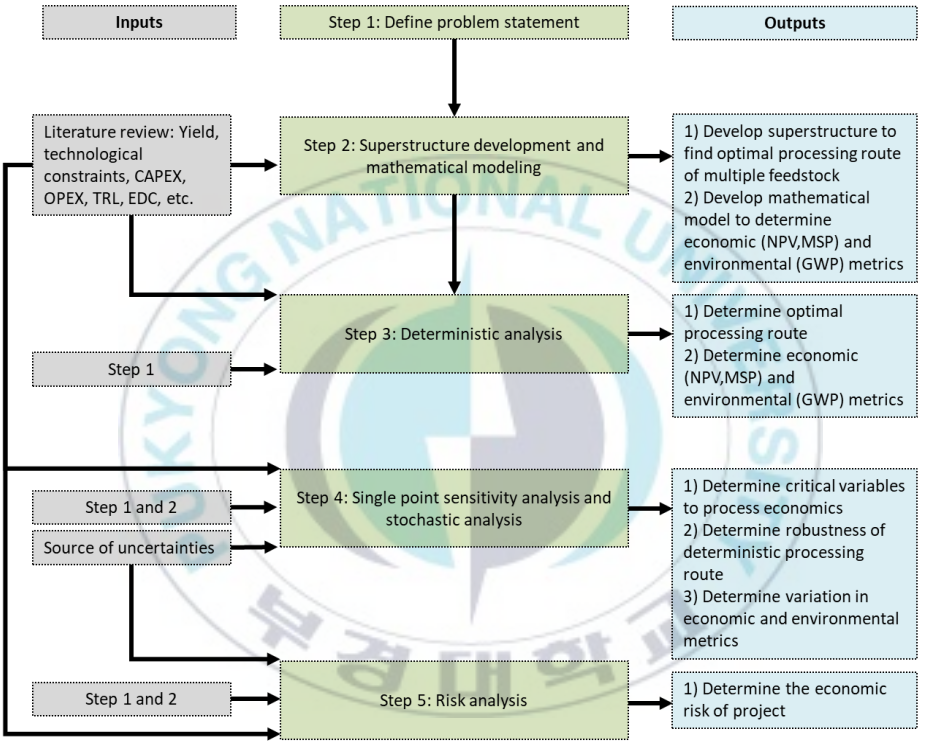

CAPEX = Capital expenditure; OPEX = Operating expenditure; TRL = technology readiness level; EDC = Environmental damage factor; NPV = Net present value; MSP = Minimum product selling price; GWP =Global warming potential

Figure 3. A procedure to determine sustainable biorefinery design.

2.1.2 Superstructure development and mathematical formulation

In this step, the superstructure is developed based on the literature review. During the literature review, data consisting of yields, capital costs, utility costs, chemical costs, feedstock availability, technological limitations, and environment damage factors etc. are also collected, which is later used by optimization model to find an optimal flowsheet from the superstructure. As shown in **Figure 4**, a superstructure is a representation of all processing alternatives including feedstocks, conversion technologies, and product portfolio as well as their interconnections that can be selected in the final flowsheet [48].

In the superstructure, each alternative is represented by two indices of which the first refers to the alternative, and the second refers to the processing stage [58]. For example, "1, 1" refers to alternative 1 in processing stage 1. White blocks are used in the superstructure to represent certain processing stages that do not involve topology (structural) decisions.

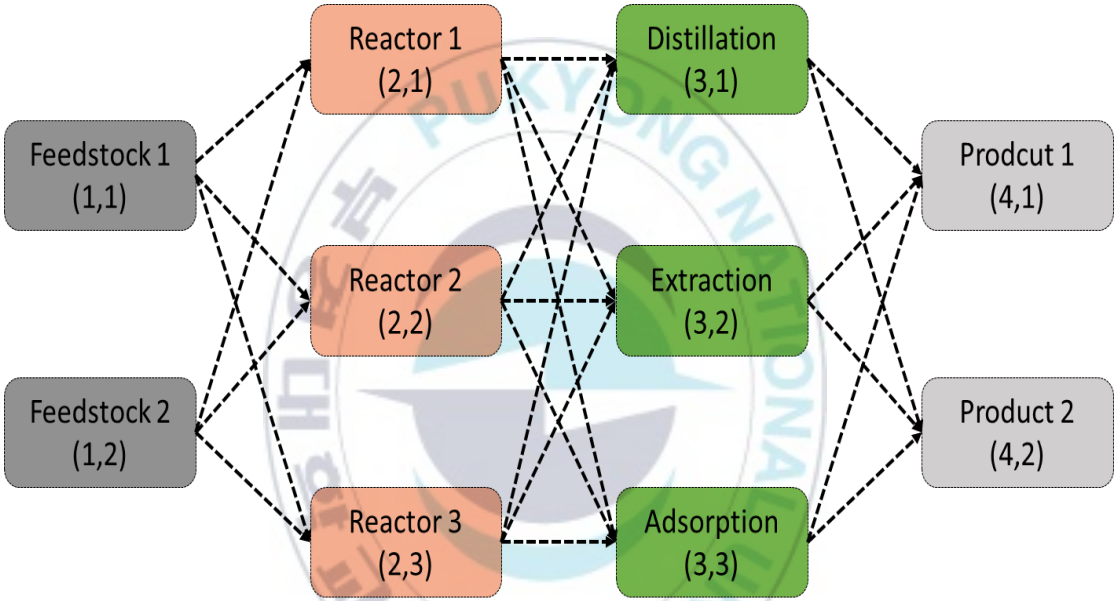

Figure 4. A generic superstructure representation.

Once the superstructure is developed then the mathematical model of the superstructure is formulated using mixed-integer linear or non-linear programming approach that yields a synthesis problem of the form [64]

$$\max z = f(x, y), \tag{1}$$

$$s.t.\ g(x, y) \geq 0, \tag{2}$$

$$h(x, y) = 0, \tag{3}$$

$$\leq x \leq x^{UP}, \tag{4}$$

$$x \in X, y \in (0, 1)^n, \tag{5}$$

where *z* is the objective function, *x* is the vector of continuous variables defined by their upper and lower bounds in a continuous feasible region *X*, *y* is the vector of discrete variables. The continuous variables *x* are related with flowrates, temperature, pressure, composition, equipment sizes, and environment (e.g. global warming potential), while discrete variables *y* are related to the existence of feedstocks, conversion technologies, and products that are postulated for the optimal flowsheet in the superstructure [65]. The inequality and equality constraints can be obtained from the superstructure to represent mass balances, energy balances, design equations, design specifications, total capital cost constraints, total manufacturing cost constraints, environmental constraints, physical

constraints, or logical conditions that should be satisfied in the flowsheet to exclude infeasible networks from the search space [64].

The single-point sensitivity analysis to investigate the main drivers of biorefinery design can be defined by [66]:

$$\theta_{min} = (1 - \%variation) \times \theta_{mean}, \quad (6)$$

$$\theta_{max} = (1 + \%variation) \times \theta_{mean}, \quad (7)$$

where θ is the vector of uncertain parameters, θ_{min} and θ_{max} are the maximum and minimum values of parameters due to uncertainty in data. These variations can be either the result of market forces (changing raw material costs, utility costs, or products demand and price), natural occurrences (variation in feedstock composition, culture crash in fermentation, or equipment failures) or physical properties (thermodynamic data or kinetic parameters) which are measured with finite accuracy equipment. Besides, models and tools that are used to support decision making of product-process development may not be accurate and hence additional uncertainty has to be considered [67]. The range (i.e. maximum and minimum values) of variations in parameters can be obtained from a literature review, process experts, or market analysis. However, some of the data used in process synthesis problems are usually limited or not available in the literature. In such cases, uncertainty in

parameters can be classified into low, medium, and high scenarios, which correspond to 5%, 25%, and 50% variations around the mean value, respectively [58,66,68]. In other words, data with high accuracy can be classified as a parameter of low uncertainty, inconsistent data as a parameter of medium uncertainty, and highly inconsistent data as a parameter of high uncertainty [58,66,68].

Finally, a general representation of the design problem under uncertainty is of the following form [69]:

$$\max z = E_\theta[f(x, y, \theta)], \tag{8}$$

$$s.t.\, g(x, y, \theta) \geq 0, \tag{9}$$

$$h(x, y, \theta) = 0, \tag{10}$$

$$x^{LO} \leq x \leq x^{UP}, \tag{11}$$

$$x \in X, \tag{12}$$

$$y \in \{0, 1\}^n, \tag{13}$$

$$\theta \in \{\theta^{LO}, \theta^{UP}\}^m, \tag{14}$$

where θ is the vector of uncertain parameters which is assumed to follow a uniform distribution, $E_\theta(f)$ is the expected value of the objective function over the θ space, and $g(x, y, \theta)$ and $h(x, y, \theta) = 0$ are the vectors of model equality and inequality constraints. The calculation of the expected value of the objective function requires the evaluation of

multidisciplinary integral, which can be approximated using the Sample Average Approximation technique [70] as follows:

$$E_{\theta}[f(x,y,\theta)] \sim \sum_{s=1}^{NS} P_s \times f(x,y,s), \quad (15)$$

$$s.t.\ g_s(x,y,s) \geq 0, \quad (16)$$

$$h_s(x,y,s) = 0, \quad (17)$$

where NS is the number of samples in the sample matrix S and P_s the probability of realization of sample s. It is also important to mention that in stochastic optimization, the number of scenarios used to approximate expected value of the decision variables (process indicators) and frequency of the occurrence of resulting optimal topology is a critical factor. Generally, the average approximation of decision variables become more accurate as the number of scenarios increased. However, increasing the number of scenarios also increase the complexity of the optimization problem due to the increased size of the synthesis problem. For a reasonable compromise, 200-500 samples are considered appropriate for synthesis problems [71].

The general optimization formulation presented by Eqs. 1-17 can simultaneously perform optimization of biorefinery topology and its operating conditions. The mathematical formulation can be written and solved using appropriate software such as General Algebraic modelling

systems (GAMS) by selecting suitable solver. The most well-known and efficient solvers for solving MILP model include CPLEX, while for MINLP model include DICOPT if a local solution is desired, alternatively, BARON or LINDOGLOBAL can be used for a global optimal solution.

2.1.3 Deterministic analysis

Step 3 deals with the deterministic analysis, where optimal processing pathway(s) of the biorefinery along with process indicators (economics and environmental) are determined by (Eqs. 1-5) maximization of the objective function *z* with nominal parameter values while disregarding the uncertainties in them. The ranking of optimal solutions can also be performed by systematically screening alternative solutions using an integer cut constraint algorithm, which can be expressed as [72]:

$$\sum_{p\in A^n}\left(y_{k,j}\right)_p - \sum_{p\in B^n}\left(y_{k,j}\right)_p \leq |B^n| - 1 \quad n = 1, \ldots\ldots, N, \qquad (18)$$

where *P* are the subsets of the integer variables $y_{k,j}$, $A^n = \{p|(y_{k,j})_p = 1\}$, $B^n = \{p|(y_{k,j})_p = 0\}$, n=1,..,N. The integer cut constraint algorithm avoids the duplication of already found solutions and allows to systematically evaluate various pathways in the superstructure.

2.1.4 Stochastic analysis

In this stage, stochastic analysis (robust optimization) is performed where single-point sensitivity analysis is performed to first identify the

critical parameters to the biorefinery design using Eqs. 6-7. The critical parameters that are identified in the single-point sensitive analysis are then used in stochastic optimization (Eqs. 15-17) to investigate the impact of uncertainties on biorefinery topology and process indicators. Unlike single-point sensitivity analysis, where only one parameter is changed at a time while other parameter remained fixed around their mean values, in stochastic optimization, all uncertain parameters are changed simultaneously in their predefined range using suitable sampling (e.g. Latin hypercube) method [73]. Once sampling method is selected, then the deterministic model (Eqs. 1-5) is solved repeatedly for each scenario generated by the selected sampling method to calculate the average expected value of decision variables including the frequency of the occurrence of resulting optimal topology. Here, a topology that maximally selected and remained economically viable is considered robust design. Thus, results from this step provide technical insights about the optimal configurations of the biorefinery from the perspective of both process indicators and topology robustness under uncertainty.

2.1.5 Risk assessment

Finally, in step 5, risk assessment is performed where economic risk is quantified based on the minimum product selling price. To perform this

analysis, the optimal solutions obtained from the previous step are analyzed as a risk. Here, we analyzed the probability of obtaining a minimum product selling price that is higher than the targeted market price. In other words, the risk assessment will reflect the probability of the biorefinery being economically non-viable, which corresponds to determining the minimum product price that is higher than the market price.

2.2 Techno-economic assessment methodology

The primary goal of the techno-economic assessment (TEA) model is to evaluate the profitability of biorefinery designs by estimating economic indicators such as NPV, MPSP, and maximum feedstock purchasing price. A 20-year discounted cash flow rate of return analysis model was developed to estimate MPSP and maximum feedstock purchasing price that makes the NPV of the project equal to zero. The assumptions in the TEA model include a discount rate of 10%, a straight-line depreciation method over 7 years, a tax rate of 30%, a 2-year construction time, a plant startup during the 3rd year, financing equity of 100%, and 8000 operating hours per year.

The TCI include total direct and indirect costs, land costs, and working capital. Note that total direct and indirect costs are subdivided into many

costs which are reported in **Table 1**, and the sum of these costs correspond to fixed capital investment. A factor methodology is used in which suitable multipliers reported in **Table 1** are applied to the installed costs of equipment to estimate total capital investment [12]. Whereas, in this study, the installed costs are scaled (using Eq. 19) to new capacity from vendor quoted equipment costs and capacity using installing factor and scaling factors that are equipment specific. Later, the installed costs of equipment are updated to the year of analysis i.e. 2019-dollar value using the Chemical Engineering Plant Cost Index in Eq. 20. **Table 2** provides a summary of the main equipment costs along with cost year, scaling exponent, and installation factors.

$$C_n = (I_n)\left(C_{n,o}\right)\left(\frac{Q_n}{Q_{n,o}}\right)^{a_n}, \tag{19}$$

where $C_{n,o}$ is the cost of the baseline equipment item n with the baseline capacity $Q_{n,o}$. C_n is the cost of the equipment item n with the new/real capacity Q_n, a_n is the scaling exponent for the kind of unit n, and I_n is the installation factor of the equipment item n.

$$UC_n = C_n\left(\frac{CEPCI_{2019}}{CEPCI_{ref}}\right), \tag{20}$$

where UC_n is the updated cost of the equipment in the year of interest and $CEPCI_{2019}$ and $CEPCI_{ref}$ are the index values in the year 2019 and the baseline year, respectively.

Total manufacturing costs consist of direct (variable), fixed, and general manufacturing costs. Direct manufacturing costs include raw material costs and utility costs. Fixed manufacturing costs include operating labor costs, maintenance and repairs, depreciation, local taxes, insurance, and plant overhead. General costs are related to administration and research and development costs. A factor methodology proposed by Turton et al. [74] is used (Eq. 21) to calculate total manufacturing cost (T_{COM}).

$$T_{COM} = f_1 C_{OL} + f_2 F_{CI} + f_3 (C_{UT} + C_{RM} + C_{WT}), \quad (21)$$

where *f1, f2, and f3* are multipliers, C_{OL} is the cost of operating labor, F_{CI} is fixed capital investment, C_{UT} is the cost of utility, C_{RM} is the cost of raw material, and C_{WT} is the cost of wastewater treatment. Cost of utility and raw materials such as biomass, process water, enzymes, and chemicals are estimated by mass and energy balance constraints. Cost of labor is calculated as 1.6% of total installed costs. The unit price of chemicals, utility and wastewater treatment are summarized in **Table 3** and **Table 4**.

The non-discounted cash flow, NCF_n for the year *n* is given as:

$$NCF_n = -r_n T_{CI} + a_n W_C + (Rev - T_{COM})(1 - tax) + D \cdot tax, \quad (22)$$

where r_n is the ratio of total capital investment consumed during year *n*, *D* is depreciation, W_C is working capital, and Rev is the process revenues obtained from the sale of products. a_n is a parameter equal to -1 during the year 3, 1 during the last year of the project, and zero for all other years.

The process revenues (Rev) obtained from the sale of products are given by:

$$Rev = \sum_{p=1}^{n_p} f_p P_p, \tag{23}$$

where n_p is the number of products, f_p is the mass flow rate of product p, and P_p is the wholesale price of product p.

The NPV is defined as:

$$NPV = \sum_{n=0}^{20} \frac{NCF_n}{(1+r)^n}. \tag{24}$$

Table 1. Methodology to determine total capital investment and total cost of manufacturing.

Parameters	**Value**	**Ref**
x_1, Total installed cost	100%	[12]
x_2, Warehouse	4% of Inside battery limits (ISBL)	[12]
x_3, Site development	9% of ISBL	[12]
x_4, Additional piping	5% of ISBL	[12]
Total direct costs (TDC)	$\sum_{i=1}^{4} x_i$	[12]
y_1, Prorateable costs	10% of TDC	[12]
y_2, Field expenses	10% of TDC	[12]
y_3, Home office & construction fee	20% of TDC	[12]
y_4, Project contingency	10% of TDC	[12]
y_5, Other costs (start-up, permits, etc.)	10% of TDC	[12]
Total indirect costs (TIDC)	$\sum_{i=1}^{5} y_i$	[12]
Fixed capital investment (FCI)	TDC + TIDC	[12]
Land	6% of installed costs	[12]
Working capital	5% of FCI	[12]
Total capital investment (TCI)	FCI + Land + Working capital	[12]
f1	2.2 times of the cost of labor	[74]
f2	1.1 times of FCI	[74]
f3	1.05 times of the cost of utility and raw material	[74]

Ref = Reference

Table 2. Equipment cost quoted by vendors and literature.

Equipment	USD	n	IF	Year	Ref
Pump	22,500	0.80	2.30	2009	[12]
Flash	511,000	0.70	2.00	2009	[12]
Mechanical separator	3,294,700	0.80	1.70	2010	[12]
Condenser	34,000	0.70	2.20	2009	[12]
Heater	92,000	0.70	2.20	2010	[12]
Cooler	85,000	0.70	2.20	2010	[12]
Acid thermal hydrolysis reactor	19,812,400	0.60	1.50	2009	[12]
Acid thermal hydrolysis reactor after deacetylation	24,600,000	0.60	1.50	2013	[75]
Alkaline hydrolysis reactor	614,000	0.70	2.20	2018	[74]
Conditioning vessel	236,000	0.70	2.00	2009	[12]
Hot water wash reactor	3,840,000	0.70	2.00	2009	[12]
Saccharification reactor	3,840,000	0.70	2.00	2009	[12]
Belt filter press	3,294,700	0.80	1.70	2010	[12]
Succinic acid fermenter	1,611,100	1.00	1.45	2007	[76]
Ethanol fermenter	10,128,000	1.00	1.50	2009	[12]
Deacetylation vessel 1	780,000	0.70	1.70	2013	[75]
Deacetylation vessel 2	110,000	0.80	1.70	2013	[75]
Micro- and nano- filtration	1000/m2	1.00	1.00	-	[33]
Centrifuge	170,000	1.00	1.45	1990	[74]
Evaporator	3,801,095	0.60	1.00	2010	[12]
Vacuum distillation	511,000	0.70	2.00	2009	[12]
Activate carbon vessel	614,000	0.70	1.00	2018	[74]
Acidification vessel	614,000	0.70	1.00	2018	[74]
Extraction column	511,000	0.70	2.00	2009	[12]
Back extraction column	511,000	0.70	2.00	2009	[12]
Ion exchange column	5,250,000	0.90	1.80	2014	[77]
Electrodialysis	1,410,000	0.70	1.00	1993	[78]
Water splitting electrodialysis	1,410,000	0.70	1.00	1993	[78]
Vacuum rotary filters	671,000	0.65	1.50	2014	[79]
Crystallizer	428,200	0.67	2.00	2014	[79]
Reactive crystallizer	428,200	0.67	2.00	2014	[79]
Thermal cracker	241,400	0.70	1.50	2011	[79]

Solvent purification vessel	614,000	0.70	1.00	2018	[74]
Dryer	10,500,000	0.60	1.00	1990	[80]
Washer	614,000	0.70	1.00	2018	[74]
Beer and rectification column	3,407,000	0.60	2.40	2009	[12]
Rectification column condenser	487,000	0.60	2.80	2010	
Open ponds	158,506,910	1.00	1.00	2011	[81]
Photobioreactors	109,000	1.00	1.00	2011	[81]
Inoculum system	18.22/m2	1.00	1.00	2011	[81]
Covered pond	233,000	1.00	1.00	2011	[81]
Open lined pond	87,000	1.00	1.00	2011	[81]
Lining for covered inoculum pond	3,097,827	1.00	1.00	2014	[81]
Air supported greenhouse for covered inoculum ponds	3/ft^2	1.00	1.00	2014	[81]
Lining for open inoculum pond	3,097,827	1.00	1.00	2014	[81]
CO_2 piping	1,400,800	1.25	0.60	2014	[81]
Storage tank immersion	70,500	1.76	1.00	2014	[81]
Trunk line	1,661,900	1.76	1.00	2014	[81]
Branch line	912,300	1.76	1.00	2014	[81]
Within plot piping	2,210,000	1.00	1.00	2014	[81]
Makeup delivery section	5,421,935	1.37	1.00	2014	[81]
Primary settler	1,715,000	1.00	1.00	2014	[81]
Hollow filter membranes	12,864,000	1.00	0.75	2014	[81]
Centrifuge for dewatering microalgae	560,000	1.00	1.00	2013	[81]
Membrane	1,000	-	-	2010	[33]
Extraction column	1,210,000	-	5.00	2012	[33]
Stripping column	114,000	0.60	3.00	2018	[33]
Decanter	569,000	0.60	2.00	2015	[33]
Hydrogenation reactor	2,026,515	0.56	2.47	2002	[33]
Molecular sieves	901,362	0.70	2.47	1998	[33]

n = scaling exponent
IF = Installation factor
Ref = Reference

Table 3. The unit price of chemicals.

Chemicals	Price (USD/t)	Year
Corn stover [82]	80	2004
S. japonica [83]	68	2008
Steam [74]	12.68	2013
Glucose [84]	988	2019
Glycerol [85,86]	750	2011
Acid [12]	87.78	2007
Ammonia [75]	550	2011
Enzymes [87]	5000	2016
Succinic acid [88]	2800	2019
Carbon dioxide [86]	30	2010
Sodium hydroxide [12]	149.16	2007
Magnesium carbonate [89]	480	2015
Magnesium hydroxide [86]	270	2001
Sodium carbonate [90]	300	2014
Activated carbon [91]	1300	1999
Octanol [87]	5000	2016
Tri-octylamine	1000	-
Tri-methyl amine	1000	-
Methanol [86]	547	2011
Ammonium bisulfate [86]	260	2011
Phosphoric acid [86]	420	2011
Dry distiller solids [84]	70	2004
Fresh water [74]	0.22	2013
Hydrogen [92]	1600	2011
Corn steep liquor [92]	12	2011
Enzyme nutrients [92]	1007	2011
Ethanol [93]	610	2017
Microalgae [94]	1000	2008

Table 4. Cost of utility and wastewater treatment.

Utility	Price	Year
Electricity [95]	0.07 USD/kWh	2019
Steam [95]	6.13 USD/GJ	2016
Cooling water [17]	0.28 USD/GJ	2015
Chilled water [96]	5 USD/GJ	2009
Wastewater [96]	0.041 USD/m^3	2009

2.3 Environmental assessment methodology

To evaluate environmental impact at the early-stage design we have developed a model to calculate the life cycle profile of biorefinery from feedstock extraction, transportation, processing, and disposal. The scope of environmental assessment model is cradle-to-gate that takes into account emissions produced from (1) raw material extraction and transportation to biorefinery (2) chemical used in different stages of processing/biorefinery (3) heat and power consumption in biorefinery, and (4) byproducts and waste released to environment. Therefore, in this study, the main goal of life cycle assessment is to identify process hotspots and to compare the environmental impact of different topologies in order to evaluate the main driver affecting the environmental profile and sustainability.

The inventory data or characterization factors required to perform life cycle assessment was taken from SimaPro V8.2.3 software using CML-IA baseline V3.03 characterization method. Eleven environmental indicators are considered in the present model: abiotic fossil fuel depletion potential (ADFF), acidification potential (AP), abiotic depletion potential (ADP), which is relative to the extraction minerals, eutrophication potential (EP), global warming potential 100 years (GWP), ozone depletion potential

(ODP), photochemical oxidation potential (POCP), terrestrial ecotoxicity potential (TEP), marine aquatic ecotoxicity potential (MAETP), freshwater aquatic ecotoxicity potential (FWAETP), and human toxicity potential (HTP). One kg product was considered as a functional unit to compare the life cycle profile of different biorefinery configuration.

3 PROCESS SYNTHESIS OF SUGAR PLATFORM: PART 1

This chapter is modified version of a research article which has been published in *Energy* as Rofice Dickson, Jun-Hyung Ryu, and J. Jay Liu (2018), “Optimal plant design for integrated biorefinery producing bioethanol and protein from *Saccharina japonica*: A superstructure-based approach.” 164(1), 1257-1270, doi:10.1016/j.energy.2018.09.007.

3.1 Introduction

The demand for biofuels is rising rapidly due to increased environmental concerns, finite fossil fuel reserves, and fluctuating petroleum prices [97]. Biofuels produce less carbon dioxide, and their application as a transport fuel has the potential to reduce atmospheric carbon dioxide levels [98]. Macroalgae, namely seaweed, are a promising biofuel feedstock owing to their fast growth and high carbohydrate content as well as low lignin levels.

Although macroalgae based biofuels are quite promising, their commercial production is currently limited due to the high cost of seaweed [83]. This challenge can be addressed by utilizing all of the components of seaweed, not merely carbohydrates. This can be achieved with a broad concept of biorefinery where carbohydrates can be processed to produce bioethanol while solid residue from the fermenter can be utilized to produce other products such as animal feed, fertilizers, and chemicals [99]. The residual solids obtained from the anaerobic digestion of brown algae are rich in protein, which can comprise as much as 50% of the residuals [100]. Tompkins has shown that the protein value of such solids could be similar to distillers' dried grain with soluble, the protein-rich byproduct of corn fermentation [101]. Similar evidence on the high protein value of

these solid residues supports its potential as a functional food [102–104]. Recently, Hou et al. have shown that the protein concentration in the solid residues collected after brown algae fermentation is 2-3 orders magnitude greater than those present in raw brown algae. They further established that the amino acid distribution in these residues is not changed [105].

Due to the aforementioned unique chemical composition of brown algae, carbohydrates in brown algae require moderate processing conditions such as low temperature and pressure [106]. This is beneficial for the recovery and extraction of sensitive bioactive components, such as vitamins, proteins, and antioxidants, from the solid residues of fermentation. Furthermore, the high demand for functional food and cheap protein products indicated the need for an integrated bioethanol and protein production biorefinery to meet these requirements.

The rest of the chapter is constructed as follows: The optimization of the superstructure is formulated as an MINLP problem. To obtain the global optimal solution, separable programming was used to approximate the MINLP problem to equivalent MILP problem. The maximum seaweed price (MSP), minimum dried distilled solid price (MDDS) and minimum ethanol selling price (MESP) were also determined. A comprehensive sensitivity analysis was conducted to identify influential model parameters

with an impact on the overall economics, thus suggesting where to focus for further improvements.

3.2 Methodology

3.2.1 Problem statement

The main objective of the optimization problem is to decide how bioethanol and dry distiller solids should be produced from SJ in the most economically way. To achieve the targets, a superstructure-based optimization model was developed that can systematically find the best strategy to produce desired products.

3.2.2 Superstructure development and process optimization

A superstructure shown in **Figure 5** is developed and optimized to find integrated biorefinery design producing bioethanol and dry distiller solids.

There are five different sections in superstructure, (1) pretreatment of biomass; (2) saccharification and fermentation; (3) production of enzymes; (4) purification of ethanol; and (5) processing of unreacted solids into useful product by centrifuge, protein recovery, and drying. For each section, a number of design alternatives are modeled to carry out the respective task. For instance, there are two different options for feed pretreatment. Feed can either be pretreated with a traditional acid pretreatment route or treated with a hot water wash method. Likewise,

there are two different technologies for separating solids and liquids coming out of the fermenter. Solid purification can be done before the beer column, in which case centrifugation (separation) can be performed at the outlet of fermenter. Alternatively, solid separation can be implemented after the beer column. Solids loading rate to beer column differs between separation routes. In the former route, solid loading to beer column is lower, while in the latter solid loading to the beer column is higher. There are two different options for obtaining enzymes for saccharification and fermentation. Enzymes can be manufactured onsite or they can be purchased. In the former case, capital and manufacturing costs are incurred, whereas in the latter case only purchase cost of enzyme will incur.

With reference to superstructure configuration, if a separation of solids and liquids take place before stripping column, then flows of stream from *spl2* to *M3* and *spl3* to *centrfiguge2* are eliminated. In the reverse scenario, when separation of solids and liquids takes place after stripping column, flows *spl2* to *centrifuge1* and *spl3* to *c5* do not occur. Disjunctions are used to model these two alternatives and are shown in **Section 3.2.4** [107].

Colored blocks shown in the superstructure were used for the selection of option k from stage j (conditional task). Here binary variables and

conditional constraints with disjunctions are used to determine the optimal processing pathways [48]. These are the primary decision variables for the selection of optimal configuration. For example, *spl1* divides the incoming stream into two streams. They go to their respective technology and are analyzed based on the objective function. There is a restriction on *spl1* that only one processing stage can be selected among various alternatives. Although *M1* can take multiple inputs from respective technologies and give single output. However, due to restrictions on *spl1* to select only one alternative, *M1* can only have one optimal input from the different technologies. The optimal input is based purely on the merit of the objective function.

The chemical composition of the SJ species is given in **Table 5** and used in this study as the input for feed in simulations. Experimental data regarding the process stage and main operating conditions for the modeling of each stage are summarized in **Table 6**.

3.2.3 Nomenclature of superstructure

Nomenclature for all alternatives in the superstructure is performed according to the methodology presented in **Section 2.1.2** and is provided in **Table 7**.

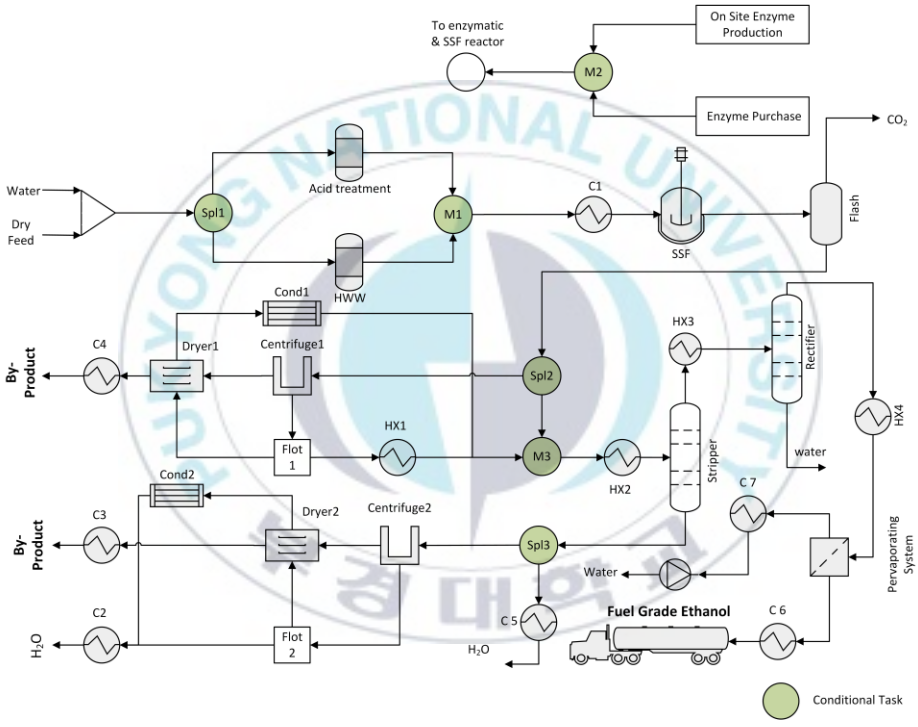

Figure 5. Superstructure of an integrated biorefinery.

Table 5. Chemical composition of the brown algae species *Saccharina japonica* [35].

Proximate analysis	**Dry basis, % w/w**
Ash	26
Volatile solids	74
Proteins	12
Lipids	2
Mannitol	12
Laminarin	14
Alginate	23
Cellulose	6
Fucoidan	5
Components	**Wet basis, % w/w**
Water	88
Total Solids	12

Table 6. Operating conditions for the process stage employed in simulation.

Process stage	Operating Condition	Reference
Acid Pretreatment 0.5 hr	120 ^{o}C	[12]
Hot water wash pretreatment 0.5 hr	85 ^{o}C	[108] [109]
Enzymatic saccharification 64 hr	48 ^{o}C	[110]
Fermentation 64 hr	30 ^{o}C	[111]
Acid loading	18 mg/g dry biomass	[12]
Cellulase loading	20 mg protein /g (Laminarin + cellulose)	[12]
Corn steep liquor in fermentation reactors	0.225 wt%	[12]
Diammonium phosphate level in fermentation reactors	0.33 g/L fermentation broth (whole slurry)	[12]

Table 7. Nomenclature of superstructure.

Nomenclature	Description	Reference
1,1	Acid route for feed pretreatment	[12]
2,1	Hot water wash route for feed pretreatment	[15]
1,2	Solid separation before stripping column	[51]
2,2	Solid separation after stripping column	[112]
1,3	*In situ* enzyme production	[12]
2,3	Purchase of enzymes	[92]

3.2.4 Superstructure mathematical modeling

Numerical representation of given superstructure contains mass and energy balance constraints, capital and operating cost constraints, and an objective function.

3.2.4.1 Mass balance constraints

Mass balance at each processing stage must be satisfied. Linear modeling is performed for mass balance constraints. The balance equation for mixers, pumps, and heat exchangers is as follows:

$$F_i^{out} = \sum_{k=1}^{n_k} F_i^k, \forall i \in I, \quad (25)$$

where F_i^k is the component *i* mass flow rate of the inlet stream *k*, F_i^{out} is the component *i* mass flow rate of the outlet stream, and n_k is the number of streams for any particular stage.

The amount of solids at any stage is controlled by the following constraint:

$$F_j^{out} \leq \sum_{k=1}^{n_k} F_i^k . \alpha_j, \forall i \in I, \forall j \in I, \quad (26)$$

where F_j^{out} is the mass flow rate of component *j* in the outlet stream and α_j is the mass fraction of component *j* in the outlet stream.

Reactors in which reactant *j* is converted to product *i* are defined by:

$$F_i^{out} = F_j^{in} \cdot \eta_{i,j} + F_i^{in}, \forall i \in I, \forall j \in I, \quad (27)$$

where F_j^{in} is the reactant *j* inlet flow rate and $\eta_{i,j}$ is the parameter and yield of product *j* from reactant *i*.

Splitters are used for the selection of option *k* from stage *j* and modeled by the following constraints:

$$F_i^{out} = \sum_{k=1}^{n_k} F_i^k, \forall i \in I, \quad (28)$$

and $$\sum_{k=1}^{n_k} F_i^k \leq y_{k,j}.UB \sum_{k=1}^{n_k} F_i^k, \forall i \in I, \forall j \in I, \quad (29)$$

where $y_{k,j}$ is the binary variable for the selection of option *k* from stage *j*, *UB* is the upper bound. The restriction for the selection on only one alternative is modeled as:

$$\sum_{k=1}^{n_k} y_{k,j} \leq 1, \forall j \in J. \quad (30)$$

In the dryer model, the recovery of water (ζ_2) is defined as the fraction of water in the feed solids that goes into the vapor stream. The recovery of ethanol (ζ_1) is related with the recovery of water by a simple flash calculation [46]:

$$\zeta_1 = \frac{\alpha_{1/2}.\zeta_2}{1+(\alpha_{1/2}-1).\zeta_2}, \quad (31)$$

where $\alpha_{1/2}$ is the relative volatility of ethanol with respect to water and taken to be constant (2.24) over temperature. The mass balance for ethanol and water in the vapor stream is given by Eq. (27) by replacing $\eta_{i,j}$ with ζ_1 and ζ_2.

$$F_i^{out} = F_j^{in}.\zeta_j, \forall i \in I, \forall j \in I. \quad (32)$$

The mass balance of ethanol and water in outlet dried solids is given by:

$$F_i^{out} = F_j^{in}.(1-\zeta_j), \forall i \in I, \forall j \in I. \quad (33)$$

The beer and rectification columns are modeled according to the method proposed by Grossmann [51], in which recovery of ethanol at the top of the column is fixed to 99.6% to reduce ethanol losses. A reflux ratio of 2 is taken for beer column and rectification column. Recovery of water is treated as a variable to provide operation flexibility. Then mass balance is given by:

$$F_i^k = F_i^{IN}.\zeta_{i,k}, \forall i \in I, \forall k \in K, \quad (34)$$

where F_i^k is the component *i* mass flow rate of the outlet stream, F_i^{IN} is the component i inlet flow rate, and $\zeta_{i,k}$ is the fractional recovery of component *i* in the outlet stream *k*.

Limit on feedstock is modeled as:

$$Feed \leq supply. \quad (35)$$

Disjunctions are used for modeling solid separation alternatives. For example, if the separation of solids and liquids takes place before the stripping column, then flow from *spl3* to *c5* must exist and can be modeled as:

$$\sum_{k=1}^{2} y^k \geq 2, \quad (36)$$

where y^k is the binary variable for outlet stream *k*. On the contrary, if separation of solids takes place after the stripping column, then flow from *spl3* to *centrifuge2* must exist and can modeled as in Eq. (36). Finally, restriction on *spl2* and *spl3* to select only one option from several options is applied by using Eq. (30).

3.2.4.2 Energy balance constraints

For each unit operation, the following energy balance constraint was used:

$$\sum_{i=1}^{n_i} F_i^{IN}.cp_i^{IN}.T^{IN} + Q_{GEN} + Q_{EXT} = \sum_{i=1}^{n_i} F_i^{OUT}.cp_i^{OUT}.T^{OUT}, \forall i \in I, \quad (37)$$

where cp_i^{IN} and cp_i^{OUT} are the specific heat of component *i* at the inlet and outlet conditions respectively. T^{IN} and T^{OUT} are the temperature of inlet and outlet conditions, and F_i^{IN} and F_i^{OUT} are the flow at inlet and outlet conditions. The above relationships are nonlinear due to the multiplication of continuous variables such as temperature and flow rate. An approximation of nonlinear equations is presented in **Section 3.2.4.5**.

Heat balance in the reboiler is determined by a simple relation proposed by [46] and rearranged as:

$$Q_{EXT} = (1 + R) \sum_{i=1}^{n_i} f_{B,i}\lambda_i. \quad (38)$$

The cooling heat load needed for the condenser is given by:

$$Q_{EXT} = -(1 + R) \sum_{i=1}^{n_i} f_{D,i}\lambda_i, \quad (39)$$

where $f_{d,i}$, $f_{b,i}$, R, and λ_i are the component molar flowrate in the distillate, component molar flowrate at the bottom, reflux ratio, and latent heat of component *i*, respectively.

3.2.4.3 Economic analysis constraints

The TEA model was formulated based on the strategy presented in **Section 2.2**. The TEA model consists of capital and manufacturing constraints to calculate discounted cash flow, which is later used to calculate the minimum selling price of products and the maximum purchasing price of feedstock. Equipment cost data including their scaling exponents and installation factors are reported in **Table 2**. Likewise, chemicals costs and utility costs are presented in **Table 3** and **Table 4** of **Section 2.2**, respectively.

3.2.4.4 Objective functions

Two different objective functions were used for this optimization, maximization of net present value and maximization of bioethanol yield.

The NPV is defined according to Eq. (24) as:

$$NPV = \sum_{n=0}^{20} \frac{NCF_n}{(1+r)^n}.$$

The yield of bioethanol can be defined as the flow of bioethanol out of the final stage and modeled as;

$$Yield = \sum_i F_i^{out}, \quad (40)$$

where F_i^{out} is the component *i* mass flow rate of the outlet final stream.

3.2.4.5 Approximation of nonlinear constraints

Energy balance equations and design constraints are the main sources of nonlinearity that may cause difficulty in solution convergence and computation of a global optimal solution [87]. In order to avoid such issues, the separable programming technique was applied to linearize the problem [113]. For example, transformation of the energy balance Eq. (37) can be expressed as follows:

$$\sum_{i=1}^{n_i} F_i^{IN}.cp_i^{IN}.T^{IN} + Q_{GEN} + Q_{EXT} = \sum_{i=1}^{n_i} F_i^{OUT}.cp_i^{OUT}.T^{OUT} \quad for\ i = 1, \dots, n_{comp},$$

where the product of two variables, mass flow rate and temperature, is taking place and causing non-linearity. The model can be transformed into a separable form by the following transformation:

1. Introduce two new variables, $Y1$ and $Y2$, into the model,
2. Relate $Y1$ and $Y2$ to F_i^{IN} and T^{IN} by:

$$\mathrm{Y1} = \frac{1}{2}\left(\mathrm{F_i^{IN}} + \mathrm{T^{IN}}\right), \tag{41}$$

and

$$\mathrm{Y2} = \frac{1}{2}\left(\mathrm{F_i^{IN}} - \mathrm{T^{IN}}\right), \tag{42}$$

3. Replace the term $F_i^{IN} \cdot T^{IN}$ in the model by:

$$\mathrm{Y_1^2} - \mathrm{Y_2^2}\ . \tag{43}$$

The model now contains the nonlinear functions Y_1^2 and Y_2^2 of single variables and is therefore separable. These nonlinear terms can be dealt with by piecewise linear approximations in which the lower and upper bounds of these variables are set and the graph is plotted between *Y1* and Y_1^2 and *Y2* and Y_2^2.

For design equations, approximations were done by using logarithms to form a separable model. Once separable equations are obtained, approximation can be done by similar methodology as described above. Care must be taken when logarithmic transformations are made to ensure that neither *Y1* nor *Y2* ever take the value 0. If this were to happen, their logarithms would go to negative infinity. It may be necessary to limit *Y1* and *Y2* to certain bounds to avoid this occurrence.

3.2.4.6 Verification of approximations

Statistically, no model is 100% accurate. It is therefore of utmost importance to investigate the results from approximations. To assess approximations, an automated model was developed in Microsoft Excel and linked with the GAMS environment by GDXXRW utility. Each time a model is compiled in GAMS; optimized variables were transported to the excel model. The model in excel then uses this information to insert the optimized variable into original nonlinear equations and compare the result

of original solution with the approximated one. Finally, it calculates the amount of error in the approximation. If the error rate is higher than 1%, then it suggests new coefficients for approximation. The newly suggested coefficient is updated in GAMS and this process continues. Normally, this process needs just one revision of the coefficient to provide the desired results.

3.3 Model solution

The previously mentioned model has been implemented in GAMS v.25.0.2. Its solution has been computed in GAMS using CPLEX solver. The model contained 1,795 continuous variables, 8 binary variables, and 2,106 equality and inequality constraints. Furthermore, the optimal solution is found in 129 iterations with an optimally gap of 0.

3.4 Results and discussions

The proposed modeling framework is implemented to determine the optimal structure for an SJ based bioethanol plant. To gain more insight into a macroalgae based biorefinery, two different optimization scenarios are investigated by using different objective functions where (i) scenario 1 sought to maximize product yield and (ii) scenario 2 sought to maximize the net present value.

3.4.1 Scenario-1: Maximization of product yield

The optimal flowsheet obtained from the superstructure for maximizing ethanol yield is given in **Figure 6**, in which the optimal pathway is composed of an acid feed pretreatment, solid separation after the stripping column, and *in-situ* enzyme production. The optimization results are presented in **Table 8**. The maximum yield of bioethanol was found to be 84.41 gal/ton of dry feed. DDS is obtained as a byproduct, and its yield is estimated to be 0.49 ton/ton of dry feed. Based on these yields, bioethanol and DDS productions of 52 Mgal/yr and 297.6 kton/yr were obtained respectively. The NPV for this plant design is found to be 3.90 million USD for 20 years project life.

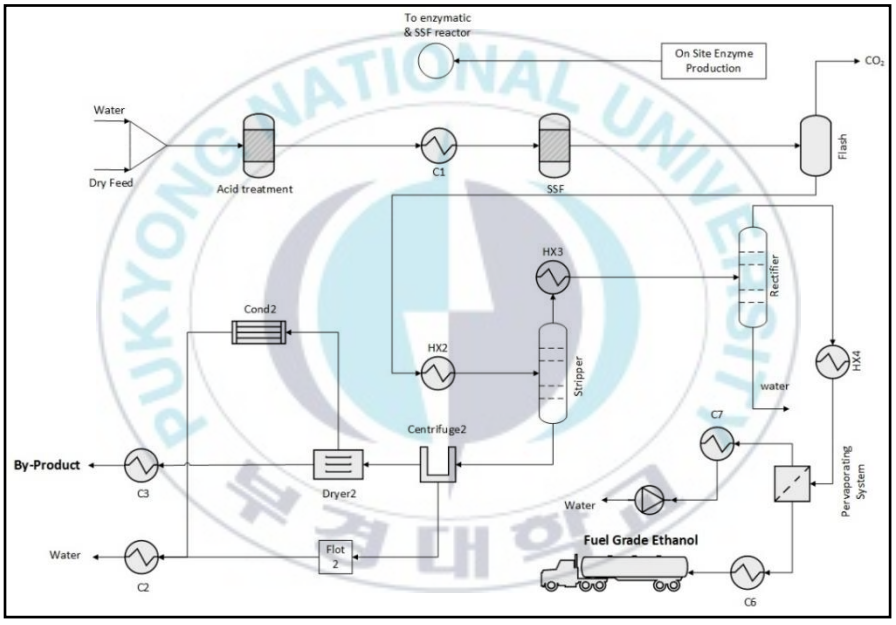

Figure 6. Optimal plant structure for scenario-1.

Table 8. Optimization results.

	Bioethanol yield[a]	DDS Yield[b]	NPV (MM$)	Bioethanol production Mgal/yr	DDS production kton/yr
Case1	84.41	0.49	3.9	52	297.6
Case2	80.57	0.51	61.5	49	311.3

[a]gal/ton
[b]ton/ton dry feed

3.4.2 Scenario-2: Maximization of NPV of the process

Scenario-2 deals with the maximization of a rigorous economic objective function, such as NPV.

The optimal processing pathway according to scenario-2 has been computed and illustrated in **Figure 7**. Interestingly, the optimal design for this scenario is completely different than the previous scenario except for the enzyme production decision. Hot water wash, solid recovery before beer column use, and production of enzymes at plant site were selected as the optimal plant configuration.

The bioethanol and DDS yields are estimated to be 80.6 gal/ton of dry feed and 0.51 ton/ton of dry feed respectively. Based on these yields, bioethanol and DDS productions of 49 Mgal/yr and 311.3 kton/yr were obtained respectively. NPV for this plant design is 61.5 million USD.

Even though the bioethanol yield in scenario-1 is 5% higher than that in scenario-2, the economic potential comparison of these two scenarios clearly shows that a plant design with respect to maximization of NPV is the better option. Hence, scenario 1 is not economically favorable and scenario-2 was selected as a base case for further investigation.

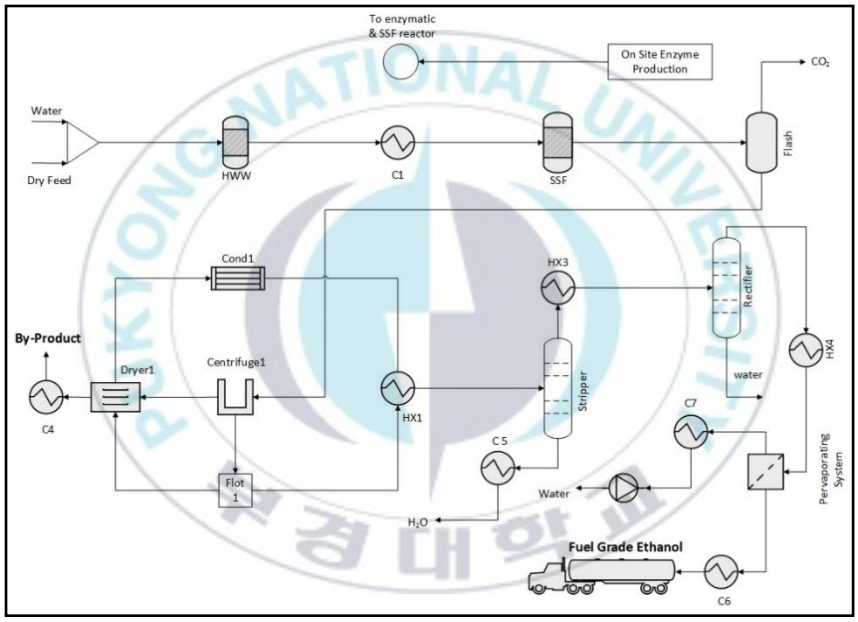

Figure 7. Optimal plant structure for scenario-2.

3.4.3 MESP and MDDS

MESP can be defined as the price of ethanol at which NPV corresponds to zero. MESP is calculated to be 1.97 USD/gal, which is on average 19.8% lower than the MESP from lignocellulose biomass [12,72,114,115]. Similarly, MDDS is also estimated by fixing the cost of ethanol to a base cost (2.24 USD/gal). The breakeven point obtained from the MDDS is 90 USD/ton, which is 30% lower than current wholesale price (130-140 USD/ton) of distillers' dried grain with soluble [116]. As MESP and MDDS are lower than their current wholesale market price, this shows that the production of bioethanol and protein rich solid from seaweed is economically viable.

3.4.4 Maximum seaweed price

Cost of seaweed is one of the biggest expenses contributing to the total manufacturing cost. It can be seen from **Figure 8A** that almost 54% of the total manufacturing cost consists of raw material cost. An increase in the cost of seaweed causes a direct increase in the cost of ethanol production. Therefore, upper limit for the price of seaweed, at which NPV become zero, was evaluated. MSP is estimated by maintaining the price of both products at base case and varying the cost of feed until the NPV value reached zero. The target seaweed price is calculated to be 88 USD/ton.

3.4.5 Manufacturing cost summary

The TCOM for the optimal base design was calculated to be 105 million USD per year. The method used to estimate TCOM is similar to that employed by Turton et al [74]. Manufacturing cost break down is reported in **Figure 8A**. Raw material cost accounts for the largest operating cost. This cost also includes the cost of transporting seaweed from the collection area to the plant site. Utilities are the second-largest portion of the manufacturing costs, which are mostly used to run distillation columns and dryer. It is expected that using heat integration and multi-effect distillation columns may decrease utility consumption at the expense of high capital cost.

3.4.6 Total capital investment

The results in **Figure 8B** illustrate that the total capital cost for optimal plant design is 220 million USD. The largest contribution to capital investment is the manufacturing capital required to purchase plant equipment. Ethanol purification and solid recovery are among the most expensive areas in terms of capital investment, due to large number of unit operations involved in dehydrating and recovering proteins. Interestingly, in this plant configuration, the capital cost of the hot water pretreatment is considerably lower than that of conventional acidic pretreatment.

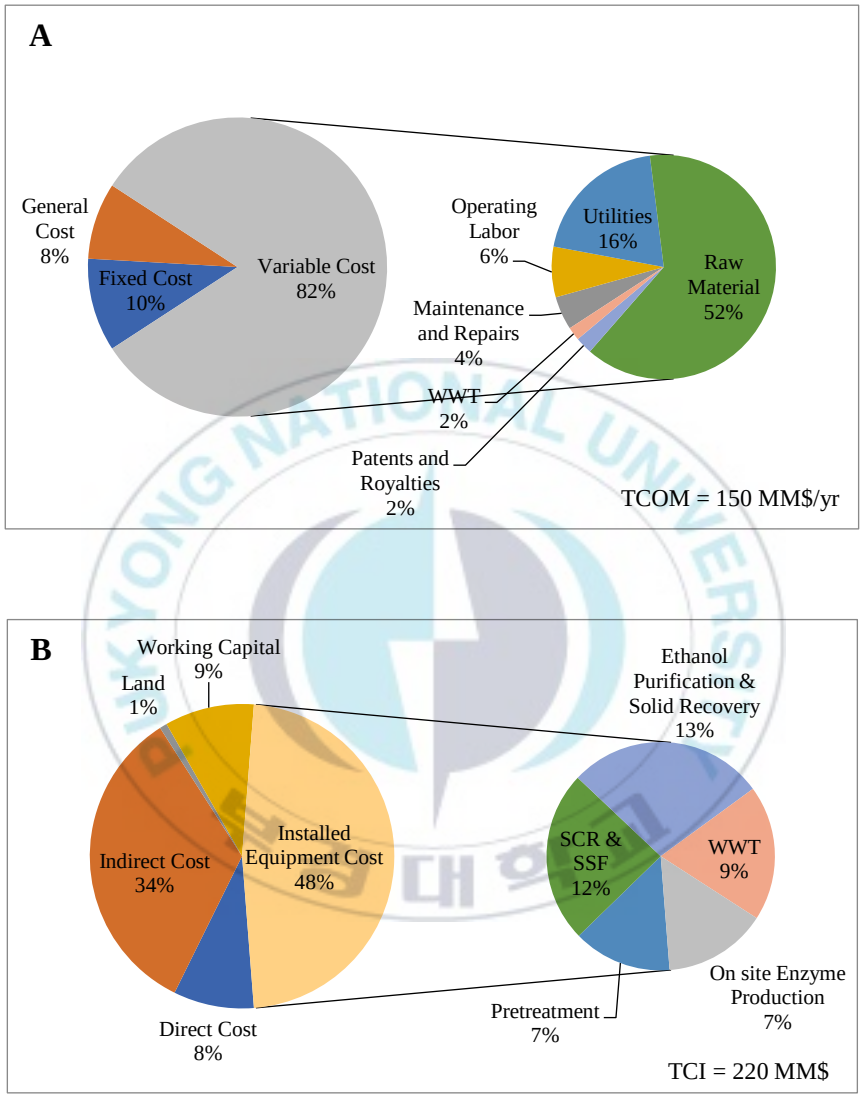

Figure 8. Total cost of the manufacturing breakdown [A]. Total capital investment breakdown [B].

3.4.7 Identification of alternative promising strategies

The generation of alternative promising strategies is done by adding integer cut constraints (Eq. 18). These promising pathways are known as sub-optimal solutions. Various solutions in **Table 9** represent the top four ordered pathways apart from pathway 1 (base case), which is the optimal solution. Pathway 6 is the least optimal pathway, which is estimated by minimizing the objective function. As it can be seen in **Table 9**, the NPV differences between the first three sub-optimal pathways is not substantial. The same is true for MESP, MDDS, and MSP. However, the solution for pathway 5 differs from the optimal pathway considerably. This is due to the selection of an acidic pretreatment instead of a hot water wash. It is further estimated that the selection of an acidic pretreatment for a brown alga based bioethanol plant would increase the TCI from 220 million USD to 289 million USD. Likewise, MESP rises from 1.97 USD/gal to 2.20 USD/gal. Additionally, the NPV for pathway 5 is close to breakeven point and becomes negative in pathway 6, which is the worst combination of unit processes corresponding to acid pretreatment, solid recovery after the beer column, and enzyme purchase. In this case, MESP rose to 2.24 USD/gal. These data strongly support the effectiveness of a hot water wash pretreatment over an acidic route.

Table 9. A set of ordered potential processing pathways.

	NPV (MM$)	**Yield (gal/ton)**	**MESP ($ /gal)**	**MSP ($/ton)**	**Promising pathways**
Pathway1 (base case)	61.5	80.5	1.97	90	2,1 1,2 1,3
Pathway2	58.7	80.5	1.98	90.2	2,1 1,2 2,3
Pathway3	57.2	80.7	1.99	90.3	2,1 2,2 1,3
Pathway4	54.5	80.7	2.0	93.1	2,1 2,2 2,3
Pathway5	8.1	84.3	2.20	124.3	1,1 1,2 1,3
Pathway6 (Worst case)	0.68	84.4	2.24	130.4	1,1 2,2 2,2

3.4.8 Sensitivity analysis

To investigate and evaluate the effect of the key model parameters on MESP and ethanol yield, a single-point sensitivity analysis was performed. The variables evaluated in the sensitivity analysis along with their variations are reported in **Table 10** and results of the sensitivity analysis on MESP are presented as a tornado chart in **Figure 9**, where the value of MESP obtained in base case is used as a reference.

Sensitivity analysis indicates that MESP is the most sensitive to the total capital investment, cost of feed, sales of DDS, amount of solid loading and glucose conversion to ethanol.

During sensitivity analysis of some variables, such as TCI and enzymes cost, the optimal design of the base case was changed to other configurations where purchased enzymes are selected as the optimal alternative. The differences between the flowsheet, relative to optimal flowsheet, during sensitivity analysis of TCI and enzyme cost are due to the total capital cost, which is increases dramatically with a 15% incremental change in these variables. Consequently, purchase of enzymes become the most favorable option.

For all other variables, there is no change in the optimal processing pathways because these variations are globally applied to whole

superstructure, thus results affect the value of objective function only with no change in optimal production route.

The results of sensitivity analysis on ethanol yield are shown in **Figure 10**, where the ethanol yield obtained in the base case is used as a reference. Conversion of glucose to ethanol is the dominant parameter for increasing the overall yield. An increase of 8%, relative to baseline yield, was observed by 10% increase of conversion ability of glucose to ethanol. Also, feed composition has a large effect on the overall ethanol yield. Increasing the carbohydrates content of feed by 50% provides an additional 5 gallons of ethanol per ton of dry seaweed.

Table 10. Assumptions and variations of the sensitivity analysis.

Assumption	Min	Base	Max	Variation (%)
Composition				
Mannitol (% w/w)	6	12	18	±50
Cellulose and Laminarin (% w/w)	10	20	30	±50
Capital				
TCI (%)	-15	-	15	±15
Internal rate of return (%)	8.5	10	11.5	±15
Brown algae cost (USD/ton)	57.8	68	78.2	±15
DDS price (USD/ton)	110.5	130	149.5	±15
Pretreatment and Saccharification reactor				
Pretreatment % solid load	16	20	24	±20
Saccharification % solid load	16	20	24	±20
Pretreatment temperature (^{o}C)	75	85	95	±12
Laminarin and cellulose to glucose (%)	72	80	88	±10
Fermentation				
Glucose to ethanol (%)	72	80	88	±10
Mannitol to ethanol (%)	72.9	81	89.1	±10

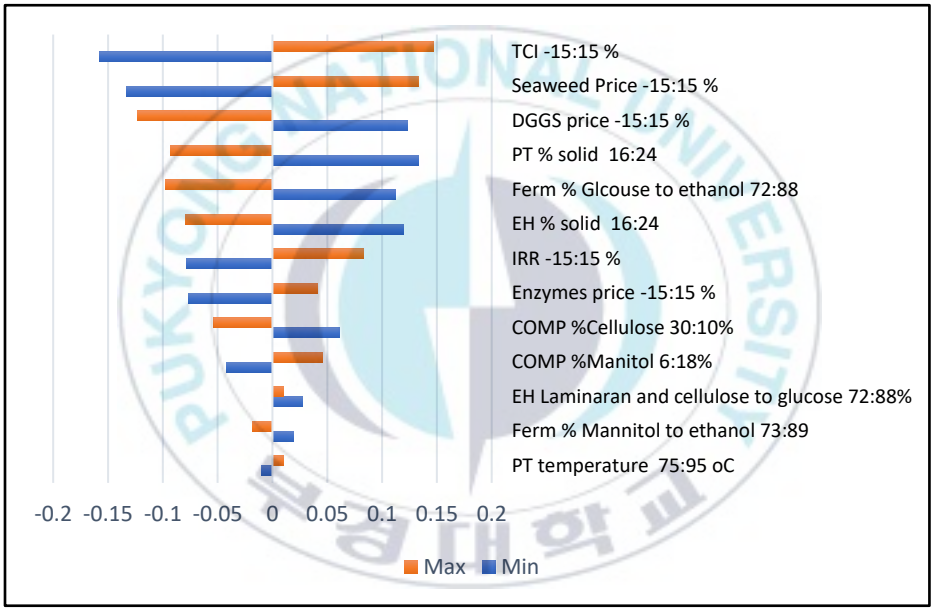

Figure 9. Sensitivity tornado chart for MESP.

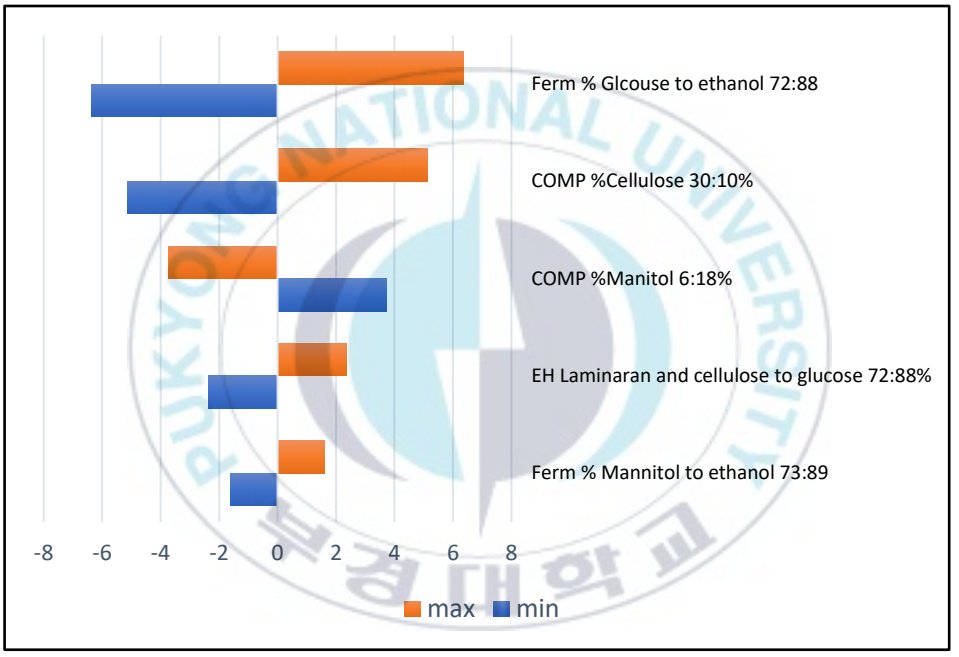

Figure 10. Sensitivity tornado chart for ethanol yield.

3.4.9 Potential improvements to plant economics

In this section, based on the results of sensitivity analysis, critical parameters are identified, and suggestions are made for potential improvements to plant economics.

3.4.9.1 Seaweed price

As can be seen in the sensitivity analysis, seaweed price is a key factor for determining the economic feasibility of a bioethanol production facility. Therefore, this is the first potential target for improvement. In this work, the base case price of dry seaweed (68 USD/ton) included the cost of macro-algae cultivation (80%) and transportation (20%) [102]. This 20% transportation cost contributes to an expenditure of 12.2 million USD for the transportation of total feed per year. However, if the location of the biorefinery is properly optimized, this can result in a significant decrease in the transportation cost. In addition, some pretreatment strategies such as drying and shredding can be applied at the feed collection area to decrease the transportation of inert (Water) materials to the factory.

At this point, a 50% reduction in transportation cost of feed, when assuming the plant location closest to feed collection area, corresponds to 61 USD/ton of dry feed. From the results given in **Table 11**, a 4.54% and

30.65% improvement in MESP and NPV respectively can be achieved relative to the base case.

3.4.9.2 Carbohydrates conversion

A goal was set for the conversion of carbohydrates to glucose. A higher carbohydrate conversion demands the use of advanced enzymes with accelerated activity for multiple substrates (cellulose, laminarin). In addition, accessory enzymes such as ferulic acid esterase may also be used for efficient hydrolysis [12]. By assuming a 10% increase in carbohydrate conversion to glucose, and combining this with the case 1, a 47.8% and 5.58% improvement in NPV and MESP can be achieved respectively.

3.4.9.3 Sugar conversion

Conversion of sugars to bioethanol is essential for the economic success of the bioethanol production process. In this study, an 80% sugar to ethanol conversion rate is used. However, in the sensitivity analysis, it is shown that a 10% increase in the conversion efficiency of sugar decreases the production cost by 5%. In order to achieve this goal, genetically engineered enzymes are required [12]. Once the activity and stability of the enzymes are optimized and properly tuned, a remarkable increase in performance is expected. In this case a 10% increase in the conversion capacity of sugar to bioethanol is assumed, and then integrated with results of goal 2, would

result in 106.5% and 10.6% improvements in NPV and MESP respectively.

3.4.9.4 DDS price

The current wholesale market price of DDS varies from 130-140 USD/ton [115]. The variation in the price of DDS is based on protein contents. Whereas the quantity of protein in DDS depends upon various factors such as protein contents present in feed (seaweed) and processing conditions (temperature, time). Prolonged or excessive heating during the process scorches the protein in DDS and reduces the availability of amino acids, particularly lysine [117]. Therefore, it is important to focus on optimal processing conditions and technologies to meet high-quality standards for DDS. Assuming a wholesale price of 150 USD/ton for high-quality DDS, and combining with previous results, would result in 150.7% and 16.3% improvements in NPV and MESP respectively.

Table 11. Effect of different policies/goals on MESP and NPV.

	Base case	**Goal1**	**Goal2**	**Goal3**	**Goal4**
NPV	61.5	82.9	90.9	127.0	154.2
Improvement (%)	0	34.8	47.8	106.5	150.7
MESP	1.97	1.89	1.86	1.76	1.65
Improvement (%)	0	4.1	5.6	10.7	16.3

3.5 Conclusions

In this work, a superstructure for the systematic assessment of a multiproduct biorefinery using SJ was developed. A rigorous techno-economic model was used to investigate different optimization scenarios such as maximization of yield and maximization of NPV. Distinct optimal structures were obtained for each optimization scenario. The MESP for scenario 1 and 2 were calculated to be 2.20 USD/gal and 1.97 USD/gal respectively. Results indicated that the acid pretreatment of feed (scenario 1) is not economically favorable over hot water wash (scenario 2) for production of SJ-based bioethanol.

A comprehensive sensitivity analysis was also performed to evaluate the major cost drivers. TCI and biomass prices were found to be the most sensitive parameters to MESP. In terms of enzymes, the capacity for the conversion of carbohydrates into sugars, and subsequently to ethanol, has a strong relation with MESP. Finally, bottlenecks were investigated, and new research targets were suggested to improve biofuel production. An MESP improvement of 16.3% was obtained by implementing these targets in simulation.

4 PROCESS SYNTHESIS OF SUGAR PLATFORM: PART 2

This chapter is a modified version of the conference paper presented in *ESCAPE-19* conference. The full-length article of this chapter is under review in *Energy* journal.

The superstructure presented in this chapter is the extension of the one presented in Chapter 3. More alternative technologies were added in the superstructure to utilize all emissions of biorefinery including carbon dioxide, wastewater, unreacted solids.

4.1 Introduction

Global warming is arguably one of the largest challenges faced by modern society [97]. Among greenhouse gases, CO_2 is of primary concern owing to its continuous increase in emission levels [118]. Therefore, a viable alternative is crucially needed in the form of biomass-derived biofuels, which could yield lower CEs. In addition, process integration techniques that can efficiently utilize CEs from industrial processes are necessary to decrease its adverse effect on the environment.

Brown algae, more specifically SJ offer multiple advantages over terrestrial biomass as presented in **Section 1.2**. The high levels of carbohydrates in SJ can be utilized to produce bioethanol. The optimal design determined in the previous chapter indicated that bioethanol production from SJ is economically viable at 1.97 USD/gal.

Despite promising economics, bioethanol processing produces significant amounts of waste streams and byproducts [119]. For example, gaseous products from the fermenter contain large quantities of CO_2 with traces of ethanol vapors [120]. The CE from fermentation in a medium-sized biorefinery processing 63 to 112 kg/s sugarcane ranges from 3.5 to 6.1 kg/s [121]. Furthermore, the stillage from the distillation column has a high chemical oxygen demand, biochemical oxygen demand, and mineral

content. Disposal of these wastes without treatment can contribute to global warming and cause severe environmental issues such as deoxygenation of water reservoirs, discoloration, odor, eutrophication, and acidification [122]. Likewise, unreacted biomass from processing offers additional challenges.

A report by the U.S. Department of Energy indicated that succinic acid is a top value-added chemical owing to its growing global market and its numerous applications in food and pharmaceutical industries [123,124]. Bai et al. [125] demonstrated that SJ biomass represents an economical alternative to petroleum-based succinic acid with high yields. Utilizing CO_2 also makes succinic acid production suitable as a method for mitigating CE from bioethanol production. Another potential method for this is microalgae-based biological utilization [126,127]. Microalgae can grow anywhere, even in wastewater; thus, they can be cultivated in the same area in which SJ is processed [128]. Davis et al. reported that 1 kg of microalgae consumes 1.93 kg of CO_2 [129]. The algal mass produced from bioethanol-emitted CO_2 is also a value-added product with applications in food and fuels [130]. The unreacted biomass can be separated from liquid products of fermentation and can be processed to produce high protein feed for animals called DDS [101]. Likewise, wastewater from all processing

can be collected to process in a wastewater treatment facility to produce clean water for biorefinery and biogas as a byproduct [131,132].

Despite several concepts of utilizing waste streams, high capital investment of such technologies is one of the major bottlenecks for their integration with standalone biorefineries. Therefore, comprehensive studies on large-scale optimization are required to investigate the optimal design of integrated biorefineries in most cost-competitive fashion.

The remainder of this chapter is organized as follows. The optimization of the superstructure is formulated as an MINLP. To determine the optimal design, various scenarios are investigated by maximizing the NPV and minimizing the CE. Once the optimal design is determined, the economic indicators of the process—such as maximum seaweed price and minimum selling prices of ethanol, dry distiller solids, succinic acid, and microalgae—are evaluated. Comprehensive single-point sensitivity analysis is then performed to identify the influential model parameters affecting the overall economics. The most influential parameters determined from sensitivity analysis are then analyzed using Monte Carlo simulation to determine the range of economic indicators and to perform the risk assessment. Finally, the impact of the biorefinery on the

environment is also investigated by optimizing CO_2 utilization and freshwater consumption.

4.2 Methodology

4.2.1 Problem statement

The optimization problem is defined as the determination of the optimal design of biorefinery that produces bioethanol and utilizes all waste streams of processing into value-added products. The optimal design in this study is defined to have superior economic potential with minimum detrimental effects on the environment.

4.2.2 Sustainable superstructure development

The traditional bioethanol process consists of acid thermal hydrolysis; enzymatic hydrolysis; fermentation; and ethanol purification by stripping column, rectification column, and molecular sieves [51]. To design an environmentally sustainable biorefinery, new technologies and their alternatives were added to the traditional bioethanol process. The superstructure given in **Figure 12** is capable of utilizing all components of seaweed and waste streams from the bioethanol processing. Seven major sections are included in the superstructure: feed pretreatment, enzymatic hydrolysis and fermentation, enzyme production, CO_2 utilization, microalgae harvesting, purification, and wastewater treatment. Multiple

design alternatives are embedded in different sections of the superstructure to perform specific tasks.

Nomenclature for all alternatives in the superstructure is performed according to the methodology presented in **Section 2.1.2** and is provided in **Table 12**. The proposed superstructure contains 30 design alternatives including different pretreatment and separation technologies and alternatives for CO_2 mitigation and enzyme production.

The biorefinery process in superstructure starts with the feed pre-treatment. Feed can either be pre-treated with acid thermal hydrolysis or hot water wash. The resulting treated feed then sent to the enzymatic hydrolysis and fermentation section, where carbohydrates are converted into glucose and ultimately to ethanol. There are two alternatives for obtaining enzymes for saccharification. Enzymes can be manufactured on-site or they can be purchased. The outlet streams from the saccharification and fermentation section consist of the gaseous, liquid, and solid product stream. The gaseous products primarily consist of CO_2 and sent to CO_2 utilization section. Two design alternatives considered for CO_2 utilization are microalgae production and succinic acid production. Based on the work of Bai et al. [125] succinic acid production from SJ is promising and can occur by consuming glucose and CO_2 in the presence of *E. Coli*. Glucose

required for the succinic acid fermentation is provided from the saccharification and fermentation section (**Figure 11**) by splitting a part of glucose to CO_2 utilization section. As glucose split for the succinic acid production will decrease the bioethanol production, therefore, upper bound on succinic acid production is applied. In alternative method, CO_2 can be utilized to produce microalgae. Microalgae can be cultivated either in open ponds or photobioreactors.

In harvesting section, five design alternatives are considered for microalgae harvesting and dewatering. The microalgae are harvested in gravity settler, which can be dewatered either by hallow filter membranes, diffused air flocculation, or electrocoagulation followed by centrifugation. Alternatively, belt filter press can be implemented at the outlet stream of gravity settler. The final concentration of microalgae from all dewatering alternative is 20 wt.%. The operating data considered for microalgae production is based on the work of Davis et al. [129]. In the purification section, various streams coming from the fermentation and CO_2 utilization section are processed to their desired level of purity. For example, succinic acid can be purified either by extractive distillation or reactive distillation processes. Unreacted solids from the fermenter can be processed either before the beer column or after the beer column. Furthermore, solid

processing can be performed either by centrifuge or belt filter press. As ethanol purification is an energy-intensive process, therefore, multiple design alternatives are considered in the superstructure to select optimal topology for its purification. In general, two pathways included in the superstructure are conventional unit operations and novel technologies such as hybrid distillation. The conventional unit operations consist of beer column, rectification column, and molecular sieves (zeolite beds) or pervaporation membranes (cross-linked vinyl alcohol). However, hybrid distillation includes the combination of distillation columns and pervaporators in series. Furthermore, ethanol purification in the beer column is energy-intensive. Therefore, to reduce energy consumption, the beer column has two design alternatives: a single distillation column and pressure swing distillation. To reduce freshwater consumption, a complete wastewater treatment network incorporated into the superstructure that will treat and recycle wastewater from various process units. Process wastewater is treated using anaerobic digestion, aerobic digestion, and reverse osmosis. The treated water is assumed to be pure and is recycled to the process. The experimental data used in the optimization are listed in **Table 13**.

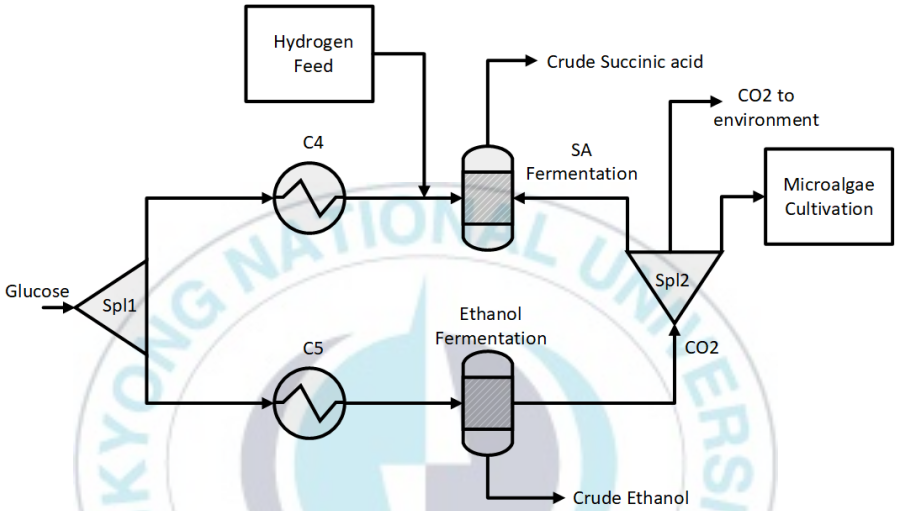

Figure 11. Alternatives for carbon dioxide utilization.

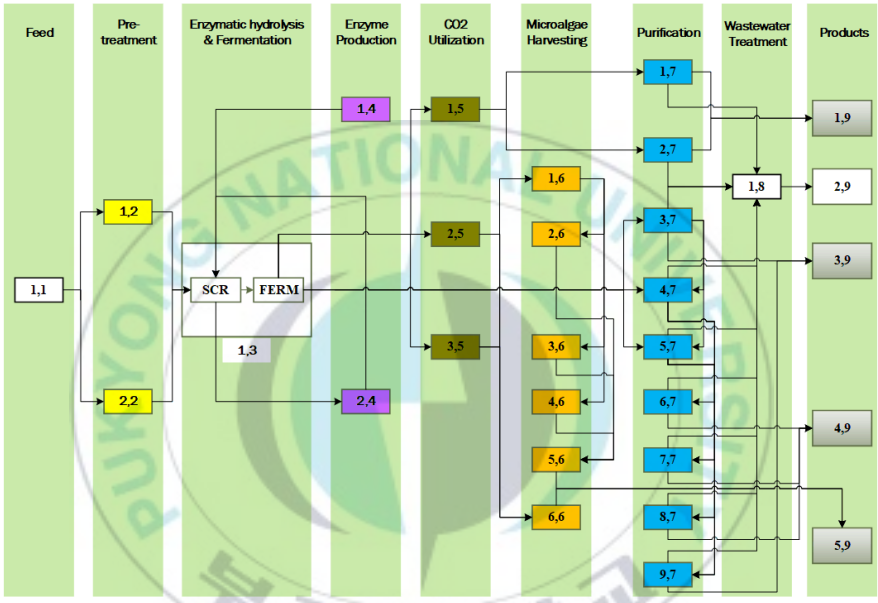

Figure 12. Superstructure of biorefinery for producing biofuel and chemicals from *Saccharina japonica*.

Table 12. Notations for the superstructure.

Notation	Description	Ref
1,1	Feed (SJ)	[102]
	Pretreatment	
1,2	Acid thermal hydrolysis	[15]
2,2	Hot water wash	[15]
	Enzymatic hydrolysis and fermentation	
1,3	Saccharification and fermentation	[133]
	Enzyme production	
1,4	Enzyme purchase	[12]
2,4	On-site enzyme production	[12]
	CO_2 utilization	
1,5	Succinic acid fermentation	[125]
2,5	Microalgae cultivation in open pond	[134]
3,5	Microalgae cultivation in photobioreactor	[134]
	Microalgae harvesting	
1,6	Gravity settler	[135]
2,6	Hollow filter membranes	[136]
3,6	Diffused air flocculation	[137]
4,6	Electrocoagulation	[138]
5,6	Centrifuge	[139]
6,6	Belt filter press	[140]
	Purification	
1,7	Reactive crystallization for succinic acid purification	[141]
2,7	Extractive distillation for succinic acid purification	[142]
3,7	Solid purification before beer column	[51]
4,7	Single beer column for ethanol purification	[12]
5,7	Thermally integrated beer column for ethanol purification	[51]
6,7	Pervaporation units for ethanol purification	[143]
7,7	Molecular sieves for ethanol purification	[51]
8,7	Hybrid distillation for ethanol purification	[144]

9,7	Solid purification after beer column	[51]
	Wastewater treatment	
1,8	Wastewater treatment	[52]
	Products	
1,9	Succinic acid	-
2,9	Recycle water	-
3,9	Dry distiller solids	-
4,9	Ethanol	-
5,9	Microalgae	-

Table 13. Operating conditions used in the optimization.

Feed pretreatment operating conditions [15]					
Process alternatives	T (K)	RT (h)	Solid loading (wt.%)	Acid loading (kg/kg dry biomass)	NH_3 loading (g/L of hydrolysate)
ATH[a]	393	0.5	30	0.018	4.8
HWW[b]	358	0.5	20	-	-

Operating conditions for various processing stages [12,108,125,133]						
Processing stage	T (K)	RT (h)	Cellulase loading[c] (kg)	CSL[d] (wt.%)	Yield (%)	DAP[e] (g/L)
SCR[f]	321	64	0.02	-	90	-
SCR[g]	321	64	0.02	-	70-80	-
Ethanol Fermentation	303	96	-	0.25	83	0.33
Seed train	301	64	-	0.5	24	0.67
SA Fermentation	310	72	-	-	73	-

Design parameters for microalgae cultivation alternatives [134]

Process alternatives	Lipid yield (%)	Algae productivity	Work for blower and mixing (kJ/m^2)	Heat removed by chillers (GJ/day)	Paddlewheel power consumption (kW)
Open pond	25	0.25 (kg/m^2/day)	-	-	11
PBR[h]	25	1.25 (kg/m^3/day)	3.5	83.4	-

Operating data for alternative dewatering technologies [134]

Process alternatives	Concentration (wt.%)	Separation efficiency (%)	Energy demand
Gravity settler	1	90	Negligible
Hollow filter membranes	13	99.5	0.144 MJ/m^3
Electrocoagulation	6	95	2.52 MJ/m^3
Diffused air flotation	6	95	0.48 MJ/kg
Centrifuge	20	99.7	4.86 MJ/m^3
Belt filter press	20	98	1.08 MJ/m^3

[a] Acid thermal hydrolysis
[b] Hot water wash
[c] kg/kg (laminarian+ cellulose)
[d] Corn steep liquor
[e] Diammonium phosphate
[f] Saccharification after acid thermal hydrolysis
[g] Saccharification after hot water wash
[h] Photobioreactor

4.2.3 Mathematical modelling of superstructure

The mathematical model of the superstructure is formulated as an MINLP model by considering mass and energy balance constraints, capital and operating cost constraints, and objective functions.

4.2.3.1 Mass balance constraints

Linear modeling is performed for the mass balance constraints. The superstructure includes two types of splitters. The first is a fractional splitter that can take any value between 0 and 1, with several possible parallel pathways available, and the second is a conditional splitter that can take either 0 or 1 as an integer value. These splitters are required to select one optimal technology from multiple alternatives. The first type of splitter is abbreviated *spl1* whereas the second is denoted *spl2*.

The mass balance constraints for the splitters are modeled as follows:

$$F_i^k = F_i^{IN} \times \mu^k, \forall k \in K, \forall i \in I, \tag{44}$$

$$\sum_{k=1}^{n_k} \mu^k = 1, \tag{45}$$

$$F_{i,j}^{IN} = \sum_{k=1}^{n_k} F_{i,j}^k, \forall i \in I, \forall j \in J, \tag{46}$$

and

$$F_{i,j}^k \leq y_{k,j} \times UB, \forall k \in K, \forall i \in I, \forall j \in J, \tag{47}$$

where F_i^k, F_i^{IN}, μ^k, $F_{i,j}^{IN}$, $F_{i,j}^k$, $y_{k,j}$, and UB are the mass flow rate of component *i* in outlet stream *k*, the mass flow rate of component *i* in the inlet stream, the split fraction for stream *k*, the mass flow rate of component

i in inlet stream *k* from stage *j*, the mass flow rate of component *i* in outlet stream *k* from stage *j*, the binary variable for the selection of option *k* from stage *j*, and the upper bound, respectively. The logical constraint for the selection of only one technology is enforced by the following:

$$\sum_{k=1}^{n_k} y_{k,j} \leq 1. \tag{48}$$

Eqs. (44) and (45) refer to *spl1*, whereas Eqs. (46–48) correspond to *spl2*.

The mass balance equation for reactors such as pretreatment, saccharification, fermentation, crystallizers, open pond, photobioreactor, and harvesting technologies in which the reactant *r* is converted to product *p* is given by

$$F_p^k = F_r^{in} \times \Phi_{p,r}^k + F_p^{in}, \forall k \in K, \forall p \in P, \forall r \in R, \tag{49}$$

where F_p^k is the mass flow rate of product *p* in outlet stream *k*, F_r^{in} is the mass flow rate of reactant *r* in the inlet stream, F_p^{in} is the mass flow rate of product *p* in the inlet stream, and $\Phi_{p,r}^k$ is the yield of product *p* of reactant *r* in outlet stream *k*.

In the dryer model, the mass balance of component *i* in outlet stream *k* is given by

$$F_i^k = F_i^{in} \times \zeta_i^k, \forall k \in K, \forall i \in I, \tag{50}$$

and

$$\sum_{k=1}^{n_k} \zeta_i^k, \forall i \in I, \tag{51}$$

where ζ_i^k is the recovery of component *i* in outlet stream *k*.

In the distillation model, the mass balance equation of component *i* in outlet stream *k* is modeled as

$$F_i^k = F_i^{in} \times \omega_{i,k}, \forall k \in K, \forall i \in I, \quad (52)$$

where $\omega_{i,k}$ is the split of components *i* in outlet stream *k* and is estimated by modeling the rigorous distillation column (Radfrac) in Aspen Plus ® V10.

The mass balance constraint for the mixer, pumps, and heat exchangers is

$$F_i^{out} = \sum_{k=1}^{n_k} F_i^k, \forall i \in I, \quad (53)$$

where F_i^k is the mass flow rate of component *i* in inlet steam *k*.

The quantity of solids present at any stage *j* is controlled by

$$F_{i,j}^k \leq \alpha_{i,j}^k \times F_j^k, \forall k \in K, \forall i \in I, \forall j \in J, \quad (54)$$

and

$$F_j^k = \sum_{i=1}^{n_i} F_{i,j}^k, \forall k \in K, \forall j \in J, \quad (55)$$

where $F_{i,j}^k$ is the mass flow rate of component *i* in stream *k* of stage *j*, F_j^k is the total mass flow rate of stream *k* of stage *j*, and $\alpha_{i,j}^k$ is the mass fraction of component *i* in stream *k* of stage *j*.

The feedstock purchase is bounded by its availability (Θ) and minimum purchase amount (Y):

$$\Theta \geq Feed \geq Y. \quad (56)$$

4.2.3.2 Energy balance constraints

The energy balance constraints were formulated exactly based on the strategy presented in **Section 3.2.4.2**.

4.2.3.3 Economic analysis constraints

Likewise, the TEA model was formulated based on the strategy presented in **Section 2.2**.

4.2.3.4 Objective functions

Two optimization scenarios were studied in the form of objective functions to fully examine the economic potential and environmental impact of the optimal design. The objective functions chosen are maximization of the NPV and minimization of CE.

The net present value is defined according to Eq. (24) as:

$$NPV = \sum_{n=0}^{20} \frac{NCF_n}{(1+r)^n}.$$

The CE from various processes can be modeled as

$$CE = \sum_{k}^{n_k} F_{CO_2}^{k}, \tag{57}$$

where $F_{CO_2}^{k}$ is the mass flow rate of CO_2 in outlet stream *k*.

4.2.4 Optimization scenarios

The following five optimization scenarios are proposed to design a sustainable biorefinery.

4.2.4.1 Scenario 1: base case

The process alternatives included in this design are pretreatment by acid thermal hydrolysis or hot water wash, on-site enzyme production or purchasing of enzymes, solid purification either before or after the beer column, and ethanol purification by classical methods or hybrid distillation. All of the remaining processes and their alternatives related to carbon utilization were excluded from the superstructure. This condition was met by forcing the binary variables involved in the selection of the carbon utilization processes to take a zero value. The base case design was solved with respect to maximizing the NPV.

4.2.4.2 Scenario 2: maximization of net present value

All restricted binary variables (carbon utilization) in the previous scenario were relaxed to determine a sustainable design. The goal of this scenario is to find candidates for the optimal flowsheet to gain the maximum NPV. In addition, only one alternative can be selected to utilize CO_2.

4.2.4.3 Scenario 3: minimizing CO_2 emissions

The goal of this scenario is to determine the optimal design from the given pool of alternatives having the least amount of CE. Therefore, the chosen objective for this scenario is minimization of CE. Except for the

objective function, all constraints are similar to those applied in Scenario 2.

4.2.4.4 Scenario 4: synergistic effect

The goal of this scenario is to investigate the synergistic effect of succinic acid and microalgae processes on the economics and environment regarding the bioethanol process. This required the removal of restrictions to select only one alternative for CO_2 utilization, as described in **Sections 4.2.4.2** and **4.2.4.3**. The chosen objective for this scenario is maximization of the NPV, whereas the second objective function was applied as a constraint in which the upper limit of the CE obtained from Scenario 3 was used.

4.2.4.5 Scenario 5: limited funds optimization

Owing to integration of the carbon utilization processes, the TCI of the biorefinery can increase significantly. Therefore, in this scenario, optimization based on limited funds was also performed, which enabled the selection of the optimal design by comparing the various economic and environmental potentials of all scenarios (1–5). Optimization was conducted for three scenarios: Cases A, B, and C, where the fund allocation to each scenario was 25%, 35%, and 45% of the base case TCI, respectively. The primary objective function was maximization of the

NPV, whereas the second objective function, minimization of CE, was applied as a constraint. Contrary to that in Scenario 4, the CE upper limit in Cases A, B, and C were relaxed by 6.2, 4.3, and 2.5 times, respectively. This is because a limited investment will decrease the capacities of the processes utilizing CO_2, which leads to poor CE utilization.

4.3 Results and discussion

The proposed process synthesis framework was implemented in GAMS (25.0.2) to determine the optimal process design with potential zero emissions from various process stages of the SJ-based biorefinery. To accomplish this task, two objective functions were optimized: maximizing the NPV and minimizing CE. The chemical composition (wt.%) of the SJ species reported in **Table 5** was used in the present study.

4.3.1 Scenario 1: base case

The optimal pathway obtained from the base case includes feed pretreatment by hot water wash, saccharification and fermentation, on-site enzyme production, ethanol purification by pressure swing distillation followed by hybrid distillation, solid purification after the beer column, and purification of polluted water in the wastewater treatment network (**Table 14**). The products obtained in this scenario are bioethanol and dry distiller solids.

The results given in **Table 15** indicate that the bioethanol yield obtained in the base case was 84.54 gal/ton of dry feed. Based on this yield, this biorefinery is able to produce 48.39 Mgal/yr of bioethanol to gain an NPV of 16.5 million USD over the 20 years of the project life. The dry distiller solids production was 296.35 kton/yr. The TCI, TCOM, and utility costs, as shown in **Figure 13A**, correspond to 241.5 million USD, 111.0 million USD/yr and 18.1 million USD/yr, respectively. The results obtained from the base case will act as an initial point in designing a better process in terms of economics and the environment.

4.3.2 Scenario 2: maximizing the net present value

The optimal flowsheet pathway given in **Table 14** includes feed pretreatment by hot water wash, saccharification and fermentation, on-site enzyme production, ethanol purification by pressure swing distillation followed by hybrid distillation, solid purification after the beer column, and purification of polluted water in the wastewater treatment network. Succinic acid was selected as the optimal technology for carbon utilization. The products obtained in this scenario are bioethanol, dry distiller solids, and succinic acid. The flow rate summary in **Table 15** shows that the utilization of glucose for succinic acid production led to a decrease in the bioethanol yield from 84.54 gal/ton to 73.97 gal/ton of dry feed. The

productions of bioethanol, dry distiller solids, and succinic acid were 42.38 Mgal/yr, 259.49 kton/yr, and 15 kton/yr, respectively. The NPV, TCI, TCOM, and utilities costs are given in **Figure 13A**. Interestingly, the NPV obtained in this scenario was 6.12 times higher than that of the base case. This improvement is attributed to the high selling price of succinic acid, which is almost 5 times that of the current wholesale price of ethanol. On the contrary, the reduction in net CE was not encouraging; an improvement of only 6% was obtained, as shown in **Figure 13B**.

4.3.3 Scenario 3: minimizing CO_2 emissions

As shown in **Figure 13B**, Scenario 1 resulted in CE of approximately 4.86 kg/s. Similarly, Scenario 2 resulted in 4.01 kg/s of CE. Therefore, the goal of Scenario 3 is to determine an environmentally friendly optimal design capable of further reducing the CE by converting them into useful products. The optimal flowsheet obtained for this scenario is different from that of Scenario 2, as illustrated in **Table 14**. The optimal pathway obtained for ethanol production and solid processing is similar to that for the base case. For carbon utilization, microalgae cultivation in open ponds, harvesting by gravity settler, and dewatering by hollow filter membranes followed by centrifuging were selected as optimal technologies. The results presented in **Figure 13B** show that a 90% reduction in net CE was

achieved relative to the base case. The remaining CE, 0.42 kg/s, is attributed to a surplus supply of CO_2, which is 10% more than the stoichiometry requirement. This surplus can account for possible variability in efficiency; otherwise, the CO_2 utilization would be too optimistic. Under this scenario, the bioethanol yield and production were 84.54 gal/ton and 48.39 Mgal/yr, respectively. These results are similar to those obtained in Scenario 1 owing to the lack of compromise on bioethanol production, as was the case of Scenario 2 in producing succinic acid. The dry distiller solids and microalgae production were 296.35 kton/yr and 58.46 kton/yr, respectively. The NPV, TCI, COM, and utilities costs are shown in **Figure 13A**. The NPV was 61.7 million USD, which is 0.39 times lower than that for Scenario 2 but 3.74 times higher than that for Scenario 1. Another interesting economic result of this scenario is the TCI of 380.4 million USD, which is 45% higher than that of Scenario 2. This large investment cost is attributed to two factors: (1) the large investment required for constructing 158 individual ponds at 10 acres each and (2) the limit on succinic acid production. It is believed that if the restriction on succinic acid production is removed, the TCI difference between the two scenarios will become marginal.

4.3.4 Scenario 4: synergistic effect

A comparison of Scenarios 2 and 3, involving succinic acid production and microalgae production, respectively, revealed that the former is an economically better option. On the contrary, the latter showed better environmental benefits. Therefore, the objective of this scenario is to study the synergistic effects of both processes on economics and the environment. The optimal pathway is given in **Table 14**, where the productions of succinic acid and microalgae were selected as optimal technologies to meet the required targets. For ethanol production, feed pretreatment by hot water wash, saccharification and fermentation, on-site enzyme production, ethanol purification by pressure swing distillation followed by hybrid distillation, solid purification after the beer column, and purification of polluted water in the wastewater treatment network were the optimal technologies. For succinic acid purification, reactive crystallization was selected as an optimal technology. For microalgae production, cultivation in open ponds, harvesting by gravity settler, and dewatering by hollow filter membranes followed by centrifuging were the optimal technologies. The products obtained from the process design of this scenario are bioethanol, dry distiller solids, succinic acid, and microalgae, corresponding to productions of 42.38 Mgal/yr, 259.49

kton/yr, 15 kton/yr, and 47.8 kton/yr, respectively. The NPV of this scenario was 144.7 million USD, which is 8.77 times higher than that of the standalone process and 1.43 and 2.34 times higher than the NPVs of Scenarios 2 and 3, respectively. The CO_2 utilization was 90%.

4.3.5 Scenario 5: optimization under limited funds

The results of the aforementioned scenarios clearly show that the process economics and environmental sustainability parameters improved significantly. However, this improvement came at the cost of a higher capital investment, at 56% more than that of the base case. Hence, the goal here is to obtain a higher NPV and a minimum 75% reduction in CE than that of base case under a limited budget for investing in carbon utilization technologies. The results indicated that for all three cases, the optimal process for CO_2 utilization is the combination of succinic acid and microalgae production and that optimal pathway is similar to that for Scenario 4. In all three cases, bioethanol, dry distiller solids, succinic acid, and microalgae were produced. As shown in **Figure 13C**, a 45% investment in CO_2 utilization technologies resulted in a 79% reduction in CE and a 6.24-fold increase in the NPV relative to the base case design.

Table 14. Optimal pathway for various scenarios.

Scenario	Optimal pathway
1	1,1 → 2,2 → 1,3 → 2,4 → 5,7 → 8,7 → 9,7 → 1,8 → 2,9 → 3,9 → 4,9
2	1,1 → 2,2 → 1,3 → 2,4 → 1,5 → 1,7 → 5,7 → 8,7 → 9,7 → 1,8 → 1,9 → 2,9 → 3,9 → 4,9
3	1,1 → 2,2 → 1,3 → 2,4 → 2,5 → 1,6 → 2,6 → 5,6 → 5,7 → 8,7 → 9,7 → 1,8 → 2,9 → 3,9 → 4,9 → 5,9
4	1,1 → 2,2 → 1,3 → 2,4 → 1,5 → 2,5 → 1,6 → 2,6 → 5,6 → 1,7 → 5,7 → 8,7 → 9,7 → 1,8 → 1,9 → 2,9 → 3,9 → 4,9 → 5,9

Table 15. Yield and flow rate summary of various scenarios.

Scenario	Ethanol yield (gal/ton)	Ethanol (Mgal/yr)	DDS (kton/yr)	MA (kton/yr)	SA (kton/yr)
1	84.54	48.39	296.35	0.00	0.00
2	73.97	42.38	259.49	0.00	15.00
3	84.54	48.39	296.35	58.46	0.00
4	73.97	42.38	259.49	47.81	15.00

DDS = Dry distiller solids; MA = Microalgae; SA = Succinic acid

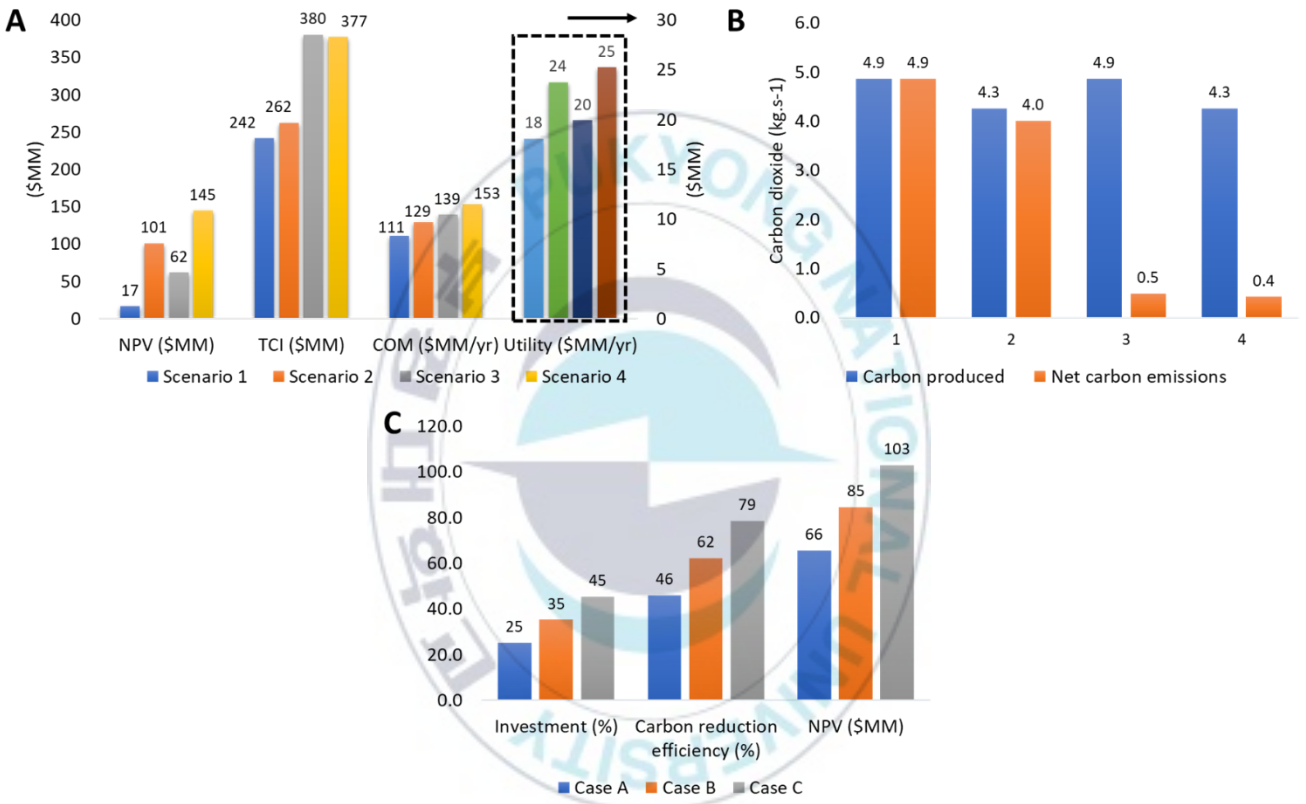

Figure 13. (A) **E**ffects of various scenarios on plant economics. (B) Net CO2 produced from various scenarios. (C) Techno-economic and environmental results for Scenario 5.

4.3.6 Optimal design

A comparison of all previous scenarios revealed that Scenario 4 is superior both economically and environmentally. One can argue that the TCI of scenario 4 is 56% more than that of the base case and 8% more than that of Case C of Scenario 5. However, if we compare the economics of Scenario 4 with those of the base case and Case C, 8.77-fold and 1.40-fold improvements in NPV were achieved, respectively. Furthermore, the CE reduction in Scenario 4 is 11% more than that of the Case C. Clearly, by investing 8% more than that for Case C, the economic and environmental benefits become significantly more favorable. Therefore, Scenario 4 was selected as the optimal design for further investigation. A simplified block flow diagram of the optimal design is shown in **Figure 14**. Unless otherwise specified, “optimal design” hereafter refers to Scenario 4.

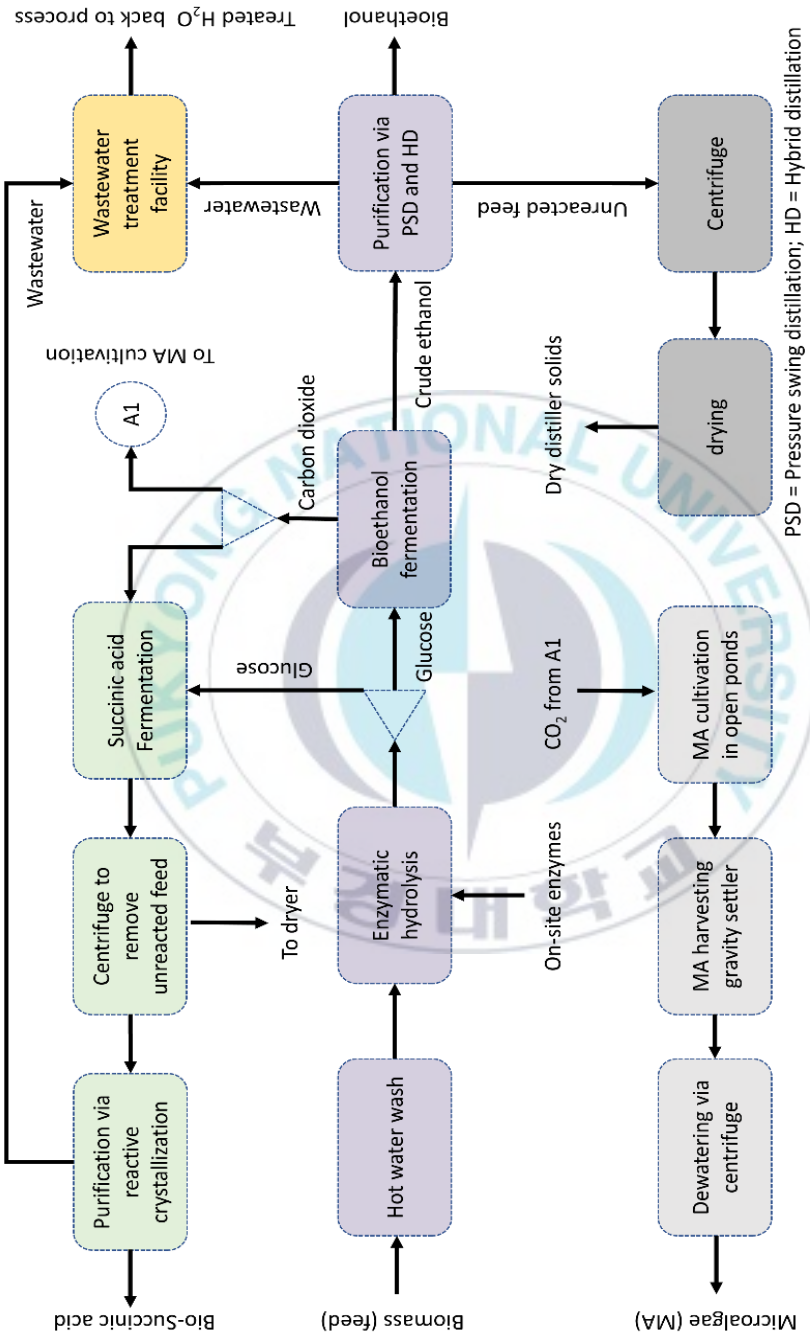

Figure 14. Simplified block flow diagram of optimal biorefinery structure.

4.3.7 Total manufacturing cost

The TCOM of the optimal design was calculated to be 161 million USD/yr. **Figure 15A** shows that the ethanol section constitutes a major portion of annual manufacturing cost. This is attributed to the large consumption of seaweed, whereas the primary raw materials required for production of succinic acid and microalgae are provided as byproducts from ethanol production. Thus, costs associated with other sections are less expensive than that in ethanol production. In the succinic acid section, the variable costs were dominant, with a 78% contribution. The distribution of manufacturing costs of the microalgae section suggests that the variable manufacturing cost constitutes most of the manufacturing expenses, in which raw material costs are dominant. Although the supply of CO_2 for microalgae cultivation is free of charge, the utilization of a large amount of fertilizers for microalgae growth results in high cost. The labor costs in microalgae production are also significant owing to the large number of operators required to maintain and service large numbers of individual ponds, corresponding to 158 individual ponds of 10 acres each.

4.3.8 Total capital cost

Similar to the total manufacturing cost, the total capital cost of the optimal design is the sum of the capital costs of individual sections. The

TCI of the optimal design is 377 million USD. The ethanol section consumes most of the capital investment required to purchase plant equipment, as illustrated in **Figure 15B**. This high investment is attributed to the large capacity of bioethanol production, whereas the capacities of other sections depend on the CO_2 evolved from ethanol fermentation. Although the capital investment required to integrate the succinic acid and microalgae carbon utilization processes is large, at approximately 42% of the ethanol section, the overall economics and CE reduction are more favorable. In the succinic acid section, purification, solid recovery, and fermentation areas are the most expensive, with a cumulative contribution of 82% of the total installed cost. Interestingly, the pretreatment sections in the bioethanol and succinic acid processes are among the least expensive. This is attributed to the unique chemical composition of seaweed, which is lack of lignin, thus eliminating harsh pretreatments such as acid thermal hydrolysis that require large amounts of steam and chemicals as well as expensive equipment to resist the acidic environment. In the microalgae section, cultivation of microalgae is the most dominant area in terms of the investment, with a 69% contribution.

4.3.9 Minimum product selling price

The minimum selling price of a product can be defined as the selling price of a product that makes the NPV equal to zero. **Table 16** shows that the MESP of the optimal design, at 1.48 USD/gal. The minimum succinic acid selling price (MSAP) is 2.00 USD/kg, which is 23% lower than that of Scenario 2. Similarly, the minimum microalgae selling price (MMAP) decreased from 0.79 USD/kg in Scenario 3 to 0.40 USD/kg in the optimal design. The minimum selling price of DDS in the optimal design is 0.03 USD/kg.

4.3.10 Maximum seaweed price

The maximum seaweed purchase price is an important economic indicator because it defines the upper price for seaweed purchase that leads to economically competitive fuel prices in the current market. Therefore, the maximum price of seaweed at which the NPV becomes zero was also calculated by keeping the price of all products to the base case price. The results in **Table 16** indicate that the base case is more sensitive to changes in the price of seaweed. For example, if the seaweed price increases from 0.08 USD/kg to 0.08 USD/kg, the NPV of the base case decreases to zero. On the contrary, the MSP for the optimal design is 0.13 USD/kg for achieving zero NPV, which is 57% higher than that of the base case.

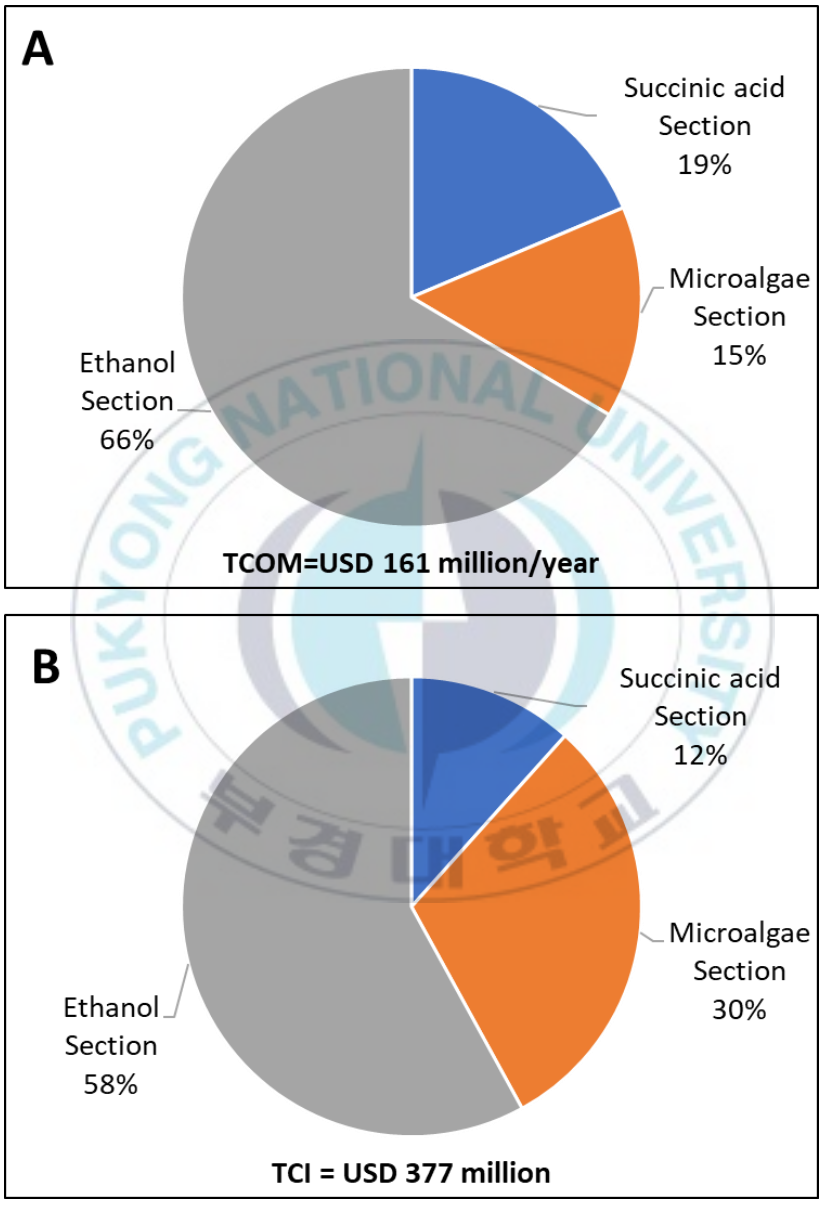

Figure 15. Breakdowns of the total (A) manufacturing costs and (B) capital costs of the optimal design.

Table 16. Minimum selling prices of products from biorefinery.

	MESP ($/gal)	**MDDS ($/kg)**	**MSAP ($/kg)**	**MMAP ($/kg)**	**MSP ($/kg)**
Scenario 1	2.16	0.14	-	-	0.08
Scenario 2	1.67	0.06	2.60	-	0.11
Scenario 3	1.89	0.10	-	0.79	0.10
Optimal design	1.48	0.03	2.00	0.40	0.13

4.3.11 Sensitivity analysis (Major cost drivers)

To estimate the major cost driver of the MESP and the ethanol yield, a single-point sensitivity analysis was conducted. The sensitivity analysis results presented in **Figure 16** show that the TCI, biomass cost, succinic acid and microalgae selling prices, internal rate of return, mannitol composition in the feedstock, DDS price, and labor costs play an important role in influencing the MESP.

The results of the sensitivity analysis on the ethanol yield are shown in **Figure 17**. Feed composition was shown to be the most dominant and important parameter for increasing the overall yield of bioethanol. In addition, glucose conversion to ethanol has a significant effect on the overall yield.

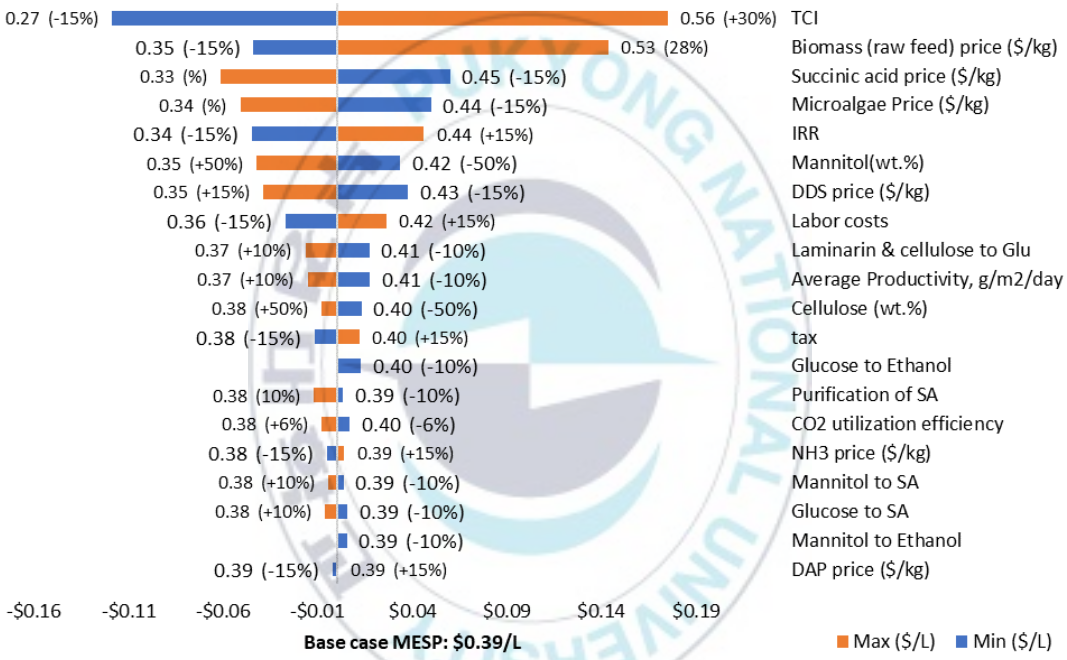

Figure 16. Sensitivity tornado chart for the minimum ethanol selling price.

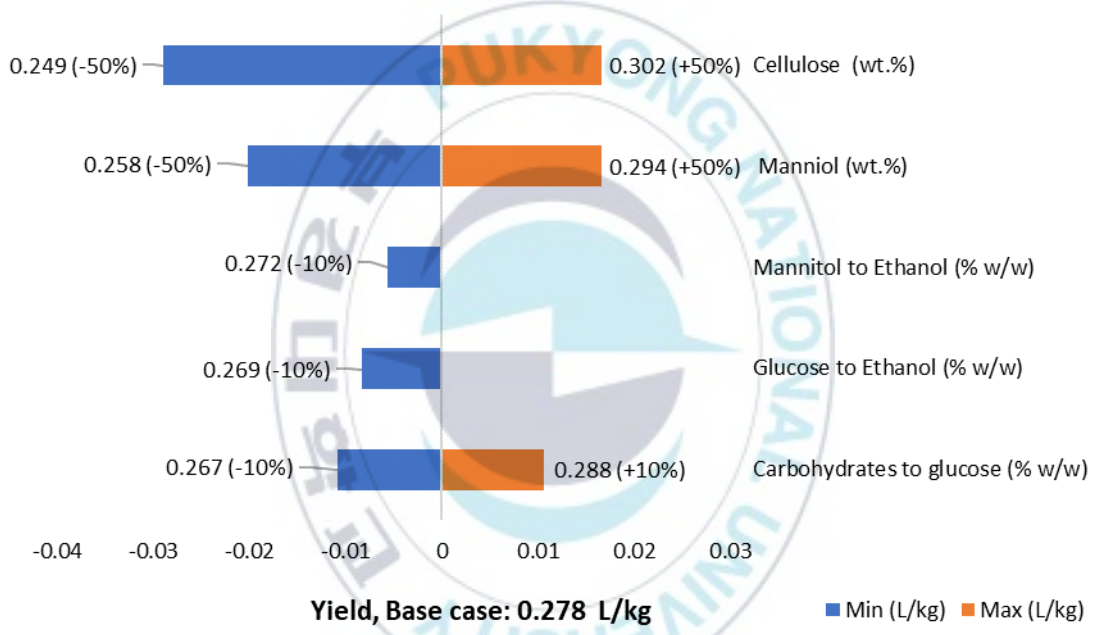

Figure 17. Sensitivity tornado chart for the ethanol yield.

4.3.12 Monte Carlo simulation (Risk assessment)

The critical parameters that were identified by single-point sensitive analysis in the previous section are used here to determine the minimum product selling range and risk using Monte Carlo simulation. 1000 samples were generated using uniform distribution between the predefined range of parameters. The most probable minimum selling price range was assumed to be one standard deviation from the mean price. The results indicated that the MESP range of the optimal design is 0.36–0.56 USD/L with a mean value of 0.46 USD/L and standard deviation of 0.097 USD/L.

Risk assessment (**Figure 18**) was performed where economic risk was quantified based on the minimum ethanol selling price. Here, we analyzed the probability of obtaining a minimum ethanol selling price that was higher than the targeted market price. Based on the current ethanol market price of 0.4 USD/L in the United States, the probability of risk for the optimal design is about 93.7% and 0% for the remaining scenarios, which geographically make the optimal design economically unfavorable for the country. However, seaweeds are largely cultivated in Asia and mainly in China, Indonesia, and South Korea, where the ethanol price varies at 0.6–0.72 USD/L. This leads to a 44–20% probability of loss for the optimal design.

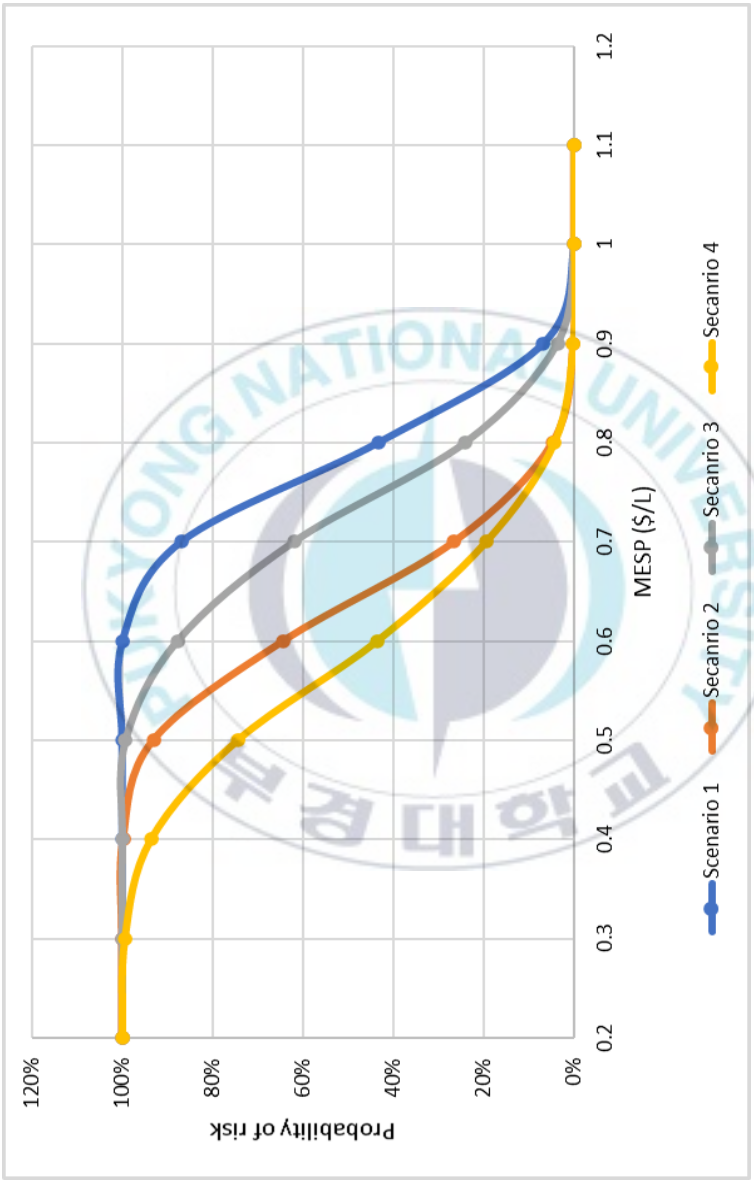

Figure 18. Cumulative density distribution for minimum ethanol selling price.

4.3.13 Wastewater treatment and water consumption

Wastewater treatment and freshwater consumption are important environmental factors in process sustainability. In the wastewater treatment process, effluent streams from various stages of ethanol and succinic acid sections are treated and recycled to the process.

The overall freshwater consumption is 6.31 gal of water/gal ethanol. It is worth noting that the water lost by evaporation in the cooling tower cannot be reused. However, it is believed that this water loss can be decreased by heat integration in the heat exchanger network.

The water loss for microalgae production is higher than that from the ethanol and succinic acid sections owing to evaporation of water from the pond surfaces. Result shows that water evaporation alone resulted in water losses of 82 wt.%. The loss of water in the blowdown is attributed to a 0.5% discharge of recovered water from the gravity settler. Microalgae contain 80% moisture in the final product stream; therefore, 5% of the water is lost in the product stream. The total makeup water required for the microalgae section is 3.1 Mgal/day.

4.4 Conclusion

In this study, a novel strategy is proposed to produce advanced biofuel and to utilize all waste streams from *Saccharina japonica*-based biorefinery. A rigorous optimization-based framework for simultaneous process synthesis and process integration of a macroalgal biorefinery was proposed. The process synthesis model features several design alternatives for bioethanol processing as well as alternatives for utilizing all waste streams from the processing in one combined superstructure. The detailed mathematical modeling of the superstructure is incorporated as large-scale mixed-integer non-linear optimization model that can be solved efficiently to determine the optimal design with superior economic and environmental performance. The framework was demonstrated by using five optimization scenarios under different objective functions, and the economic viability and environmental sustainability of each case study were presented.

The novelty of this work includes utilization of *Saccharina japonica* as a feedstock, which itself is self-sustaining, and integration of the carbon sequestration processes with traditional bioethanol processing to utilize all waste streams. The minimum ethanol selling price range of the optimal design is 0.36–0.56 USD/L. A comparison of the CO_2 emissions in the optimal design with that in the base case revealed a strong potential for

environmental sustainability, with a decrease from 4.86 kg/s in the latter to 0.42 kg/s in the former, representing a 90% reduction. Similarly, the freshwater requirement in the optimal design is 6.31 L H_2O/L ethanol, representing a 38.6% reduction compared with the base case. Risk assessment suggested that the proposed seaweed-based biorefinery design would be economically favorable in Asia, with a 20–44% probability of risk. According to the sensitivity analysis, seaweed cost and chemical composition are critical parameters that should be improved by intensified farming via artificial cultivation techniques to decrease the probability of risk.

5 PROCESS SYNTHESIS OF VOLATILE FATTY ACIDS PLATFORM

This chapter is a modified version of the conference paper presented in *ESCAPE-19* conference. The full-length article of this chapter is under review in *Green Chemistry*.

5.1 Introduction

The current pace of utilizing petroleum resources is causing ecosystem damages. Global warming is a serious environmental issue, common to all mankind [145]. CEs from burning fossil fuel are thought of as one major contribution to global warming [2]. To mitigate climate change impacts, highly efficient biorefineries utilizing sustainable biomass must be developed to replace fossil-based energy infrastructure [145]. Macroalgae (seaweed) have been considered as more sustainable biomass compared to crops since they do not compete for land and freshwater [35]. In order to use the macroalgae in a commercial scale biorefineries, it is necessary to evaluate various potential pathways into value-added products as well as intermediate components and technologies. Furthermore, the potential processes must be designed with minimum carbon and other waste emissions, while simultaneously have to be economically competitive to operate. This in turn presents a large decision-making problem with a significant combinatorial complexity.

Biofuels can be produced from SJ via VFAP. In this platform, VFAs consisting of acetic acid, propionic acid, and butyric acid are produced by the partial anaerobic digestion of biomass using a mixed culture bacterial ecosystem [17]. VFAs have numerous applications in the chemical, food

and pharmaceutical industries. They are important precursors of biopolymers—e.g., polyhydroxyalkanoates —and other valuable products such as aldehydes and ketones [146]. Therefore, VFAs can be separated and sold as the main products of a biorefinery. Alternatively, VFAs can be hydrogenated to produce mixed alcohols consisting of ethanol, propanol, and butanol, which can be sold as renewable transportation fuels.

In the literature, numerous studies have demonstrated that the VFAP has a higher product yield than the SP [147]. This is primarily owing to the ability of anaerobes to digest all the non-lignin components of the biomass, including carbohydrates, proteins, and lipids, whereas, in the case of the SP, only the carbohydrate content of the biomass is converted to bioethanol [17]. Furthermore, unlike the SP, the VFAP does not require aseptic conditions and does not utilize expensive enzymes and capital-intensive fermenters [18]. Despite the promising yields and simple digestion process, the design of effective and economically viable separation technologies for the dehydration of aqueous VFAs is a major obstacle to the industrial-scale application of the VFAP [17]. This is mainly because water and acetic acid have similar boiling points, which makes their separation by distillation difficult and energy-intensive. Another challenge associated with the VFAP is the significant production of carbon dioxide

during the fermentation of biomass. Bonfim-Rocha et al. demonstrated that the CEs produced by the fermentation-based biorefinery processing of 2–3.5 Mt/yr amount to approximately 110–193 kton/yr [121]. A potential method of mitigating direct CEs from the VFAP is microalgae-based biological utilization. Davis et al. reported that 100 ton of algal biomass fixes approximately 193 ton of carbon dioxide, which make it a suitable candidate for reducing the CEs produced by the VFAP [129]. There is also an indication that the water footprint of a biorefinery is quite high. Approximately 13 gals of wastewater are produced when one gal of corn ethanol is refined [4]. This level of water consumption is alarming and must be reduced by reusing the wastewater from processing.

In order to address this problem, the study presented in this chapter utilizes a superstructure process design approach for a seaweed biorefinery producing mixed alcohols and mixed organic acids via anaerobic digestion/volatile fatty acid route. Seventeen design alternatives have been proposed to determine the optimal design and technical feasibility by maximizing the NPV in the most environmentally beneficial fashion.

The remainder of this chapter is organized as follows. The optimization of the superstructure is formulated as an MINLP. To determine the optimal design, various scenarios are investigated by maximizing the NPV. Once

the optimal design is determined, the economic indicators of the process are evaluated. Comprehensive single-point sensitivity analysis is then performed to identify the influential model parameters affecting the overall economics. Finally, the impact of the biorefinery on the environment is also investigated by optimizing CO_2 utilization and freshwater consumption.

5.2 Methodology

The main objective of the optimization problem is to determine the optimal design of the biorefinery from the given superstructure by maximizing the NPV as well as minimizing the environmental impact of the biorefinery by integrating waste streams utilization technologies. The major decision variables include: technology selection for the VFAP and carbon dioxide utilization; the mass flow rate of each species in every stream; the heat and power consumption of each piece of equipment; the capital cost and the operating cost required for economic evaluation; and all emissions required for environmental evaluation.

5.2.1 Superstructure development

A superstructure containing seventeen design alternatives at the various processing stage of a biorefinery is illustrated in **Figure 19**. Seven major sections are included in the superstructure: anaerobic digestion, VFA

extraction, mixed alcohol synthesis, carbon dioxide utilization, harvesting, purification, and wastewater treatment.

The biorefinery process starts with the anaerobic digestion of SJ. Anaerobic digestion consists of four stages; and in order to produce VFAs, partial anaerobic digestion is carried out using inhibitor such as iodoform, which eliminates methanogenesis step [17]. The operating conditions for anaerobic digestion are 13 wt.% solid loading; a retention time of 120 h; an inhibitor loading of 30 ppm; a digestion temperature of 35 °C, and a yield of 0.35 g VFA/g of dry feed [147]. After anaerobic fermentation, the outlet stream from the digester consists of solid, liquid, and gaseous products, which is sent to the purification section. In the purification section, gaseous- and solid-products are separated from liquid products. Liquid products consisting of VFAs are sent to VFA extraction section, in which two alternative technologies are considered: classical dehydration and hybrid dehydration [17,148]. The main equipment of the classical dehydration contains an extraction column, a rectification column, a stripping column, and a decanter. The hybrid process involves the combination of membranes and the classical dehydration process. The main goal in VFA extraction section is to concentrate VFAs from 5 wt.% to 95 wt.%. Once the VFAs are concentrated, they can be hydrogenated in

the mixed alcohols synthesis section to produce mixed alcohols consisting of ethanol, propanol, and butanol [149].

Alternative, hydrogenation can be bypassed and concentrated VFAs are separated into pure compounds [150]. Mixed alcohols and mixed acids will be produced as the main products of biorefinery in the former (hydrogenation) and latter (bypass), respectively. If the latter is selected as an optimal decision, an upper limit of utilizing 30 wt.% of the VFAs is set for mixed acids production, because the main objective of the biorefinery is to produce biofuels. In CO_2 utilization section, the key objective is to convert CO_2 into microalgae either in open ponds or photobioreactor. If the production of microalgae is not economically favorable then the CO_2 is vented to the environment by paying a carbon tax of 20 USD/ton. For microalgae harvesting and dewatering, six process alternatives are included in microalgae harvesting section. The microalgae can be harvested in gravity settler, which can be dewatered either by hollow filter membranes, diffused air flocculation, or electrocoagulation followed by centrifugation. Alternatively, a belt filter press can be implemented at the outlet stream of gravity settler. The operating data and equipment costs considered for microalgae production are based on the work of [134] and outlined in **Table 13**. In purification section, separation of non-

condensable gases, VFAs, MAs, and DDS take place in pressure swing adsorption, distillation columns, pervaporation or molecular sieves followed by distillation, and centrifuge and dryer, respectively [150–154]. A complete wastewater network consisting of anaerobic digestion, aerobic digestion, and reverse osmosis is included in the superstructure that treats polluted water from various processing stages back to the process [12,51].

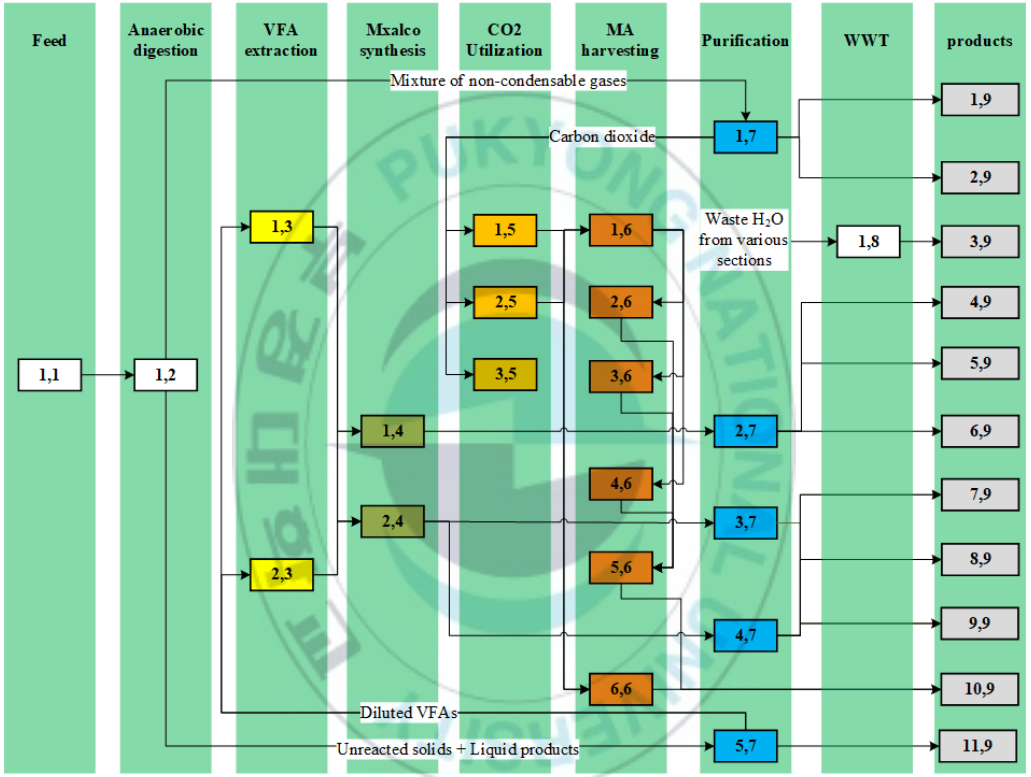

Figure 19. Superstructure of biorefinery for producing biofuel and chemicals from Saccharina japonica.

5.2.2 Mathematical modeling of superstructure

5.2.2.1 Mass balance constraints

The mass balance constraints for the splitters were modeled using Eqs. (44-48).

The mass balance equation for reactors such as the anaerobic digester, open ponds, photobioreactors, and harvesting technologies where the reactant *r* is converted to the product *p* is given by

$$F_p^k = F_r^{in} \times \Phi_{p,r}^k + F_p^{in}, \forall k \in K, \forall p \in P, \forall r \in R, \quad (58)$$

where F_p^k is the mass flow rate of product *p* in the outlet stream *k*, F_r^{in} is the mass flow rate of reactant *r* in the inlet stream, F_p^{in} is the mass flow rate of product *p* in the inlet stream, and $\Phi_{p,r}^k$ is the yield of product *p* from reactant *r* in the outlet stream *k*.

The mass balance of component *i* in the outlet stream *k* in the pressure swing adsorption, mechanical separator, dryer, and decanter is given by

$$F_i^k = F_i^{in} \times \zeta_i^k, \forall k \in K, \forall i \in I, \quad (59)$$

and

$$\sum_{k=1}^{n_k} \zeta_i^k = 1, \forall i \in I, \quad (60)$$

where ζ_i^k represents the recovery of component *i* in the outlet stream *k*.

The mass composition (X_i^k) of component *i* in the stream *k* is given by

$$\sum_{k=1}^{n_k} X_i^k = \sum_{k=1}^{n_k} \frac{F_i^k}{F^k}, \forall i \in I, \quad (61)$$

where F^k is the overall mass flow rate of the stream *k*.

In the flash column, the mass balance of component *i* in the outlet stream *k* can be determined by

overall mass balance: $F_i^{in} = \sum_{k=1}^{n_k} F_i^k, \forall i \in I,$ (62)

Antoine relation: $log_{10} VP_i^{in} = A_a^i - \frac{A_b^i}{T^{in} + A_c^i}, \forall i \in I,$ (63)

Henry relation: $logVP_i^{in} = H_a^i + \frac{H_b^i}{T^{in}} + H_c^i \times logT^{in} + H_d^i \times T^{in}, \forall i \in I,$ (64)

equilibrium relation: $K1_i^{in} = \frac{VP_i^{in}}{P^{in}}, \forall i \in I,$ (65)

bottom composition: $X1_i^{k1} = \left(\frac{LV+1}{LV+K1_i^{in}}\right) \times X_i^k, \forall k1 \in K, \forall i \in I,$ (66)

top composition: $Y1_i^{k2} = X1_i^{k1} \times K1_i^{in}, \forall i \in I, \forall k1, k2 \in K,$ (67)

top overall flowrate: $F^{k2} = \left(\frac{F^{in}}{LV+1}\right), \forall i \in I, \forall k2 \in K,$ (68)

top component flowrate: $F_i^{k2} = F^{k2} \times Y1_i^{k2}, \forall i \in I, \forall k2 \in K,$ (69)

logical constraint 1: $\sum_i^{n_i} X1_i^{k1} = 1,$ (70)

and logical constraint 2 : $\sum_i^{n_i} Y1_i^{k2} = 1,$ (71)

where VP_i^{in} is the vapor pressure of component *i* in the inlet stream, A_a^i, A_b^i, and A_c^i are the Antoine parameters of component *i*, H_a^i, H_b^i, H_c^i, and H_d^i are the Henry parameters of component *i*, T^{in} is the inlet temperature, $K1_i^{in}$ are the K-values of component *i* in the inlet stream, LV is the liquid

to vapor ratio, $X1_i^{k1}$ is the bottom composition of component *i* in the stream *k1*, $Y1_i^{k2}$ is the top composition of component *i* in the stream *k2*, F^{k2} is the flowrate of the top stream, and F^{in} is the mass flowrate of the inlet stream.

In the extraction column, the mass balance of component *i* in the outlet stream *k* can be determined by

overall mass balance: $F_i^{in} + F_{MTBE}^{in} = \sum_{k=1}^{n_k} F_i^k, \forall i \in I,$ (72)

extraction solvent: $F_{MTBE}^{in} = F^{in} \times \sum_{sf=1}^{sf_n} \lambda_{sf} \times b1_{sf},$ (73)

stages (*N*): $N = \sum_{st=1}^{st_n} \sum_{sf=1}^{sf_n} \nu_{st} \times b2_{sf}^{st},$ (74)

extract mass balance: $F_i^{k1} = F_i^{in} \times \sum_{st=1}^{st_n} \sum_{sf=1}^{sf_n} \xi_{i,sf}^{st} \times b2_{sf}^{st}, \forall k1 \in K, \forall i \in I,$ (75)

raffinate mass balance: $F_i^{k2} = F_i^{in} - F_i^{k1}, \forall k2 \in K, \forall i \in I,$ (76)

logical Constraint 1: $\sum_{sf=1}^{sf_n} b1_{sf} = 1,$ (77)

logical Constraint 2: $\sum_{st=1}^{st_n} \sum_{sf=1}^{sf_n} b2_{sf}^{st} = 1,$ (78)

and logical Constraint 3: $\sum_{sf=1}^{sf_n} b1_{sf} = \sum_{st=1}^{st_n} \sum_{sf=1}^{sf_n} b2_{sf}^{st},$ (79)

where F_{MTBE}^{in} is the mass flow rate of the extraction solvent in the inlet stream, λ_{sf} is the parameter corresponding to the solid to feed ratio, $b1_{sf}$ is the binary variable for selecting the optimal solid to feed ratio, ν_{st} is the parameter indicating the number of stages, $b2_{sf}^{st}$ is the binary variable for

selecting the optimal number of stages, F_i^{k1} is the mass flow rate of component *i* in the extract stream, $\xi_{i,sf}^{st}$ is the split fraction of component *i* in the outlet stream *k*, and $F_i^{k2}$is the mass flow rate of component *i* in the raffinate stream.

In the stripping column, the mass balance of component *i* in the outlet stream *k* can be determined by

overall mass balance: $F_i^{in} + F_{LP}^{in} = \sum_{k=1}^{n_k} F_i^k, \forall i \in I,$ (80)

LP-steam balance (F_{LP}^{in}): $F_{LP}^{in} = \frac{F^{in} \times \varphi}{\sum_{i=1}^{n_i} K1_i^{in}},$ (81)

absorption factor (A_i): $\frac{\varphi - 1}{\varphi^{N+1} - 1} = 1 - \Upsilon,$ (82)

stages (N): $A_i = \frac{F_i^{in}}{K1_i^{in} \times F_{LP}^{in}}, \forall i \in I,$ (83)

stripping factor (S_i): $S_i = \frac{K1_i^{in} \times F_{LP}^{in}}{F_i^{in}}, \forall i \in I,$ (84)

fraction of components not absorbed ($\gamma 1_i$): $\gamma 1_i = \frac{A_i - 1}{A_i^{N+1} - 1}, \forall i \in I,$ (85)

fraction of components not stripped ($\gamma 2_i$): $\gamma 2_i = \frac{S_i - 1}{S_i^{N+1} - 1}, \forall i \in I,$ (86)

bottom mass balance (F_i^{k1}): $F_i^{k1} = F_i^{in} \times \gamma 2_i + F_{LP}^{in} \times (1 - \gamma 1_i), \forall k1 \in K, \forall i \in I,$ (87)

and top mass balance (F_i^{k2}): $F_i^{k2} = F_i^{in} - F_i^{k1}, \forall k2 \in K, \forall i \in I,$ (88)

where φ is the stripping factor and Υ is the recovery of the key component.

In the distillation model, it is assumed that all components heavier than the heavy key component would accumulate in the bottom stream. Similarly, all components lighter than the light key component will accumulate in the distillate. The mass balance equations of the light key (*lk*) and heavy key (*hk*) components in the distillate **(***d*) and bottom (*b*) stream can be modeled as

$$F_{lk}^{d} \geq F_{lk}^{in} \times \omega_{lk}^{D}, \ \forall d \in K, \forall lk \in I, \tag{89}$$

$$F_{lk}^{b} \leq F_{lk}^{in} \times (1 - \omega_{lk}^{D}), \ \forall b \in K, \forall lk \in I, \tag{90}$$

$$F_{hk}^{d} \leq F_{hk}^{in} \times \omega_{hk}^{D}, \ \forall d \in K, \forall hk \in I, \tag{91}$$

$$F_{hk}^{b} \geq F_{hk}^{in} \times (1 - \omega_{hk}^{D}), \ \forall b \in K, \forall hk \in I, \tag{92}$$

where ω_{lk}^{D} and ω_{hk}^{D} are the split fractions of the light key and heavy key components in the distillate, which can be estimated by modeling the rigorous distillation column (Radfrac) in the Aspen Plus ® V10 software.

The mass balance constraint for the mixers, pumps, compressors, and heat exchangers is

$$F_{i}^{out} = \sum_{k=1}^{n_k} F_{i}^{k}, \forall i \in I, \tag{93}$$

where F_{i}^{k} is the mass flowrate of component *i* in the inlet steam *k*.

The amount of solids at any stage *j* is controlled by

$$F_{i,j}^{k} \leq \alpha_{i,j}^{k} \times F_{j}^{k}, \forall k \in K, \forall i \in I, \forall j \in J, \tag{94}$$

and

$$F_{j}^{k} = \sum_{i=1}^{n_i} F_{i,j}^{k}, \forall k \in K, \forall j \in J, \tag{95}$$

where $F_{i,j}^{k}$ is the mass flowrate of component i in the stream k of stage j, F_{j}^{k} is the total mass flowrate in stream k of stage j, and $\alpha_{i,j}^{k}$ is the mass fraction of component i in the stream k of stage j.

The feedstock purchase is bounded by its availability (Θ) and minimum purchase amount (Y):

$$\Theta \geq Feed \geq Y. \tag{96}$$

5.2.2.2 Energy balance constraints

The Eq. (37) energy balance constraint was used for each unit operation. Heat balance in the reboiler and condenser is determined by Eqs. (38-39).

The temperature and pressure of the outlet stream of the flash, distillation, and stripping columns and membranes can be determined using Eqs. (63) and (64), and the bubble point and due point equations.

The power (kW) required for the pumps and compressors can be determined by

$$Power = \frac{\sum_{i=1}^{n_i} \rho_i \times \left(P^{out} - P^{in}\right)}{\eta_{pump}}, \tag{97}$$

and $Power = \sum_{k=1}^{n_k} \sum_{i}^{n_i} \frac{F_i^k}{MW_i^k} \times T^k \times r \times \left(\frac{\gamma}{\gamma-1}\right) \times PR^{\left(\frac{\gamma}{\gamma-1}-1\right)} \times \frac{1}{\eta_{comp}} \times n_{comp}$, (98)

where ρ_i is the volumetric density of component i, P^{out} is the outlet pressure, P^{in} is the inlet pressure, η_{pump} is the pump efficiency, MW_i^k is

the molecular weight of component *i* in the stream *k*, *r* is the general gas constant, γ is the heat capacity ratio, η_{comp} is the compressor efficiency, n_{comp} is the number of stages in the compressor, and *PR* is the pressure ratio. *PR* can be determined by

$$(PR)^{n_{comp}} = \frac{P^{out}}{P^{in}}. \quad (99)$$

The inter-stage cooling load (kW) between the stages of a multi-stage compressor can be determined using Eq. (37).

5.2.2.3 Economic analysis constraints

The TEA model was formulated based on the strategy presented in **Section 2.2**.

5.2.2.4 Objective function

The objective functions chosen are maximization of the NPV, which is defined according to Eq. (24) as:

$$NPV = \sum_{n=0}^{20} \frac{NCF_n}{(1+r)^n}.$$

5.2.3 Optimization scenarios

Three optimization scenarios are investigated to design a sustainable biorefinery. This approach will enable to quickly compare strength and weakness of different processing configuration obtained in each scenario.

5.2.3.1 Scenario 1

The base case is an unrestricted scenario where no limit on TCI is set. In addition, carbon dioxide utilization alternatives are deactivated in this scenario. Therefore, according to this scenario, the result with a focus on the process economics and CEs of the biorefinery process by maximizing the NPV is obtained. The solution obtained from this scenario will act as a reference point for evaluating other scenarios in terms of economics and the environment issue.

5.2.3.2 Scenario 2

All binary variables denoting carbon utilization in the initial model and the scenario 1 are relaxed. Regarding carbon emission, it is important to mention that two sources of CEs from the biorefinery should be considered: direct and indirect emissions. The former originate explicitly from various process stages such as anaerobic digestion and degassing from open ponds. Indirect emissions, however, originate from the heat and power required to power-up the processing facilities. The objective here is to focus on direct emissions only. The goal of this scenario is to find optimal flowsheet that has better process economics and environmental performance than that achieved in the base case by maximizing the NPV.

5.2.3.3 Scenario 3

Owing to the integration of the carbon utilization processes, the TCI of the biorefinery may increase significantly. Therefore, in this scenario, further optimization based on limited funds is performed. Specifically, optimization is conducted for three scenarios: Cases A, B, and C, where the fund allocated to each scenario are 20%, 30%, and 40% of the base case TCI, respectively.

5.3 Results and discussion

The proposed process synthesis MINLP model was implemented in GAMS (25.0.2) and its solution was computed using DICOPT solver. The model contained 7,476 continuous variables, in which 1,680 variables are nonlinear, 22 variables are binary, and the remaining variables are linear, and 6,517 equality and inequality constraints. The chemical composition (wt.%) of the SJ species reported in **Table 5** was used in the present study. An upper limit of 400 kton/yr (dry basis) is set on the SJ supply. Three different optimization scenarios were investigated to gain greater insight into a macroalgae-based biorefinery.

5.3.1 Scenario 1 results

The optimal flowsheet of the base case is an integrated biorefinery producing both mixed acid and mixed alcohols. The optimal pathway is

given in **Figure 20**. It consists of anaerobic digestion, extraction followed by distillation, partial bypass and hydrogenation, venting carbon dioxide to the atmosphere, hydrogen purification via pressure swing adsorption, the distillation of mixed acid, the dehydration of mixed alcohols using molecular sieves followed by distillation, DDS purification, and wastewater treatment. In the integrated design, 30 wt.% of the concentrated VFAs are utilized to produce mixed acids, whereas the remaining VFAs are utilized to produce mixed alcohols. The NPV, TCI, and TCOM are 19.49 million USD, 147.74 million USD, and 98.02 million USD/yr, respectively.

The products obtained in this scenario are mixed alcohols, mixed acids, hydrogen, and DDS. Their production rates are given in **Table 17**. The biorefinery utilizes 400 kton/yr biomass. It produces 24 Mgal/yr mixed alcohols and 11 Mgal/yr mixed acids as main products and 0.98 kton/yr hydrogen and 111.8 kton/yr DDS as byproducts. The CEs of the base case are 64 kton/yr. The cost of venting carbon dioxide to the atmosphere is 1.2 million USD/yr.

5.3.2 Scenario 2 results

The optimal flowsheet obtained for this scenario is different from that for Scenario 1, as illustrated in **Figure 20**. The optimal pathway obtained

for mixed acids and mixed alcohols production is similar to that of the base case. Microalgae production was selected as the optimal pathway for carbon dioxide utilization. The optimal pathway of microalgae production includes cultivation in open ponds, harvesting by gravity settler, and dewatering by hollow filter membranes followed by centrifuge were selected as optimal technologies. The products obtained in this scenario are mixed acids, mixed alcohols, hydrogen, DDS, and microalgae. Their production rates are reported in **Table 17**. In this scenario, a 90% reduction in net CEs was achieved relative to the base case. Only 6 kton/yr of carbon dioxide is released to the environment. This surplus can accommodate the possible variation in efficiency; otherwise, the carbon dioxide utilization will be too optimistic. The cost of CEs to the environment is 0.12 million USD/yr, which is 90% lower than the carbon tax in Scenario 1. In terms of process economics, the NPV of this scenario is 2.23 times higher than in the base case. The TCI and COM are 215.34 million USD and 102.39 million USD/yr, respectively.

5.3.3 Scenario 3 results

As indicated in Scenario 2, the NPV and CEs are improved by 223% and 90%, respectively, compared to the base case. However, these improvements are achieved by investing 1.46 times more than the capital

investment in the base case. Therefore, it was of interest to investigate the effect of investment on the process economic and environmental performance of a sustainable biorefinery. As illustrated in **Figure 21**, reducing the TCI budget by 17.6% (Case A) of the TCI in Scenario 2 increases the CEs by 6.32 times, and reduces the NPV by 60%. As investment increases in the remaining cases, the process economics and environmental performance start improving. The carbon taxes in Cases A, B, and C are 0.76 million USD/yr, 0.51 million USD/yr, and 0.26 million USD/yr, respectively.

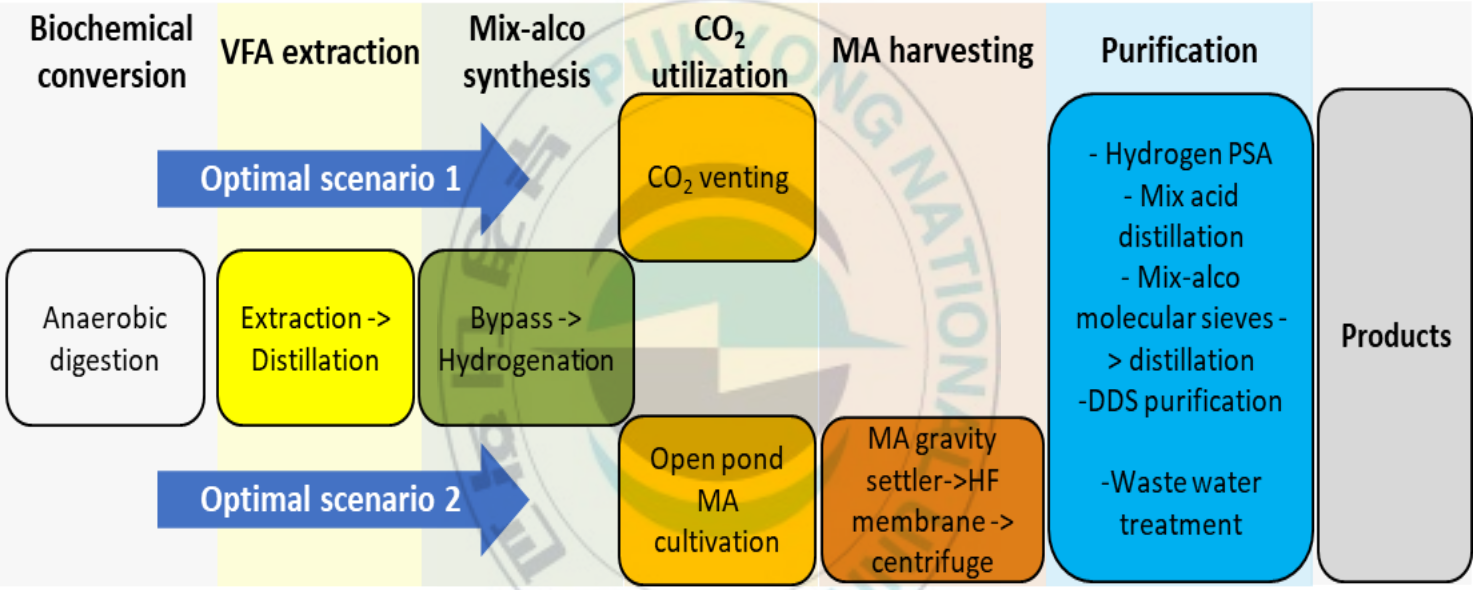

Figure 20. Optimal pathway for various scenarios.

Table 17. Mass balance summary of various scenarios for 400 kton/yr plant capacity.

Scenarios	Mixed alcohols (Mgal/yr)			Mixed acids (Mgal/yr)			Byproducts due to utilizing waste streams of biorefinery (kton/yr)		
	ETH	PRO	BUA	AA	PA	BA	MA	H_2	DDS
1	14.00	6.00	4.00	6.00	3.00	2.00	0.00	0.98	111.8
2	10.00	4.00	3.00	11.00	5.00	3.00	28.17	0.98	111.8

ETH = Ethanol; PRO = Propanol; BUA = Butanol; AA = Acetic acid; PA = Propanoic acid; BA = Butyric acid; MA = Microalgae; DDS = Dry distiller solids.

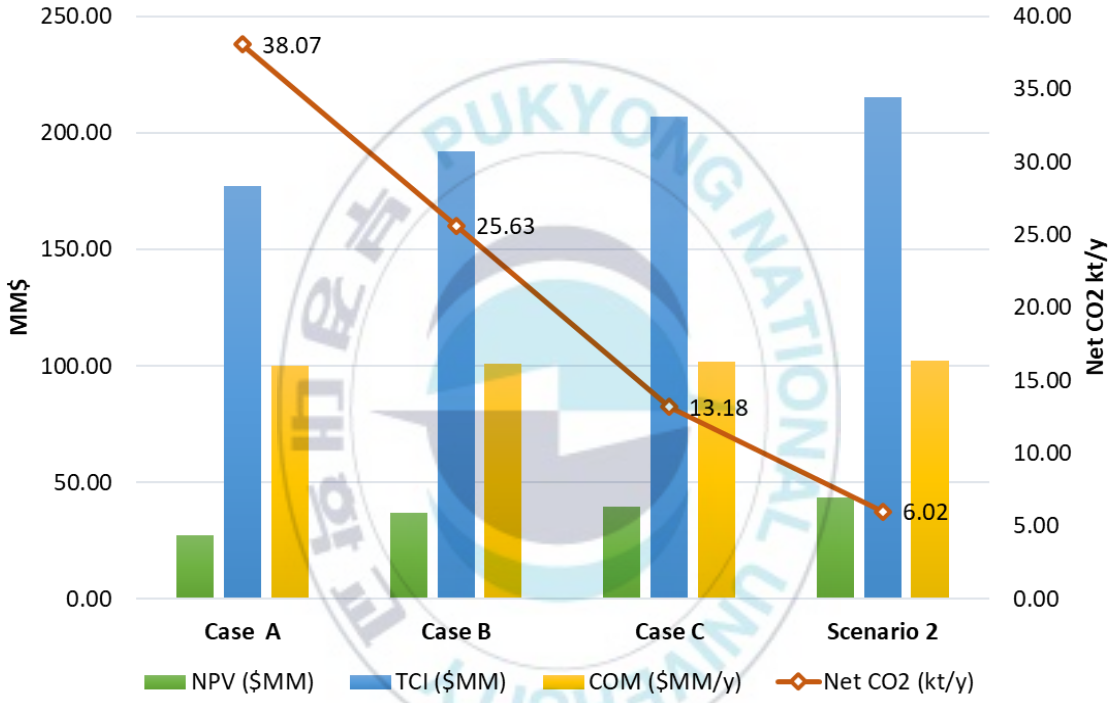

Figure 21. Effect of investment on process economics (bars) and environmental performance (line with markers).

5.3.4 Optimal design

When all previous scenarios are compared, it can be seen that Scenario 2 is the most expensive process design: 46% more expensive than the base case and 4% more expensive than Case C. Despite a capital-intensive process design, Scenario 2 offers a 2.23-times higher NPV than the base case and a 1.09-times higher NPV than Case C. Moreover, Scenario 2 utilizes 12% more CEs than Case C. Based on the improved performance, Scenario 2 was selected as the optimal design. The topology of the optimal design is shown in **Figure 22**. The overall product yield of anaerobic digestion was calculated to be 29%, which is 7% higher than the yield calculated by [155] via an SP.

The total capital cost was calculated to be 215 million USD. The VFA section consumes 69% of the TCI owing to the large volume of mixed alcohols and mixed acids produced, whereas the microalgae section consumes 31% of the TCI, and its cost depends on the carbon dioxide evolved from anaerobic digestion. The total installed cost breakdown of the integrated biorefinery is shown in **Figure 23A**. Wastewater treatment, cultivation of microalgae, and anaerobic digestion and DDS production are the most dominant areas in terms of investment, with a 73% cumulative contribution.

The TCOM of the optimal design is 102.39 million USD/yr. The VFA section accounts for 89% of the TCOM, whereas the microalgae section accounts for only 11%. Variable costs are one of the main contributors to the total manufacturing cost and are dominated by raw material costs. The raw material costs of the VFA and microalgae sections account for 53% and 22% of the TCOM, respectively. The seaweed purchasing cost alone accounts for 35% of the TCOM. Utility costs are the second dominant factor in the TCOM. The total utility cost of the biorefinery is 24.8 million USD/yr.

As already pointed out, the cost of seaweed is one of the biggest expenses and accounts for up to 35% to the TCOM. Therefore, the MSP at which the NPV becomes zero was also calculated. The results in **Table 18** indicate that the base case is more sensitive to changes in the price of seaweed. For example, if the seaweed price increases from 90 USD/t to 100 USD/t, the NPV of the base case decreases to zero. In contrast, the MSP for the optimal design is 112 USD/t for achieving zero NPV, which is 12% higher than that of the base case.

Table 18 shows that the MESP of the optimal design is 1.18 USD/gal, which is 23% lower than the base case and 35% lower than the current wholesale price (1.82 USD/gal) of ethanol. Moreover, the MESP obtained

from the VFAP is 9.4% lower than the MESP reported by [155] via SP. This demonstrates that the VFAP is superior to the SP.

5.3.5 Water consumption

The freshwater requirement is an important environmental factor in process sustainability. The results presented in **Table 19** highlight that the overall freshwater consumption of the VFA section is 6.26 gal of water/gal of alcohols and acids. Approximately 73% of the overall water makeup is due to water evaporation in the cooling tower.

The water loss during microalgae production is higher than that from the VFA section owing to the evaporation of water from the pond surfaces. The water evaporation alone accounts for 90 wt.% of the total water loss. The total water requirement for the microalgae section is 157.7 t/h.

Table 18. Minimum selling and maximum purchasing price of ethanol and seaweed.

	MESP (USD/gal)	MSP (USD/ton)
Scenario 1	1.54	100
Scenario 2 (Optimal design)	1.18	112
Scenario 3 (Case A)	1.42	104
Scenario 3 (Case B)	1.28	109
Scenario 3 (Case C)	1.24	110

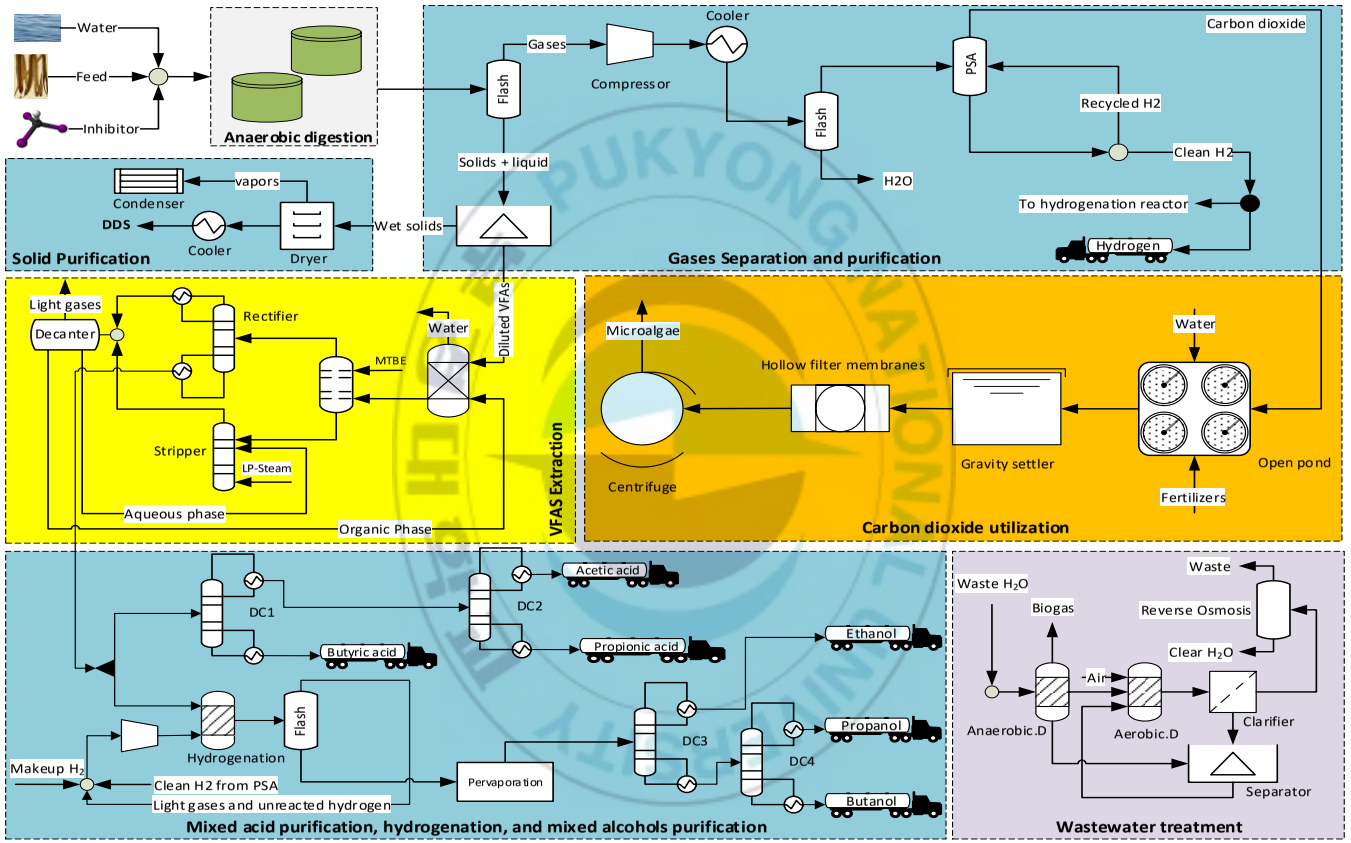

Figure 22. Optimal biorefinery structure.

Table 19. Makeup water requirement of biorefinery.

Sections	Makeup water (t/h)	Freshwater consumption (gal of A[a]/B[b])
VFA	103.7	6.26
Microalgae	157.7	9.52

a. A: water
b. B: mixed alcohols and acids

5.3.6 Sensitivity analysis

The optimization model also performs sensitivity analysis on 16 parameters of the biorefinery to evaluate the impact of key model parameters on the NPV. The investigated parameters are given in the tornado chart (**Figure 23B**) along with their limits and percentage variations.

The results indicate that fixed capital investment, the seaweed price, and the internal rate of return are the most important parameters for determining the economic viability of a biorefinery. As it is already indicated, 35% of the TCOM is due to the seaweed purchasing cost. When the seaweed purchasing price increases by 20%, the NPV decreases from 44 million USD to 9 million USD. Therefore, to ensure the economic viability of a seaweed-based biorefinery, efficient farming is necessary to increase the seaweed productivity. The selling prices of ethanol and microalgae are critical parameters for viable biofuel production.

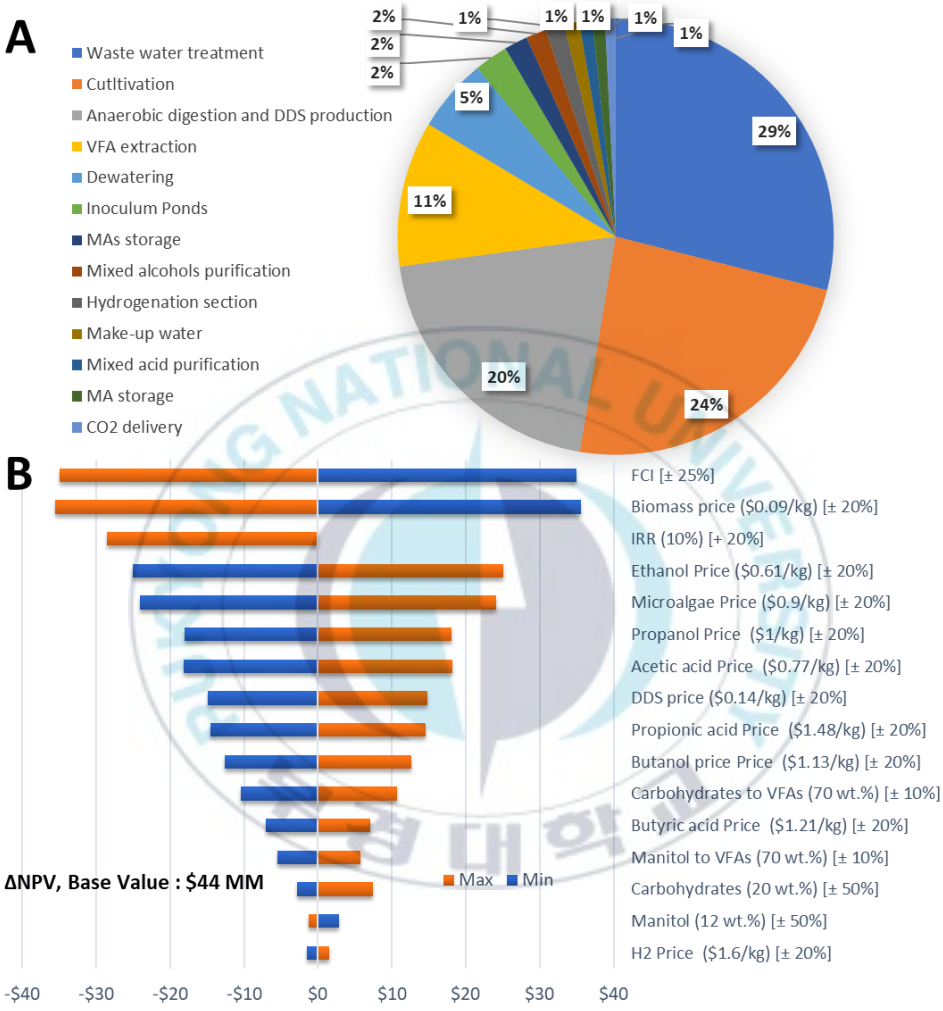

Figure 23. Total installed cost breakdown [A]; Sensitivity analysis of biorefinery parameters [B].

5.3.7 Potential improvements to plant economics

The results of the sensitivity analysis suggest several potential improvements to plant economics. It is important to note that some of the biorefinery parameters—such as the market prices of the products—are based on the geographical and political situation, and therefore cannot be controlled. However, parameters related to biorefinery processing can be tuned, thereby providing room for further improvements.

5.3.7.1 Seaweed price (Goal 1)

The sensitivity analysis demonstrated that the biomass purchasing price is a key factor for determining the economic feasibility of a biorefinery. The base case price of dry biomass (90 USD/t) includes the cost of macroalgae cultivation (80%) and transportation (20%) [102]. The latter accounts for 18 USD/t of the total biomass cost. In other words, the cost of transporting biomass from the seaweed farm to the biorefinery is equal to 7.2 million USD/yr. If the location of the biorefinery is properly optimized the transportation cost can be reduced significantly. A 25% reduction in the transportation cost of biomass owing to optimized biorefinery location corresponds to 84.5 USD/t of dry feed. The results presented in **Table 20** demonstrate that a 24.5% improvement in NPV can be achieved relative to the NPV of the optimal design.

5.3.7.2 Carbohydrates conversion (Goal 2)

Another important parameter of biorefinery processing is the conversion of carbohydrates to VFAs. In the present study, carbohydrates to VFAs conversion rate of 70 wt.% was assumed. Higher rates of carbohydrate conversion require the use of novel bioreactors such as multistage continuous high cell density reactors, in which the VFAs are extracted continuously with a solvent mixture. Once these targets are met and properly tuned, a marked improvement in the performance of up to 0.5 g VFA/g of seaweed can be expected, as reported by Chang et al. [156]. By assuming a 10% increase in carbohydrate conversion to VFA, and combining this with goal 1, a 48.7% improvement in the NPV can be achieved.

Table 20. Effect of different goals on NPV.

	Base case	**Goal 1**	**Goal 2**
NPV	44.25	55.11	65.80
% improvement in NPV	0	24.5	48.7

5.4 Conclusions

The optimal design for the SJ based biorefinery using the volatile fatty acid platform was determined using a superstructure-based approach. To determine the optimal design, a rigorous process synthesis mixed-integer non-linear model was developed that takes into accounts both process economics and the environmental impact. A techno-economic assessment indicated that the production of biofuels and value-added chemicals results in a minimum ethanol selling price of 1.18 USD/gal, which is 9.4% lower than the minimum ethanol selling price achieved through sugar platform. The NPV of the optimal design is 43 million USD for 20-year project life. An environmental assessment indicated that the optimal design is environmentally friendly process because it utilizes 90% of CEs produced by the biorefinery processing. The VFA section consumes approximately 6 gallons of water per gallon of mixed acids and mixed alcohols. A sensitivity analysis suggested a few goals that could improve the process economics of optimal design by up to 49%. Therefore, R&D on artificial seaweed cultivation is vital to increase the yield and lower the cultivation costs to make brown algae an economical and sustainable biomass resource for biofuels production. Furthermore, optimization of biorefinery location is crucial to decrease biomass transportation cost, and

development of low energy and capital cost processes coupled with novel digester design are important targets for the enhancement of the process economics.

6 PROCESS SYNTHESIS OF BIO-SUCCINIC ACID

This chapter presents a strategy of bio-succinic acid production through optimization of a superstructure that contains multiple biomass sources and technology alternatives as potential candidates of the optimal flowsheet. A MILP model was developed that performs optimization under deterministic and stochastic conditions. Besides, the optimization model also performs economic risk assessment and cradle-to-gate life cycle assessment.

The main reason of this chapter is to find best process design of bio-SA that can be integrated with standalone bio-refineries to improve their economics – as the market value of succinic acid is 2–3 times higher than that of ethanol. Besides, all three generations of biomass are studied to find optimal process design using the best feedstock.

The presented chapter is an extended version of the conference paper submitted to *ESCAPE-2020*, while the full-length article is in progress.

6.1 Introduction

SA is an important precursor for producing more than 30 commercially valuable products in pharmaceutical, food, and agriculture industries [157]. SA is largely produced from petroleum feedstock. However, technological advances in biorefinery have facilitated its production from renewable feedstock [158]. Bio-SA acid is reported by both the European Commission and the U.S. Department of Energy one of the top growing products within bio-based market, which is projected to reach 7–10 billion USD per year [123,159]. Despite its numerous applications and growing market, bio-SA production is still at its fancy and not economically lucrative compared with that from petroleum.

It has been estimated that bio-SA leads to greenhouse gas saving of 4.5–5 kg per kg of SA when compared to petrochemical-based SA [160]. However, bio-SA is not cost-competitive with its petrochemical rival, mainly due to its high production cost. Purification of SA from the fermentation broth is estimated to account 60–70% of the total production costs, while only 20–25% of the costs can be allocated to the upstream process including biomass pretreatment and fermentation process, and only 10–15% to the purchase of the feedstock itself [161]. Therefore, bio-SA can only be a viable replacement for petroleum-derived SA if upstream

and downstream technologies can lower the production cost by increasing the product yield and selectivity in former while lowering the purification cost in latter [159].

The necessity of major technological improvements to lower production cost makes the bio-SA process design, a complex combinatorial optimization problem. For instance, bio-SA can be produced from different feedstock including 1st (sugar/starch), 2nd (lignocellulose) and 3rd (aquatic biomass) generation [76,125,158,162,163]. Different feedstock sources require different pretreatments, which in turn decides the formation of fermentation process inhibitors. To achieve high yield and selectivity of SA, fermenter design and its operating condition, selection of appropriate microorganism and buffer are crucial decision variables that will decide the downstream purification [88,164]. The potential technological decision variables in bio-SA purification include: centrifugation or microfiltration for cell separation, evaporation, solvent extraction, activated carbon, ultrafiltration, precipitation, ion exchange, reactive extraction, bipolar membrane, electrodialysis, direct crystallization and nanofiltration for SA separation [88]. Combining all process alternatives from feedstock selection to downstream processing makes the bio-SA production process very complicated in order to find

best flowsheet for large-scale production taking into account technology readiness level of these various technologies. Therefore, the goal of this study is to provide clearer guidance based on multicriteria analysis (technical, economic, and environmental) about (1) what feedstock should be used to produce bio-SA? (2) what utilization strategy (processing route) should be used for specific feedstock to decrease the production cost of bio-SA? and (3) what is the impact of the processing on the environmental?

6.2 Methodology

To achieve research targets, a multi-stage framework shown in **Figure 3** and described in **Section 2** was used that systematically perform (1) deterministic optimization and analysis, (2) sensitivity analysis, and stochastic optimization and analysis, (3) economic risk assessment, and (4) environment assessment.

6.2.1 Problem statement

The scope of this study is to identify the best process for commercial-scale bio-SA production that has maximum economics as well as minimum investment, risk, and environmental impact in the given search space of processing alternatives. To solve this problem, we have selected a rigorous economic objective function i.e., NPV that should be maximized under deterministic and stochastic conditions. To evaluate environmental impact

at the early-stage design we have developed a model that performs cradle-to-gate analysis in order to evaluate the life cycle profile of different manufacturing configurations/topologies.

6.2.2 Superstructure development

This section will outline the key sections of the bio-SA biorefinery superstructure given in **Figure 24**. The novelty of the proposed process synthesis superstructure features a comprehensive network of 39 process alternatives with technology readiness level of 5–9 as the basis for optimal design identification. This is to ensure that the resulting solution from superstructure optimization is appealing from an implementation point of view. Ten major sections or processing intervals are included in the superstructure: feedstock, pretreatment, fermentation, cell mass removal, concentration pre-isolation, isolation, concentration post-isolation, color impurities removal, purification, and drying.

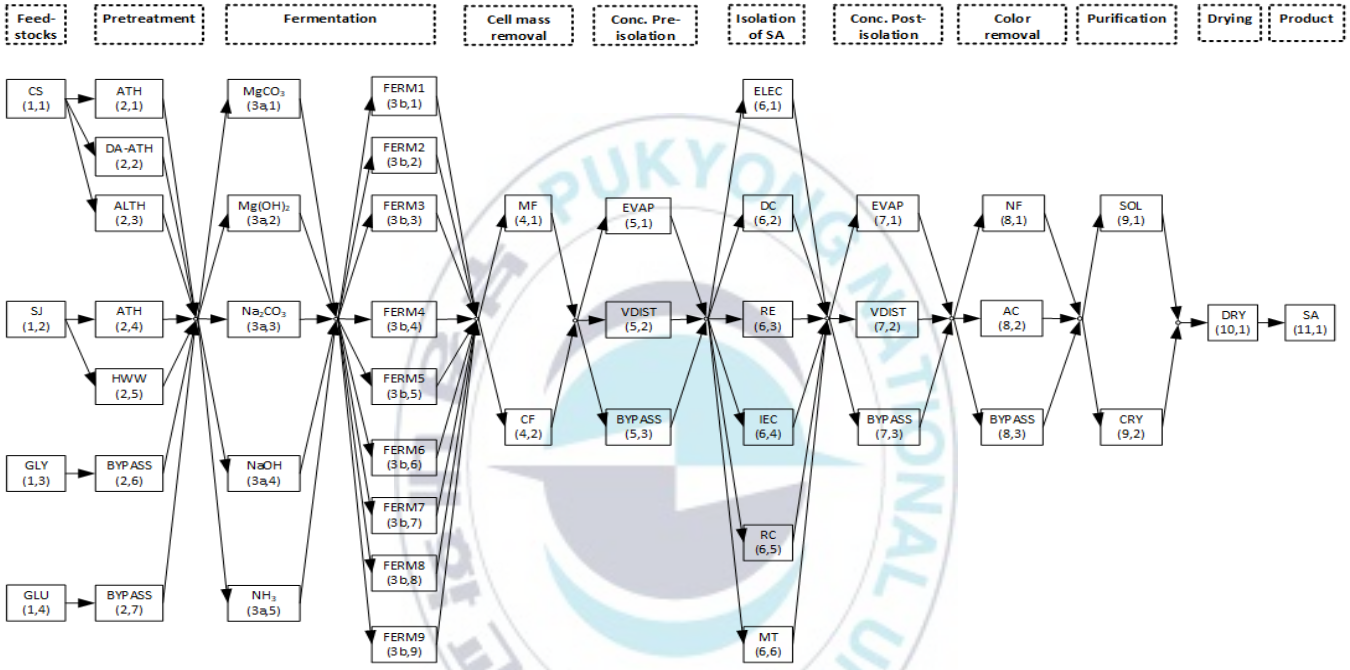

Nomenclature: CS = Corn Stover; SJ = *Saccharina japonica*; GLY = Glycerol; GLU = Glucose; ATH = Acid thermal hydrolysis; DA- ATH = Deacetylation followed by ATH; HWW = Hot water wash; ALTH = Alkaline thermal hydrolysis; FERM = Fermentation; MF = Microfiltration; CF = Centrifuge; EVAP = Evaporation; VDIST = Vacuum distillation; AC = Activated carbon; NF = Nanofiltration; ELEC = Electrodialysis; DC = Direct crystallization; RE = Reactive extraction; IEC = Ion exchange column (chromatography); RC = Reactive crystallization; MT = Membrane technology; SOL = Solvent; CRY = Crystallization; DRY = Dryer; SA = Succinic acid crystals

Figure 24. Biorefinery superstructure for production of bio-SA from multiple feedstock including corn stover, S. japonica, glycerol, and glucose.

As indicated in **Figure 24**, bio-SA can be produced using glucose, glycerol, corn stover, and SJ. It is assumed that glycerol is obtained from biodiesel industries, whereas glucose is obtained from sugar beet industries. The chemical composition reported by NREL [12] and in **Table 5** is used for corn stover and SJ, respectively. For effective utilization of biomass (corn stover and SJ) in fermentation, five pretreatment technologies are included in the superstructure: acid thermal hydrolysis of corn stover, deacetylation followed by acid thermal hydrolysis, alkaline (sodium hydroxide) hydrolysis, acid thermal hydrolysis of SJ, and hot water wash hydrolysis. The experimental data pertaining to pretreatment technologies are shown in **Table 21**. Note that glucose and glycerol are pure at refinery gates and do not require any pretreatment and therefore, they will bypass this processing interval as shown in **Figure 24**. Once the biomass is pretreated, it is processed using enzymatic hydrolysis in the presence of cellulase enzyme. The fermentation (production) of sugars can be carried out in batch or fed-batch fermenter in the presence of different microorganism and buffers. Nine fermentation technologies are included in the superstructure, which corresponds to different titer (g/l), yield (g/g), and productivity (g/l/h) of SA. The relevant operating data of fermentation technologies are given in **Table 22**. As indicated before the choice of a

buffering agent is very important regarding economics, therefore, five buffering agents including magnesium hydroxide, magnesium carbonate, sodium hydroxide, sodium carbonate, and ammonia are included in the superstructure. The choice of the appropriate buffer will be made based on the cost of a buffering agent and downstream purification technology cost. After fermentation, cell mass can be removed using microfiltration or centrifuge [76,165]. The broth can be then concentred either before or after isolation of SA using evaporation or vacuum distillation [88]. Isolation can be defined as recovering SA from its salt. Since isolation is energy-intensive, six processing alternatives namely electrodialysis [166], direct crystallization [167], reactive extraction [168], ion exchange column [169], reactive crystallization [170], and membrane technology (a combination of micro- and nano-filtration) [165] are included in the superstructure. The colour impurities and protein can be removed from the free acid (isolated) broth using activated carbon or nanofiltration [165], which is then purified using solvents, (such as methanol) or crystallization [87], and finally dried to remove moisture to desired purity.

Table 21. Summary of operating conditions and yields for various pretreatment technologies.

Processing conditions	P1		P2			P3		P4		P5	
	ATH	EH	DEA	ATH	EH	ALTH	EH	ATH	EH	HWW	EH
Solid loading (w/w%)	30	20	8	12	12	10	20	30	20	25	25
Residence time (mins)	5	84	120	10	84	10	120 (5 days)	15	84	20	48
Temperature ©	158	50	80	160	50	120	50	121	50	121	50
Catalysis loading	22.1[a]	20[b]	0.4[c]	8[a]	20[b]	55[a]	20[b]	18[a]	20[b]	0	20[b]
Glucose yield (%)	-	91	6.2	-	91	-	90	-	91	-	78.2
Xylose yield (%)	90	-	-	81	-	70	-	-	-	-	-
Mannitol yield (%)	-	-	-	-	-	-	-	95	-	78.2	-

P1-P5 = pretreatment; ATH = Acid thermal hydrolysis; EH = Enzymatic hydrolysis; DEA = Deacetylation; ALTH = Alkaline thermal hydrolysis

P1 and P4: acid thermal hydrolysis followed by enzymatic hydrolysis for corn stover [12,171] and *S.japonica* [15,125], respectively

P2: Deacetylation followed by acid thermal- and enzymatic – hydrolysis [172,173]

P3: Alkaline hydrolysis followed by enzymatic hydrolysis [174]

P5: Hot water wash followed by enzymatic hydrolysis [163]

[a]mg/g dry biomass; [b]mg/g cellulose; [c]w/w%

Table 22. Summary of operating conditions and yields for various fermentation technologies for corn stover (F1-F3), *S. japonica* (F4-F5), glucose (F6-F7), and glycerol (F8-F9).

No.	Strain name	Fermentation Type	Caron Source	Titer (g/L)	Yield (g/g)	Productivity (g/L/h)	Ref
F1	*A. succinogen*	SHF	Glu and Xyl	56.40	0.73	1.08	[1]
F2	*A. succinogen*	Batch	Glu and Xyl	42.80	0.74	0.30	[5]
F3	*A. succinogen*	SSF	Glu and Xyl	47.40	0.72	0.99	[9]
F4	*E. coli*	Dual Phase	Glu and Man	17.40	0.73	0.24	[3]
F5	*A. succinogen*	SHF	Glu and Man	33.78	0.63	0.70	[8]
F6	*E. coli*	Dual Phase	Glu	99.20	1.10	1.31	[10]
F7	*A. succinogen*	Batch	Glu	105.80	0.82	1.36	[11]
F8	*E. coli*	Fed-batch	Gly	66.78	1.24	0.93	[12]
F9	*A. succinogen*	Fed-batch	Gly	49.62	0.87	0.64	[13]

F1–F9: Fermentation 1–9; SHF: Separate hydrolysis and fermentation; SSF: Simultaneous hydrolysis and fermentation
Glu: Glucose; Xyl: Xylose; Man: Mannitol; Gly: Glycerol

6.2.3 Mathematical modeling of superstructure

The mathematical model of the superstructure represents large-scale MILP model that considers mass and energy balance constraints, capital and operating cost constraints, environmental constraints and an objective function. Note that energy balance equations and design constraints are non-convex that may cause difficulty in solution convergence and computation of a global optimal solution due to large combinatorial problem involving more than 125 binary decision variables. Therefore, separable programming and piecewise linearization are employed by approximating the initial mixed-integer non-linear programming problem into mixed-integer linear programming.

6.2.3.1 Mass balance constraints

The component mass flow rate of feedstock *b* in the stream *k* can be modelled as follows:

$$F_{b,i}^{k} = F_{b}^{k} \times x_{b,i}^{k}, \forall b \in B, \forall i \in I \forall, k \in K, \quad (100)$$

where $F_{b,i}^{k}$ is the mass flow rate of component *i* in the stream *k*, F_{b}^{k} is the overall mass flow rate in the stream *k*, and $x_{b,i}^{k}$ is the feedstock composition of component *i* in the stream *k*.

The overall mass balance of feedstock *b* in the stream *k* is given by:

$$F_{b}^{k} = \sum_{i} f_{b,i}^{k}, \forall b \in B, \forall k \in K. \quad (101)$$

The logical constraint to select feedstock *b* is modeled as:

$$F_b^k \leq \phi \times y1_b^k, \forall b \in B, \forall k \in K, \quad (102)$$

where ϕ represents upper bound for mass flow rate according to the big-M method and $y1_b^k$ represent binary variables to select feedstock *b*. These binary variables must select one optimal feedstock.

The logical constraint to select multiple feedstocks is modeled as:

$$\sum_b y1_b^k \leq 4, \forall b \in B, \forall k \in K. \quad (103)$$

Splitters are used for optimizing the topology of biorefinery by the selecting option *g* from stage *j*. The constraints pertaining to the splitters are given by:

$$\sum_{k1} F_{b,i,j}^{k1} - \sum_{k2} F_{b,i,j}^{k2} = 0, \forall b \in B, \forall i \in I, \forall j \in J, \quad (104)$$

and

$$F_{b,j}^{k2} \leq \phi \times y2_{b,j}^{k2}, \forall b \in B, \forall k2 \in K, \forall j \in J, \quad (105)$$

where $F_{b,i,j}^{k1}$ and $F_{b,i,j}^{k2}$ are the mass flow rate of component *i* in the inlet (*k1*) and the outlet (*k2)* stream of stage *j* when utilizing feedstock *b*, and $y2_{b,j}^{k2}$ are the binary variables for the selection of option *g* from stage *j*.

The constraint that enforces the selection of only one technology is given by:

$$\sum_b y2_{b,j}^k \leq 1, \forall k \in K, \forall j \in J. \quad (106)$$

Disjunctions are used for implementing a concentration step either before or after the isolation step as follow:

$$\sum_{k2=1}^{2} y2_{b,j1}^{k2} \leq 1, \forall b \in B, \forall j1 \in J, \quad (107)$$

where $y2_{b,j1}^{k2}$ are the binary variables pertaining to the outlet stream *k2 of* concertation stage *j1* in the superstructure.

To find a realistic processing pathway from the superstructure, logical constraints are used to ensure a feasible match of various processing stages. For instance, electrodialysis cannot deal with the divalent ions such as Mg^{+2} and Ca^{+2}, therefore, in fermentation, the feasible match should be monovalent buffer i.e., sodium hydroxide that will generate monovalent ion such as Na^{+1}. Likewise, the acidification of broth before electrodialysis would be an infeasible match. These logical conditions are modeled as:

$$\sum_{k2} y2_{b,j1}^{k2} - y2_{b,j2}^{k2} \leq 0, \forall b \in B, \forall j1 and\ j2 \in J, \quad (108)$$

where $y2_{b,j1}^{k2}$ and $y2_{b,j2}^{k2}$ are the binary variables corresponding to the outlet stream *k2* of stage *j1* and *j2*.

The mass balance equation for reactors and purification technologies such as the pretreatment, deacetylation, enzymatic hydrolysis, fermenter, conditioning vessel, acidification vessel, water splitting electrodialysis, reactive crystallization, and thermal cracker, where the reactant *r* is converted to the product *p* is given by

$$F_{b,p,j}^{k2} = F_{b,r,j}^{k1} \times \Phi_{b,p,r,j}^{k2} + F_{b,p,j}^{k1}, \forall b \in B, \forall k1 \,\&\, k2 \in K, \forall p \,\&\, r \in I \quad , \tag{109}$$

where $F_{b,p,j}^{k2}$ is the mass flow rate of product *p* in the outlet stream *k2* of stage *j* when utilizing feedstock *b*, $F_{b,r,j}^{k1}$ is the mass flow rate of reactant *r* in the inlet stream *k1* of stage *j* when utilizing feedstock *b*, $F_{b,p,j}^{k1}$ is the mass flow rate of product *p* in the inlet stream of stage *j* when utilizing feedstock *b*, and $\Phi_{b,p,r,j}^{k2}$ is the yield of product *p* from reactant *r* in the outlet stream *k* of stage *j* when utilizing feedstock *b*.

The mass balance constraint for the feedstock storage and handling, mixers, pumps, bypass, and heat exchangers are given by

$$F_{b,i}^{k2} = \sum_{k1=1}^{n_k} F_{b,i}^{k1}, \forall i \in I, \forall k2 \in K, \tag{110}$$

where $F_{b,i}^{k1}$ is the mass flow rate of component *i* in the inlet stream *k* when utilizing feedstock *b* and $F_{b,i}^{k2}$ is the mass flowrate of component *i* in the outlet stream *k2* when utilizing feedstock *b*.

The amount of solids at any stage *j* is controlled by

$$F_{b,i,j}^{k} \leq \alpha_{b,i,j}^{k} \times F_{b,j}^{k}, \forall b \in B, \forall k \in K, \forall i \in I, \forall j \in J, \tag{111}$$

and

$$F_{b,j}^{k} = \sum_{i=1}^{n_i} F_{b,i,j}^{k}, \forall b \in B, \forall k \in K, \forall j \in J, \tag{112}$$

where $F_{b,i,j}^{k}$, $F_{b,j}^{k}$, and $\alpha_{b,i,j}^{k}$ is the mass flow rate of component *i*-, the total mass flow rate-, and the mass fraction of component *i*- in the stream *k* of stage *j* when utilizing feedstock *b*, respectively.

The catalyst loading at any stage *j* is controlled by

$$F_{b,j}^{k} \leq \sum_{i'} F_{b,i,j}^{k} \times \beta_{b,j}^{k}, \forall k \in K, \forall j \in J, \quad (113)$$

where $\beta_{b,j}^{k}$ is the catalyst loading per kg of incoming feed in the stream *k* of stage *j* when utilizing feedstock *b*.

The mass balance of component *i* in the outlet key-stream *k* in the separator, washer, microfiltration, belt filter press, centrifuge, nanofiltration, evaporation, distillation, activated carbon column, reactive extraction, back extraction, electrodialysis, crystallization, ion exchange column, solvent purification, flash column, and dryer is given by

$$F_{b,i,j}^{k2} = F_{b,i,j}^{k1} \times \zeta_{b,i,j}^{k2}, \forall b \in B, \forall k1 \; and \; k2 \in K, \forall i \in I, \forall j \in J, \quad (114)$$

and $$F_{b,i,j}^{k1} = F_{b,i,j}^{k1} \times \left(1 - \zeta_{b,i,j}^{k2}\right), \forall b \in B, \forall k1 \in K, \forall i \in I, \forall j \in J, \quad (115)$$

where $\zeta_{b,i,j}^{k2}$ represents the recovery of component *i* in the outlet stream *k* when utilizing feedstock *b*, $F_{b,i,j}^{k1}$ is the mass flowrate of component *i* in the inlet stream *k* when utilizing feedstock *b* and $F_{b,i,j}^{k2}$ is the mass flowrate of component *i* in the outlet stream *k2* when utilizing feedstock *b*.

The feedstock purchase is bounded by its availability (Θ) and the minimum purchase amount (Y):

$$\Theta \geq Feed \geq Y. \tag{116}$$

6.2.3.2 Energy balance constraints

The power ($P_{b,j1}$) consumed during the processing of feedstock b in stage $j1$ is given by

$$P_{b,j1} = \sum_{k1} F_b^{k1} \times \emptyset_{j1}, \forall b \in B, \forall j1 \in J, \tag{117}$$

where $\emptyset_{j1}$ is the power required per kg of feed rate in stage $j1$.

The power consumed during the processing of feedstock b in desalting electrodialysis ($P_{b,DED}$) and water splitting electrodialysis ($P_{b,WSED}$) is given by

$$P_{b,DED} = \sum_{k1} F_{b,i}^{k1} \times \emptyset_{DED}, \forall b \in B, \forall i1 \in I, \tag{118}$$

and

$$P_{b,WSED} = \sum_{k1} F_{b,i}^{k1} \times \emptyset_{WSED}, \forall b \in B, \forall i1 \in I, \tag{119}$$

where $\emptyset_{DED}$ and $\emptyset_{WSED}$ are power required per kg of sodium succinate in desalting electrodialysis and water splitting electrodialysis, which is ~3.5 and ~2.5 kWh per kg of sodium succinate, respectively [161].

The power consumed during the processing of feedstock b in crystallizer ($P_{b,CRYS}$) is given by

$$V_{b,CRYS} = \sum_{(k1,i)} \frac{F_{b,i}^{k1}}{\rho_{b,i}^{k1}} \times \tau_{CRYS}, \forall b \in B, \tag{120}$$

and $$P_{b,CRYS} = V_{b,CRYS} \times \emptyset_{CRYS}, \forall b \in B, \quad (121)$$

where $V_{b,CRYS}$ is the volume of crystallizer in m^3, $\rho_{b,i}^{k1}$ is the density of component *i* in the inlet stream *k1*, τ_{CRYS} residence time (1200 s), and $\emptyset_{CRYS}$is the power required in a crystallizer, which is 2 kW per m^3 [76].

The power consumed during the processing of feedstock *b* in filtration ($P_{b,FIL}$) is given by

$$A_{b,FIL} = \frac{\sum_{(k1,i)} \frac{F_{b,i}^{k1}}{\rho_{b,i}^{k1}}}{\psi_{FIL}}, \forall b \in B, \quad (122)$$

and $$P_{b,FIL} = A_{b,FIL} \times \emptyset_{FIL}, \forall b \in B, \quad (123)$$

where $A_{b,FIL}$ is the area of rotary vacuum filter in m^2, ψ_{FIL} is flux, which is 400 $L.m^{-2}.h^{-1}$, and $\emptyset_{FIL}$is the power required (0.8 kW per m^2) in crystallizer [76].

The energy ($E_{b,j1}$) required in kWh per m^2 during the processing of feedstock *b* is determined by a relation proposed by[175] and as follows:

$$E_{b,j1} = \frac{\beta_{j1}}{(\psi_{j1} \times \eta_{j1})}, \forall b \in B, \forall j1 \in J, \quad (124)$$

where *J = {Microfiltration, Nanofiltration}*, β_{j1} is the energy required at the membrane surface, which is 50 W per m^2, ψ_{j1} is membrane flux, which is 20 $L.m^{-2}.h^{-1}$ for microfiltration and 50 $L.m^{-2}.h^{-1}$ for nanofiltration, and η_{j1} is membrane efficiency (50%).

Once the energy required is calculated then the power consumption ($P_{b,j2}$) in the membrane can be calculated as follows:

$$A_{b,j1} = \frac{\sum_{(k1,i)} \frac{F_{b,i}^{k1}}{\rho_{b,i}^{k1}}}{\psi_{j1}}, \forall b \in B, \forall, \forall i \in I, \forall j1 \in J, \quad (125)$$

and $$P_{b,j2} = A_{b,j1} \times E_{b,j1}, \forall b \in B, \forall j1 \in J, \quad (126)$$

where $A_{b,j1}$ is an area of micro- and nano-filtration in m^2.

The power ($P_{b,pump}$) consumed in the pump can be calculated as:

$$P_{b,pump} = \frac{\sum_{i=1}^{n_i} \rho_{b,i} \times \left(P_b^{k2} - P_b^{k1}\right)}{\eta_{pump}}, \quad (127)$$

where $\rho_{b,i}$ is the volumetric density of component *i*, P_b^{k2} is the outlet pressure, $P_b^{k1}$is the inlet pressure, η_{pump} is the pump efficiency.

For each unit operation involved in the processing of feedstock *b*, the following energy balance constraint was used:

$\sum_{i=1}^{n_i} F_{b,i,j}^{k1}.cp_{b,i,j}^{k1}.T_{b,j}^{k1} + Q_{b,j} = \sum_{i=1}^{n_i} F_{b,i,j}^{k2}.cp_{b,i,j}^{k2}.T_{b,j}^{k2}, \forall b \in B, \forall j \in J, \forall k1 \; and \; k2 \in K,$ (128)

where $Q_{b,j}$ is the heat duty of stage *j*, $cp_{b,i,j}^{k1}$and $cp_{b,i,j}^{k2}$ are the specific heat of component *i* at the inlet (*k1*) and outlet (*k2*) conditions of stage *j* respectively. $T_{b,j}^{k1}$ and $T_{b,j}^{k2}$are the temperature of inlet and outlet conditions of stage *j*.

Heat balance in the reboiler is determined by a relation proposed by [46] and rearranged as:

$$Q_{b,j1} = (1 + R) \sum_{i=1}^{n_i} f_{b,i}^{btm} \lambda_i. \quad (129)$$

The cooling heat load needed for the condenser is given by:

$$Q_{b,j1} = -(1 + R) \sum_{i=1}^{n_i} f_{b,i}^{dis} \lambda_i, \quad (130)$$

where $f_{b,i}^{dis}$ and $f_{b,i}^{btm}$ are component molar flow rate in distillate and bottom, respectively, and λ_i is the latent heat component i.

6.2.3.3 Economic analysis constraints

The TEA model was formulated based on the strategy presented in **Section 2.2**.

6.2.3.4 Environmental analysis constraints

An environmental assessment model was developed to calculate the life cycle profile of bio-SA acid production. The scope of analysis is cradle-to-gate that consider environmental impact caused by four categories: raw material extraction and transportation to biorefinery ($\delta 1_{b,e}$), chemicals used in different stages of processing/biorefinery ($\delta 2_{b,i,e}$), heat and power consumption in biorefinery $\delta 3_{b,l,e}$, and byproducts and waste released to the environment $\delta 4_{b,m,e}$. These categories are quantified using Eqs. (131-134), respectively.

$$\delta 1_{b,e} = \frac{F_b^k \times \gamma 1_{b,e}}{Pc}, \forall b \in B, \forall e \in E, \quad (131)$$

$$\delta 2_{b,i,e} = \frac{F_{b,i}^k \times \gamma 2_{b,i,e}}{Pc}, \forall b \in B, \forall i \in I, \forall e \in E, \quad (132)$$

$$\delta 3_{b,l,e} = \frac{U_l \times \gamma 3_{b,l,e}}{Pc}, \forall b \in B, \forall l \in L, \forall e \in E, \quad (133)$$

and $$\delta 4_{b,m,e} = \frac{F_{b,i}^k \times \gamma 4_{b,m,e}}{Pc}, \ \forall b \in B, \forall m \in M, \forall e \in E, \quad (134)$$

where $\gamma 1_{b,e}, \gamma 2_{b,i,e}, \gamma 3_{b,l,e}, \gamma 4_{b,m,e}$ are the characterization factors or inventory data to describe the environmental influence of each impact category e caused by the aforementioned categories ($\delta 1_{b,e}, \delta 2_{b,i,e}, \delta 3_{b,l,e}$, and $\delta 4_{b,m,e}$).

The total impact category $\delta_{b,e}$ is determined as follows:

$$\delta_{b,e} = \delta 1_{b,e} + \delta 2_{b,e} + \sum_l \delta 3_{b,l,e} + \sum_m \delta 4_{b,m,e}. \quad (135)$$

The inventory data or characterization factors required to perform life cycle assessment was taken from SimaPro V8.2.3 software using CML-IA baseline V3.03 characterization method. Eleven environmental indicators described in **Section 2.3** are considered in the present model. One kg product (bio-SA) was considered as a functional unit to compare the life cycle profile of different biorefinery configuration.

6.3 Results and discussion

6.3.1 Deterministic analysis

6.3.1.1 Optimal feedstock and its processing route

The optimal feedstock and its processing route to produce bio-SA is investigated by maximizing the NPV with the nominal parameters reported in **Table 23** and **Table 24**. Note that all uncertainties in the parameters are disregarded here. The summary of process indicators including NPV, TCI, TCOM, and MPSP are presented in **Figure 25A**, while the total capital cost breakdown is presented in **Figure 25B**. Results in **Figure 25A** indicate that utilizing glycerol via the processing pathway presented in **Figure 26A** leads to the highest NPV of 50 million USD compared to processing pathways of all remaining feedstock for a plant scale of 15,000 t/y and 20 years of project life. The optimal upstream processing route encompasses a fed-batch fermenter using *E. coli* and sodium hydroxide as a bacterial strain and buffer, respectively. The optimal downstream processing route consists of microfiltration, nanofiltration, vacuum distillation, crystallization, and drying to produce high-grade SA of 99.2 wt% purity. The total investment cost of the biorefinery is 43 million USD, where 71% of the TCI corresponds to fermentation and 29% to purification, as shown in **Figure 25A** and **Figure 25B**, respectively. The

main reason for high upstream investment is found to be the utilization of large volume fermenters up to 2600 m^3 due to the long fermentation time of 72 hours. Therefore, efficient strains are crucial to decrease the fermentation time in order to decrease capital investment. The minimum product selling price is calculated to be 2.07 USD/kg.

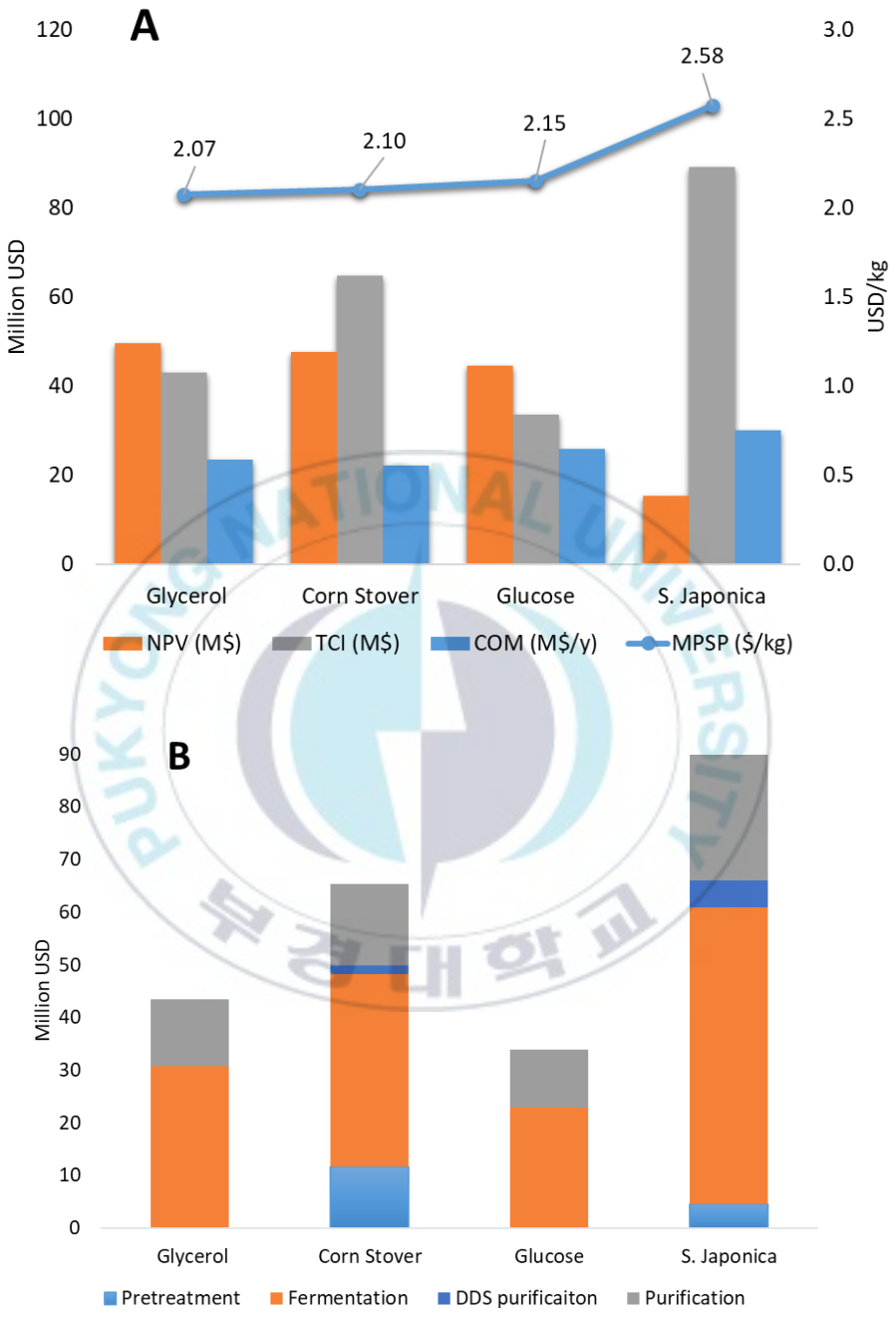

Figure 25. Process economic indicators of optimal topologies [A]. Total capital investment breakdown of optimal topologies [B].

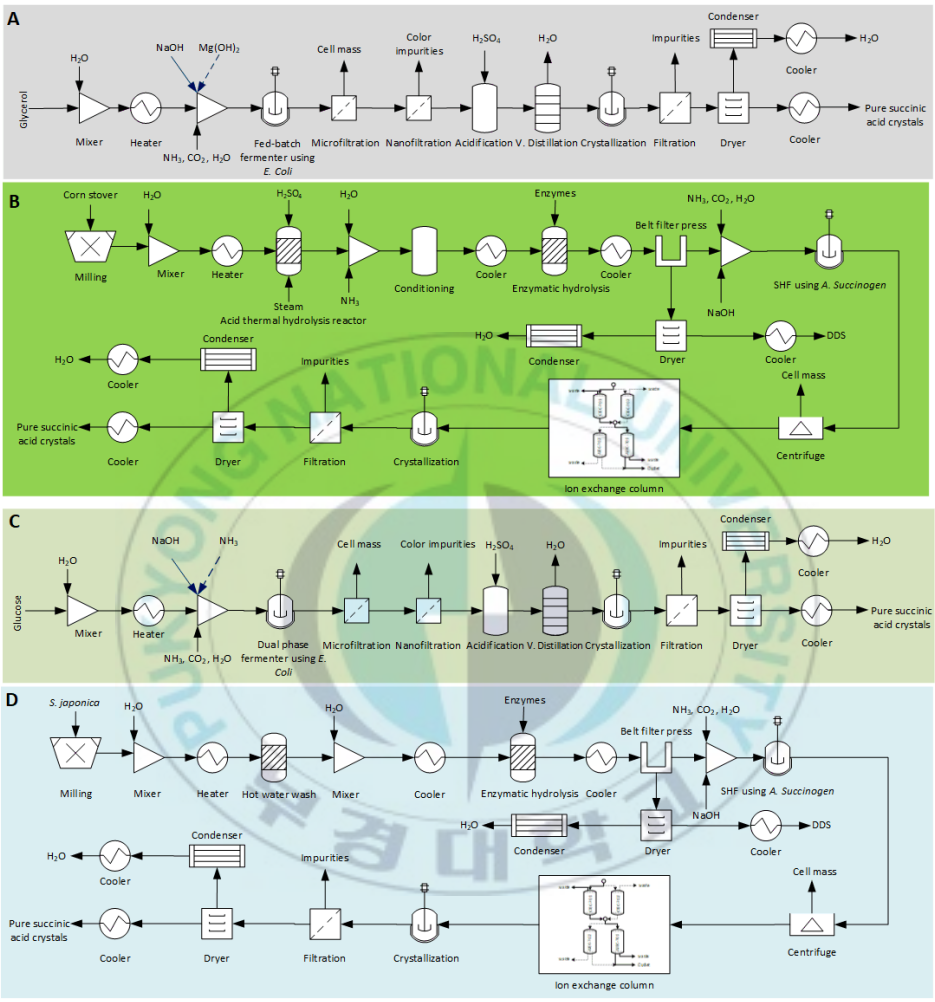

Figure 26. Optimal processing pathway for glycerol (A), corn stover (B), glucose (C), and S. japonica (D) through deterministic optimization (dark blue solid arrows) and stochastic optimization (dark blue dashed arrows). Black solid lines are common unit operations in both deterministic and stochastic optimization.

6.3.2 Comparison of optimal feedstock and its processing route with suboptimal solutions

An integer cut algorithm (Eq. 18) is used to find suboptimal topologies [72]. Corn stover is found the second-, glucose is third-, and SJ is the least-optimal feedstock to produce bio-SA via the processing pathway presented in **Figure 26B–5D** that leads to an NPV value of 47.6, 44.4, 15.29 million USD, respectively. The optimal processing route of corn stover consists of acid thermal hydrolysis, separate hydrolysis and fermentation using *A. succinogenes* and sodium hydroxide buffer, centrifuge, ion exchange column, crystallization and drying. As in the processing pathway of glycerol, bio-SA production from glucose does not require pretreatment. Indeed, its upstream processing pathway consists of dual-phase fermentation using *E. coli* and sodium hydroxide as a bacterial strain and buffer, respectively. The downstream processing pathway is similar to that of glycerol. For SJ, the hot water wash was found to be the optimal pretreatment technology compared to acid thermal hydrolysis in the case of corn stover. Regarding the optimal topology of SJ, the fermenter type, bacterial strain, buffer, and downstream processing pathway is similar to that of corn stover.

Overall economic results shown in **Figure 25** indicate large variability in bio-SA selling price from 2.07–2.58 USD/kg. Likewise, the total cost of investment varies between 34–89 million USD, being lowest for the glucose processing pathway and highest for the SJ processing pathway. The total capital cost breakdown shows that in the processing pathway of all feedstock, fermentation and purification are the most expensive process areas with 56–70% and 23–32% contributions to the total capital cost, respectively.

6.3.3 Sensitivity analysis

A single-point sensitivity analysis was performed on the optimal topologies mentioned in **Figure 26** in order to evaluate the most critical parameters on the NPV. The variables evaluated include the cost of feed, price of the product, utility cost, TCI, income tax rate, and plant capacity, while the variation i.e., maxima and minima pertaining to these variables are reported in **Table 23** and **Table 24**. Results in **Figure 27** indicate that optimal topologies of different feedstock have different critical parameters that affect the process economics. Except for the feedstock cost, glucose topology was found to be the least sensitive to uncertainties compared to topologies of other raw materials. Product price, total capital investment, and feedstock cost are the most influential parameters to NPV in all cases.

In all topologies, the bio-SA selling price was found to be one of the most dominant parameters for the economic viability of the process. Likewise, increasing plant capacity was found economically favorable for all processing pathways. Feedstock cost was found to be a very crucial parameter for all processing pathways, most sensitive in processing pathway of glucose that can increase NPV up to 30 million USD when glucose cost is at 0.58 USD/kg or can decrease NPV to 15 million USD when glucose cost is 15% more than the current market price of 0.99 USD/kg. The above-mentioned sources of uncertainty indicate that recommending an optimal feedstock and its processing route based on deterministic condition alone is not reliable. It is quite possible that the deterministic optimal pathways only perform well under the nominal scenarios and is not a robust solution when the uncertainties are present. Thus, in this study, the above-mentioned sources of uncertainty are taken into account and analyzed further to find optimal feedstock and its processing pathway under uncertainty.

Table 23. Uncertainties in chemical prices based on historical prices. Uncertainties presented in color cells applicable to both single-point sensitive analysis and stochastic analysis.

Chemicals	**Min**	**Max**	Chemicals	**Min**	**Max**
Corn Stover	31.3%	37.5%	Steam	19.6%	8.8%
S. Japonica	0.0%	50.0%	Acid	15.0%	16.2%
Glucose	41.3%	15.0%	H3PO4	48.1%	7.1%
Glycerol	20.0%	15.0%	DDS	40.0%	57.1%
Succinic acid	20.0%	20.0%	CO_2	15.0%	15.0%
Trioctylamine	15.0%	15.0%	NH_3	58.7%	54.7%
Trimethylamine	15.0%	15.0%	Enzymes	15.0%	15.0%
Ammonium bisulphate	36.5%	15.4%	Methanol	48.4%	0.0%

Note that ±15 variation is assumed for chemicals that don't have historical cost data available in literature. The variation of chemical prices is around mean value which is reported in **Table 3**.

Table 24. Uncertainties in the process economic and environmental indicators [12,34,74,176]. Uncertainties presented in color cells applicable to both single-point sensitive analysis and stochastic analysis.

	Min	**Max**
Equipment costs	20%	50%
Utility costs	20%	20%
Environmental parameters	20%	20%
Plant capacity	20%	20%
Discount rate	20%	20%
Income tax rate	20%	20%
Yield in reactors[a]	10%	10%
Efficiency in purification technology[b]	10%	10%

[a]Reactors = Acid thermal hydrolysis, deacetylation followed by acid thermal hydrolysis, alkaline pretreatment, hot water wash, enzymatic hydrolysis, fermentation 1–9

[b]Purification = Electrodialysis, direct crystallization, reactive extraction, ion exchange column, reactive crystallization and membrane technology

The variation of indicators is around mean value which is reported in **Table 2** and **Table 4**.

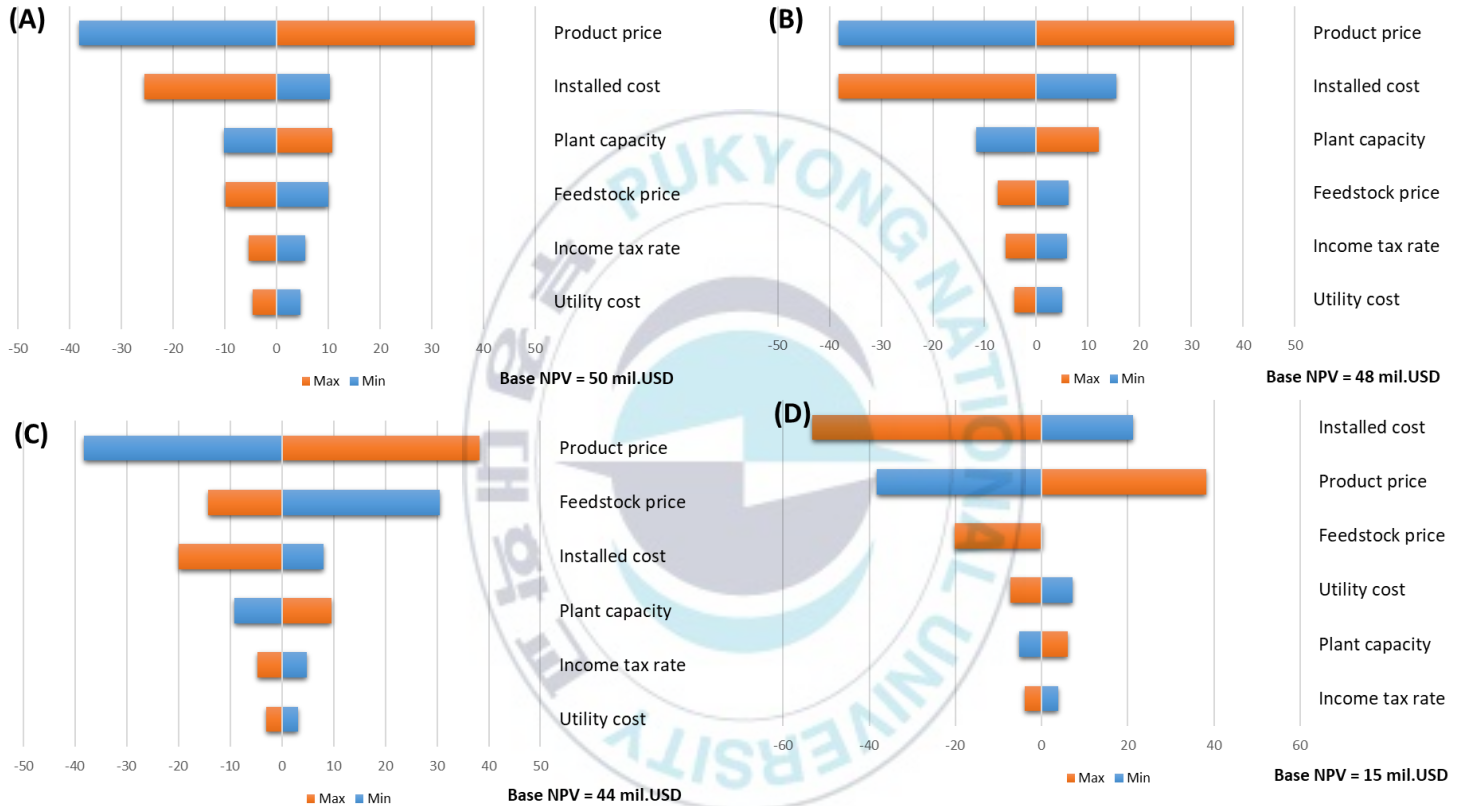

Figure 27. Singles point sensitivity analysis on net present value for bio-succinic acid production from glycerol (A), corn stover (B), glucose (C), and S. japonica (D).

6.3.4 Stochastic optimization

Robust (stochastic) optimization was performed to determine the most promising feedstock and its processing pathway. The main objective here is to determine the processing pathway that maximally remains economically viable compared to all other processing pathways under uncertain conditions. Therefore, the most influential sources of uncertainties determined by the single-point sensitivity analysis are now characterized using a uniform distribution function. In addition, parameters related to life cycle assessment, and yields in pretreatment, enzymatic hydrolysis, fermentation, and purification are taken into account to calculate process indicators and risk assessment under uncertainty. Therefore, for further analysis, the scenario to be analyzed was set-up based on historical cost data on the raw materials and uncertainty range suggested in literature for process indicators. The data regarding the range of uncertain parameters are given in **Table 23** and **Table 24**.

6.3.5 Optimal feedstock and processing route under uncertainty

In order to identify an optimal feedstock and its processing route under uncertainty, 500 scenarios were generated, and the results are mapped and statistically analyzed. The frequency of selection of glucose, glycerol, and corn stover are 235/500 (47.0%), 145/500 (29.0%), and 120/500 (24.0%),

respectively, which makes the glucose 1st in the ranking, followed by glycerol and corn stover. It can be seen that the results of the feedstock-ranking from robust optimization are different than those from deterministic optimization, which indicate that the uncertainty in the dataset indeed has a large impact on the selection of optimal feedstock. SJ is not selected a single time in 500 scenarios which indicate that at the current technology level of efficiency and feedstock cost, the production of bio-SA is not economically viable from it.

Regarding the topologies of the selected feedstock, 37 unique pathways are found as shown in **Figure 28**; 11 for glucose, 10 for glycerol, and 16 for corn stover. Here, only the highest frequency pathway can be considered as a robust optimal processing pathway for further analysis. Results presented in **Figure 28** show that the highest frequency processing pathway for glucose, glycerol, and corn stover are similar to their deterministic pathway except for the glucose where different buffering agent i.e., ammonia instead of sodium hydroxide is selected. The similarities of stochastic based biorefinery structures to the one achieved in the deterministic optimization indicate the robustness of deterministic based processing pathways. Even though SJ is not selected even a single time in 500 scenarios, however, to present a rigorous comparative analysis

between all feedstock and their processing pathways, an optimal processing route of SJ obtained from deterministic calculation was also included in further calculations.

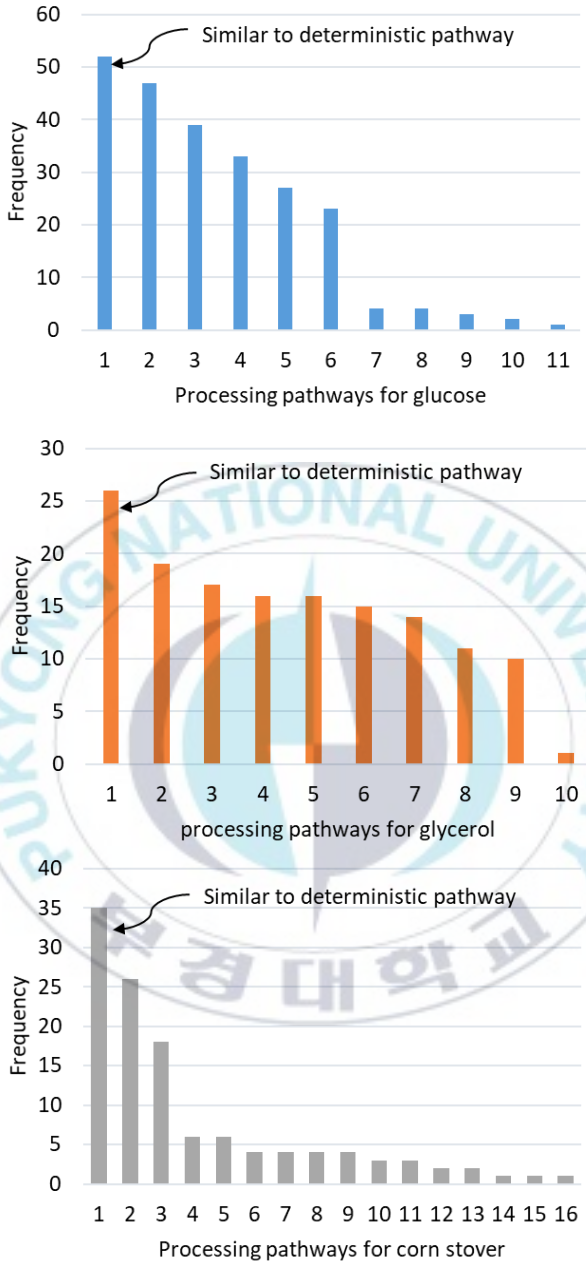

Figure 28. Frequency of selection of pathways for glucose, glycerol, and corn stover using stochastic optimization for 500 scenarios.

6.3.6 Process indicators distribution

The highest frequency optimal topologies shown in **Figure 28** i.e. pathway 1 for glucose, glycerol, and corn stover as well as a deterministic optimal pathway for SJ presented in **Figure 26D** are further analyzed to evaluate the distribution of process indicators under uncertainty. Here the binary variables corresponding to the aforementioned optimal pathways of all feedstock are fixed and the optimization problem is solved for 1000 times using Monte Carlo simulation for all uncertain parameters listed in **Table 23** and **Table 24** to evaluate the distribution of process indicators.

Results in **Figure 29A–B** indicate that SA production from glucose and glycerol have comparable NPV and MPSP, 37.74 million USD and 2.26 USD/kg in former and 34.50 million USD and 2.31 USD/kg in later, respectively. However, variations in NPV and MPSP of glucose-based SA is slightly higher than glycerol-based SA, which is according to the results of single-point sensitivity analysis where glucose is found most sensitive to feedstock cost. Despite the comparable process economic indicators and aforementioned variations, SA production from glucose through pathway 1 is still much more promising due to the fact that TCI required is 31% lower compared to SA production from glycerol through pathway 1. This indicates that the rate of return on investment is much higher in glucose-

based biorefinery, which is a very important economic parameter from the perspective of investors. A significant change in NPV and MPSP are observed in processing pathway of corn stover in which 30% decrease and 7% increase in former was observed compared to glucose-based SA. SJ has the worst process economics with a negative NPV that corresponds to the average of -20.26 million USD and MPSP of 3.10 USD/kg, which is 154% lower and 37% higher than that of pathway 1 for glucose, respectively.

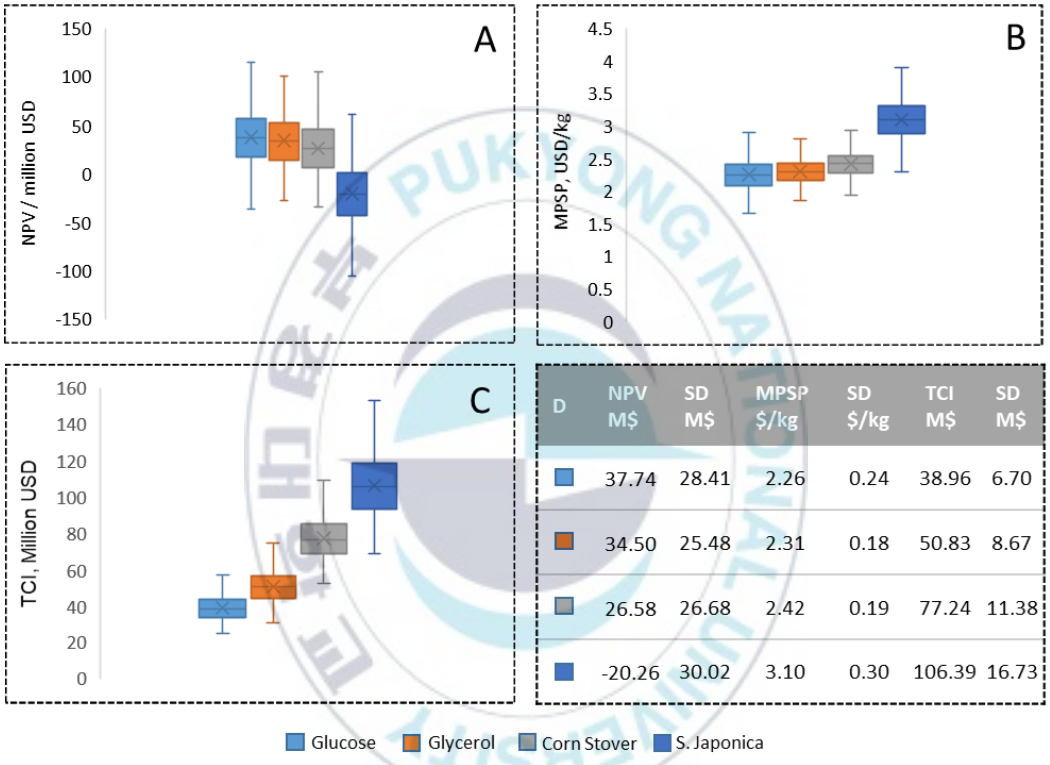

D	NPV M$	SD M$	MPSP $/kg	SD $/kg	TCI M$	SD M$
	37.74	28.41	2.26	0.24	38.96	6.70
	34.50	25.48	2.31	0.18	50.83	8.67
	26.58	26.68	2.42	0.19	77.24	11.38
	-20.26	30.02	3.10	0.30	106.39	16.73

Figure 29. Net present value range (A), minimum product selling price range (B), total capital investment range (C), and summary of average economic results with one-standard deviation (SD) for optimal topologies of all feedstock (D).

6.3.7 Risk assessment

Risk is evaluated based on the MPSP by comparing the current market selling price of petro-chemical based SA with the bio-based SA. In this study, the risk is defined as the probability at which the manufacturing process produces bio-SA at a price higher than the target petro-chemical based SA price. To evaluate the risk, we assumed that the petro-chemical based SA price lies between 1.6–2.0 USD/kg. Results in **Figure 30** show that the bio-SA production through pathway 1 of glucose is potentially the best investment alternative since it has lower risk. The risk associated with bio-SA production via the optimal processing pathway of glucose, glycerol, corn stover and SJ at the market selling price of 2 USD/kg is 85%, 97%, 99%, and 100%, respectively. It was of interest to calculate the market selling price of bio-SA at which the probability of risk becomes 100% for all optimal topologies. The results indicate that the selling price of bio-SA at 1.65 USD/kg for glucose, 1.85 USD/kg for glycerol, 1.87 USD/kg for corn stover, and 2.30 USD/kg for SJ leads to 100% of the risk.

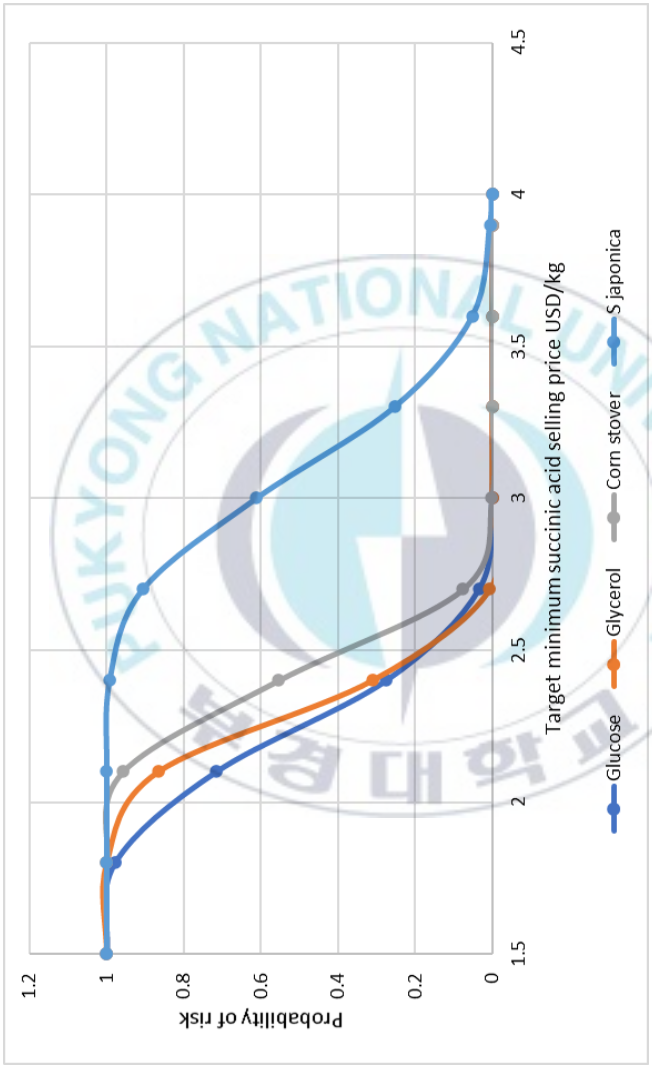

Figure 30. Cumulative density distribution for the minimum product selling price.

6.3.8 Environmental assessment

The overall environmental assessment results shown in **Figure 31** indicate that bio-SA production from the processing pathway of glucose is the most environment-friendly option compared to the processing pathways of glycerol > corn stover > and SJ. The main reason of better life cycle profile for the processing pathway of glucose is found to be high yield and titer, which decrease both upstream and downstream size (capacity) as well as process energy and chemical requirement compared to other processing pathways. SJ is the worst environmental scenario due to the large consumption of feedstock, which increases the size of biorefinery, utility and chemical consumption in both upstream and downstream. In addition, the necessity of two extra processing areas i.e., pretreatment and DDS purification in corn stover and SJ, increase their environmental impact scores more than that of glucose and glycerol.

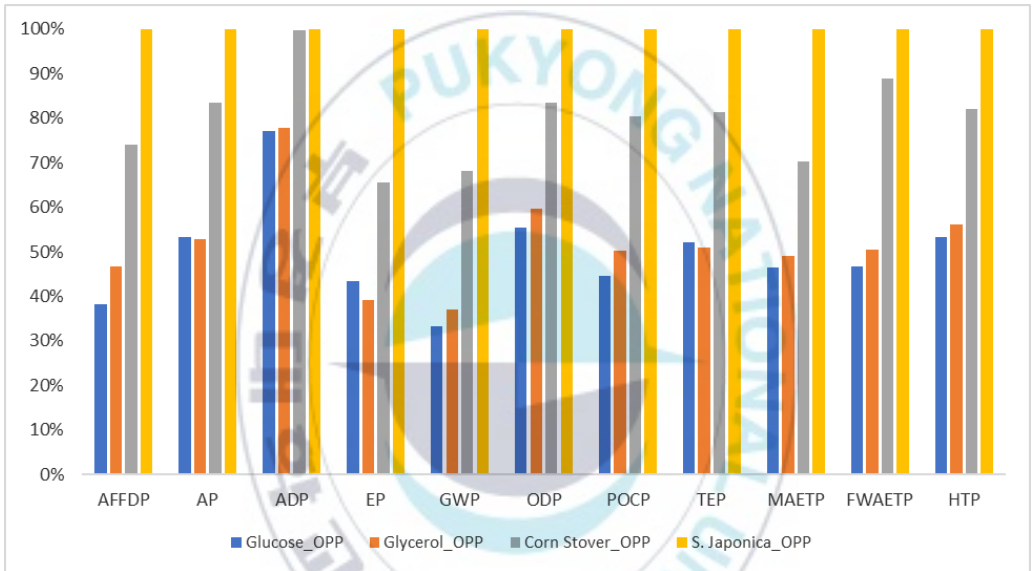

Figure 31. Comparison of environmental impact by the production of one kg biosuccinic acid from the optimal processing pathway (OPP) of glycerol, corn stover, glucose and S. japonica.

A better insight can be obtained by comparing the breakdown of feedstock and all biorefinery areas including pretreatment, fermentation, and purification in order to understand the critical parameters to environmental indicators. **Figure 32** presents the relative contribution of feedstock and biorefinery areas to the life cycle profile. Abiotic depletion potential is largely affected by the emissions from the purification area, in which a large amount of sulfuric acid used to regenerate free SA from its salts is the main cause. About 0.92–1.15 kg of sulfuric acid is consumed to produce one kg of SA. High agitation power needed in the fermenter and large consumption of heating utility in the purification area is the main contributor of abiotic fossil fuel depletion potential. The greenhouses gases released (1) during the consumption of fossil fuels to power the biorefinery, (2) from the processing to the atmosphere, and (3) from the extraction, preprocessing, and transportation of the raw materials to biorefinery gates have a significant impact on the global warming potential indicator. The heating utility in the purification area is the main driver for global warming potential. Indeed 66.0%, 78.7%, 72.3%, and 71.5% of the total process energy consumption is dedicated to downstream in the processing pathway of glycerol, corn stover, glucose, and SJ, respectively. Consequently, 50–70% greenhouse gases emissions that are generated

from the utility consumption are contributed to downstream, where phase change operations such as distillation, evaporation, and drying take place. In the upstream, power consumption due to agitation in the fermenter is found the main contributor to global warming indicator. Overall, cradle to gate analysis indicates that the optimal processing pathway of glucose, glycerol, corn stover, and SJ has global warming potential of 3.99, 4.33, 8.19, 12.02 kg CO_2/kg SA, respectively. A large amount of buffering agent (2 moles of NaOH per mole of SA) in fermentation area and acid utilization in downstream purification are the main contributors to ozone depletion potential, human toxicity potential, freshwater aquatic ecotoxicity potential, marine ecotoxicity potential and terrestrial ecotoxicity potential. Besides, utility consumption, especially in downstream, is found another critical parameter to these indicators. Note that the environmental burden only from the buffering agent is 38.3–48.3%, 38.5–46.2%, 43.3–49.8%, and 22.7–28.9% to human toxicity potential, freshwater aquatic ecotoxicity potential, marine ecotoxicity potential, and terrestrial ecotoxicity potential, respectively. Drivers for the acidification potential include sulfuric acid (20.7–31.5%), utility (26.6–54.7%), and a buffering agent (15.5–24.5%). In the pretreatment of corn stover by acid thermal hydrolysis, the contribution of ammonia in the feed neutralization step is

about 6%. In photo-oxidant formation potential, the almost identical trend to acidification potential is observed. The emissions from the wastewater treatment area are the key driver for eutrophication indicator.

To this end, analysis of the distribution of environmental impacts and their comparison with other topologies suggest (1) neutral fermentation should be replaced with the acidic fermentation to avoid utilization of a large amount of buffer in upstream and a large amount of acid in downstream, (2) heat integration should be performed to reduce high utility requirement. It is believed that the efficient use of utility via heat integration not only improves the energy utilization but would also significantly decrease numerous impacts (abiotic depletion, ozone depletion, radiation, global warming potential, and to lower extent acidification and human toxicity) and will hence improve the overall environmental performance.

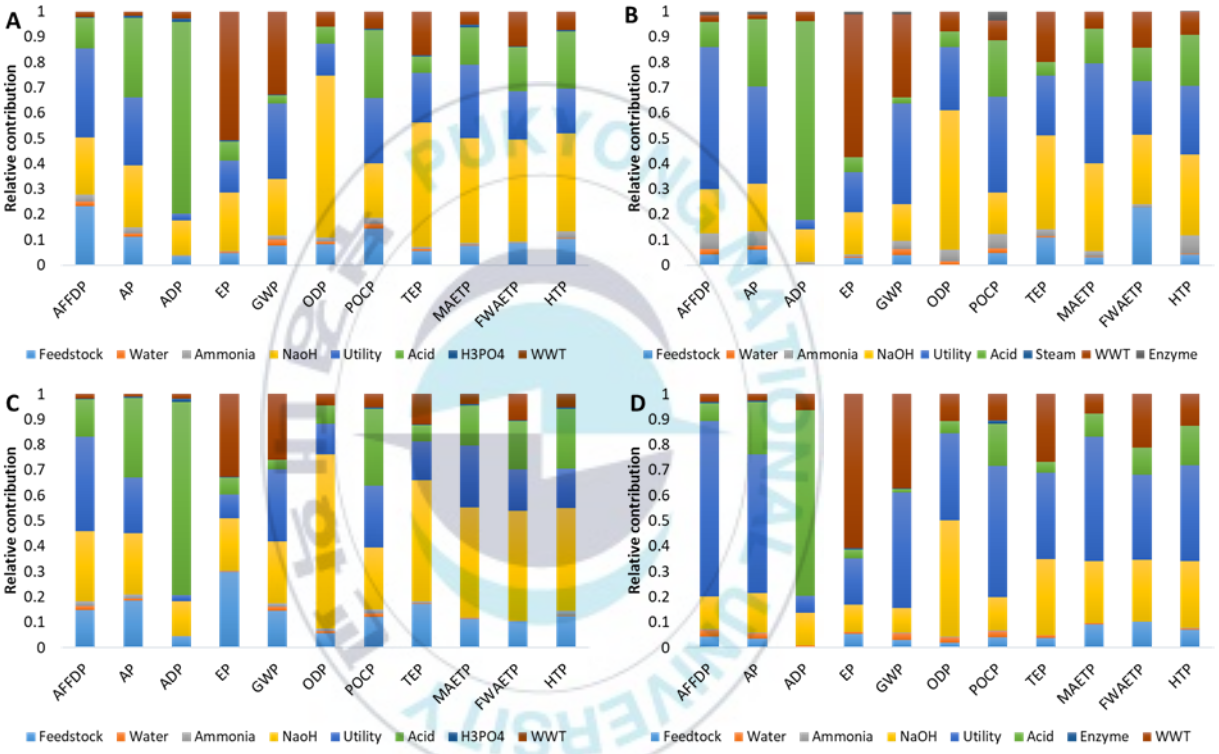

Figure 32. Relative distribution of environmental indicators to produce one kg bio-succinic acid from the optimal processing pathways of glucose (A), corn stover (B), glycerol (C), and *S. Japonica*.

6.4 Conclusion

A superstructure-based optimization model is developed for the synthesis of bio-succinic acid from different biomass sources. The proposed model performs multi-level analysis to provide robust decision-making support.

The overall results indicated that bio-succinic acid production via the optimal pathway of glucose is economically and environmentally better option.

7 CONCLUSIONS AND FUTURE PERSPECTIVES

The objective of this thesis was the process synthesis of macroalgal biorefinery through biochemical pathways. A superstructure-based optimization approach was used to develop models to find optimal raw material, product portfolio, and process technology via sugar platform and volatile fatty acid platform. The results showed that the production of biofuels and biochemicals from brown algae, *Saccharina japonica* are economically viable. Process integrations showed that both process economics and environmental profile can be improved significantly compared to standalone biorefinery design.

The results of the chapter of 3 and 4 for sugar platform indicated that bioethanol and biochemicals production from *Saccharina japonica* is economically viable over lignocellulosic biomass by having lower capital costs, energy consumption, and minimum ethanol selling price. The process economic results detailed in chapter 3 indicated that the MESP of the optimal design was 1.97 USD/gal. On the contrary, in chapter 4, when process integrations were performed via bio-SA- and microalgae-production with the standalone bioethanol processing, the MESP of optimal design decreased to 1.31 USD/gal. This represents an improvement of 33% in MESP. Concerning environmental sustainability,

the optimal design in chapter 4 achieved a 90% reduction in CO_2 emissions, as well as a 38.6% reduction in freshwater consumption. The risk of the optimal design was found to be 20–44% based on the MESP.

The results of chapter 5 for volatile fatty acid platform indicated that the production of biofuels and value-added chemicals via optimal design results in a minimum ethanol selling price of 1.18 USD/gal, which is 9.4% lower than the minimum ethanol selling price achieved through sugar platform. An environmental assessment indicated that the optimal design is an environmentally friendly process because it utilizes 90% of CEs produced by biorefinery processing. The water footprint is calculated to be 6 gals/gal of mixed acids and alcohols from VFA section. The techno-economic results revealed that biofuel and biochemical production via the volatile fatty acid platform consumes less capital investment compared to that of sugar platform. This because the VFAP does not require aseptic conditions and does not utilize expensive enzymes and capital-intensive fermenters. Furthermore, the VFAP has a higher product yield than the SP. This is primarily owing to the ability of anaerobes to digest all the non-lignin components of the biomass, including carbohydrates, proteins, and lipids, whereas, in the case of the SP, only the carbohydrate content of the biomass is converted to bioethanol.

In chapter 6, results from robust optimization indicated that glucose is the first- and glycerol is the second-best feedstock to produce bio-SA at the lowest selling price of 1.7–2.6 USD/kg and 1.9-2.5 USD/kg assuming one standard deviation, respectively through their optimal processing pathways. Corn stover can be excellent feedstock to produce bio-SA, however, it needs a major technological breakthrough to avoid expensive pretreatment and high capital investment up to 67–87 USD million which is much higher compared to optimal processing pathway of glucose. SJ is not suitable for standalone bio-SA production due to the inability of enzymes to process alginate which is a major carbohydrate 25–30 wt% to bio-SA. However, as presented in chapter 4 (See Scenario 2 in Table 16), integration of bioethanol production from alginate and bio-SA production from laminaria and mannitol increase the process economics compared to standalone production of bio-SA. Risk assessment shows that bio-SA production from an optimal pathway of glucose is the best alternative due to less associated risk. The environmental profile indicates that the optimal pathway of glucose is the most environmentally friendly process followed by glycerol, corn stover, and SJ.

Overall conclusions indicate that future seaweed biorefinery design through a biochemical pathway should be like as shown in **Figure 33**. The

seaweed is first processed to extract the most valuable components from it, second, production of biofuels through anaerobic digestion to produce mixed alcohols, and finally, process integrations through succinic acid production and wastewater treatment facility to improve process economics and environmental sustainability.

Considering the general trend of increasing energy demand, the efforts required for diversifying energy supplying sources cannot be underestimated: more environment friendly energy sources should replace the existing climate change causing ones. At the same time the corresponding energy generation processes should be improved in terms of reducing the carbon emission. In order to transform the efforts into reality, the new energy sources and the associated energy generation processes should be economically competitive. Consequently, significant research and development efforts are required in evaluating their economic feasibility due to the existence of a large number of intermediate processing routes. The presented superstructure-based framework plays an important role in evaluating optimal design, economics, and environmental sustainability of a macroalgae-based biorefinery under uncertainty. It can be further utilized in the decision-making framework of new energy systems.

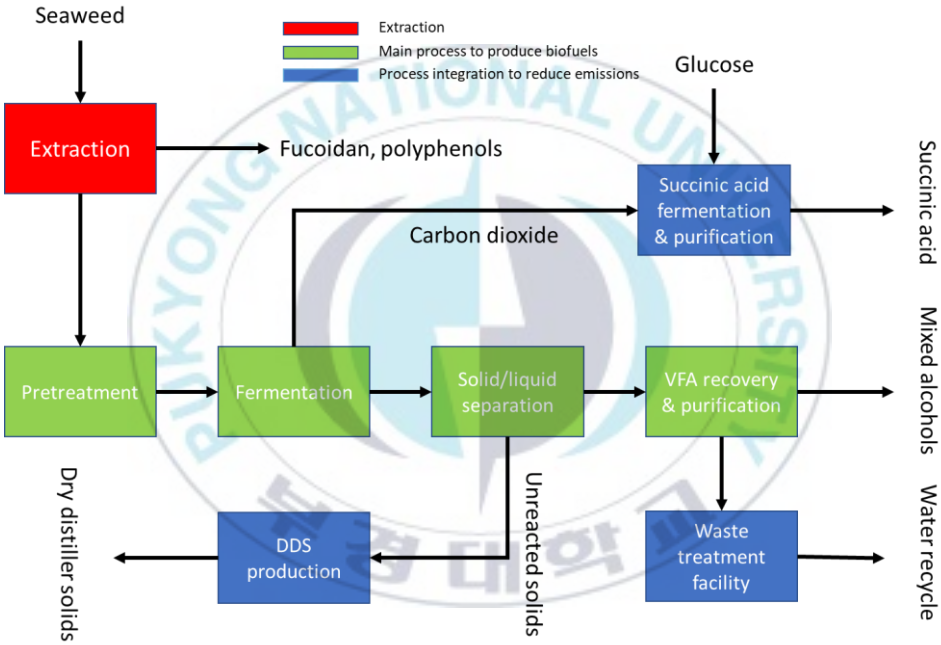

Figure 33. Proposed block flow diagram for seaweed biorefinery.

7.1 Future perspectives and research directions

This study has used superstructure-based optimization approach to support the development of seaweed-based biorefinery concepts. However, several issues presented below could still benefit substantially from further development.

1) The optimal topologies are the function of number of alternatives included in the superstructure. Therefore, the design space should be further extended to identify more promising solutions
2) The developed superstructures should be combined and extended to incorporate thermochemical conversion concepts to find more sustainable solutions for seaweed based biorefinery
3) Process synthesis approach should be integrated with supply chain network analysis for more robust solutions
4) Generic models should be formulated that allows managing a large complex process synthesis problem in a reasonable time
5) The databases and optimization models, which are formulated to investigate seaweed biorefinery design are not fully user-friendly. A graphical interface would eliminate such demerits.

REFERENCES

[1] Rogelj J, Luderer G, Pietzcker RC, Kriegler E, Schaeffer M, Krey V, et al. Energy system transformations for limiting end-of-century warming to below 1.5 °C. Nat Clim Chang 2015;5:519–27. https://doi.org/10.1038/nclimate2572.

[2] International Energy Agency n.d. https://www.iea.org/.

[3] World Energy Outlook n.d. https://www.iea.org/weo/.

[4] Bhowmick G De, Sarmah AK, Sen R. Zero-waste algal biorefinery for bioenergy and biochar : A green leap towards achieving energy and environmental sustainability. Sci Total Environ 2019;650:2467–82. https://doi.org/10.1016/j.scitotenv.2018.10.002.

[5] Carbon Dioxide Information Analysis Center n.d. https://cdiac.ess-dive.lbl.gov/trends/emis/glo_2014.html.

[6] Leung DYC, Caramanna G, Maroto-Valer MM. An overview of current status of carbon dioxide capture and storage technologies. Renew Sustain Energy Rev 2014;39:426–43. https://doi.org/10.1016/j.rser.2014.07.093.

[7] Naik SN, Goud V V., Rout PK, Dalai AK. Production of first and second generation biofuels: A comprehensive review. Renew Sustain Energy Rev 2010;14:578–97. https://doi.org/10.1016/j.rser.2009.10.003.

[8] Hellsmark H, Söderholm P. Innovation policies for advanced biorefi nery development: key considerations and lessons from Sweden. Biofuels, Bioprod Biorefining 2017;11:28-4.

[9] Bludowsky T, Agar DW. Thermally integrated bio-syngas-production for biorefineries. Chem Eng Res Des 2009;87.

[10] Lindorfer J, Lettner M, Hesser F, Fazeni K, Rosenfeld D, Annevelink B, et al. Technical, Economic and Environmental Assessment of Biorefinery Concepts. 2019.

[11] Hackl R, Harvey S. Opportunities for Process Integrated Biorefinery Concepts in the Chemical Cluster in Stenungsund 2010.

[12] Humbird D, Davis RE, Tao L, Kinchin CM, Hsu DD, Aden A, et al. Process Design and Economics for Biochemical Conversion of Lignocellulosic Biomass to Ethanol. 2011.

[13] Lope T, Adapa P, Kashaninejad M. Biomass Feedstock Pre-Processing– Part 1: Pre-Treatment. Biofuel's Eng. Process Technol., Croatia: InTech; 2011, p. 411–39. https://doi.org/10.1016/j.colsurfa.2011.12.014.

[14] Kucharska K, Rybarczyk P, Hołowacz I, Łukajtis R, Glinka M, Kamiński M. Pretreatment of lignocellulosic materials as substrates for fermentation processes. Molecules 2018;23:1–32. https://doi.org/10.3390/molecules23112937.

[15] Fasahati P, Woo HC, Liu JJ. Industrial-scale bioethanol production from brown algae: Effects of pretreatment processes on plant economics. Appl Energy 2015;139:175–87. https://doi.org/10.1016/j.apenergy.2014.11.032.

[16] Mohd Azhar SH, Abdulla R, Jambo SA, Marbawi H, Gansau JA, Mohd Faik AA, et al. Yeasts in sustainable bioethanol production: A review. Biochem Biophys Reports 2017;10:52–61. https://doi.org/10.1016/j.bbrep.2017.03.003.

[17] Fasahati P, Liu JJ. Impact of volatile fatty acid recovery on economics of ethanol production from brown algae via mixed

alcohol synthesis. Chem Eng Res Des 2015;98:107–22. https://doi.org/10.1016/j.cherd.2015.04.013.

[18] Granda CB, Holtzapple MT, Luce G, Searcy K, Mamrosh DL. Carboxylate platform: The MixAlco process part 2: Process economics. Appl Biochem Biotechnol 2009;156:107–24. https://doi.org/10.1007/s12010-008-8481-z.

[19] Dickson R, Fasahati P. Optimal design for integrated macroalgae-based biorefinery via mixed alcohol synthesis. 29th Eur. Symp. Comput. Aided Process Eng., vol. 46, Elsevier Masson SAS; 2019, p. 253–8. https://doi.org/10.1016/B978-0-12-818634-3.50043-6.

[20] Rodriguez C, Alaswad A, Mooney J, Prescott T, Olabi AG. Pre-treatment techniques used for anaerobic digestion of algae. Fuel Process Technol 2015;138:765–79. https://doi.org/10.1016/j.fuproc.2015.06.027.

[21] Miura T, Kita A, Okamura Y, Aki T, Tajima YMT, Kato J, et al. Evaluation of marine sediments as microbial sources for methane production from brown algae under high salinity. Bioresour Technol 2014;169:362–6.

[22] Miura T, Kita A, Okamura Y, Aki T, Matsumura Y, Tajima T, et al. Improved methane production from brown algae under high salinity by fed-batch acclimation. Bioresour Technol 2015;187:275–81. https://doi.org/10.1016/j.biortech.2015.03.142.

[23] Tedesco S, Benyounis KY, Olabi AG. Mechanical pretreatment effects on macroalgae-derived biogas production in co-digestion with sludge in Ireland. Energy 2013;61:27–33. https://doi.org/10.1016/j.energy.2013.01.071.

[24] Fasahati P, Saffron CM, Woo HC, Liu JJ. Potential of brown algae for sustainable electricity production through anaerobic digestion. Energy Convers Manag 2017;135:297–307. https://doi.org/10.1016/j.enconman.2016.12.084.

[25] Staniforth J, Kendall K. Biogas powering a small tubular solid oxide fuel cell. J Power Sources 1998;71:275–7.

[26] Dave A, Huang Y, Rezvani S, McIlveen-Wright D, Novaes M, Hewitt N. Techno-economic assessment of biofuel development by anaerobic digestion of European marine cold-water seaweeds. Bioresour Technol 2013;135:120–7.

https://doi.org/10.1016/j.biortech.2013.01.005.

[27] Basu P. Biomass Gasification, Pyrolysis and Torrefaction: Practical Design and Theory. Elsevier; 2018.

[28] Williams CL, Westover TL, Emerson RM, Tumuluru JS, Li C. Sources of Biomass Feedstock Variability and the Potential Impact on Biofuels Production. Bioenergy Res 2016;9:1–14. https://doi.org/10.1007/s12155-015-9694-y.

[29] Gollakota ARK, Kishore N, Gu S. A review on hydrothermal liquefaction of biomass. Renew Sustain Energy Rev 2018;81:1378–92. https://doi.org/10.1016/j.rser.2017.05.178.

[30] Searchinger T, Heimlich R. Avoiding Bioenergy Competition for Food Crops and Land. Creat a Sustain Food Futur 2015:44.

[31] Okoli CO, Adams TA, Brigljević B, Liu JJ. Design and economic analysis of a macroalgae-to-butanol process via a thermochemical route. Energy Convers Manag 2016;123:410–22. https://doi.org/10.1016/j.enconman.2016.06.054.

[32] Oh YH, Eom IY, Joo JC, Yu JH, Song BK, Lee SH, et al. Recent

advances in development of biomass pretreatment technologies used in biorefinery for the production of bio-based fuels, chemicals and polymers. Korean J Chem Eng 2015;32:1945–59. https://doi.org/10.1007/s11814-015-0191-y.

[33] Fasahati P, Liu JJ. Application of MixAlco® processes for mixed alcohol production from brown algae: Economic, energy, and carbon footprint assessments. Fuel Process Technol 2016;144:262–73. https://doi.org/10.1016/j.fuproc.2016.01.008.

[34] Brigljević B, Liu JJ, Lim H. Comprehensive feasibility assessment of a poly-generation process integrating fast pyrolysis of S. japonica and the Rankine cycle. Appl Energy 2019;254:113704. https://doi.org/10.1016/j.apenergy.2019.113704.

[35] Roesijadi G, Jones SB, Zhu Y. Macroalgae as a Biomass Feedstock: A Preliminary Analysis. 2010. https://doi.org/10.2172/1006310.

[36] Jung KA, Lim SR, Kim Y, Park JM. Potentials of macroalgae as feedstocks for biorefinery. Bioresour Technol 2013;135:182–90. https://doi.org/10.1016/j.biortech.2012.10.025.

[37] Saravana PS, Choi JH, Park YB, Woo HC, Chun BS. Evaluation of

the chemical composition of brown seaweed (Saccharina japonica) hydrolysate by pressurized hot water extraction. Algal Res 2016;13:246–54. https://doi.org/10.1016/j.algal.2015.12.004.

[38] Jiang R, Ingle KN, Golberg A. Macroalgae (seaweed) for liquid transportation biofuel production: What is next? Algal Res 2016;14:48–57. https://doi.org/10.1016/j.algal.2016.01.001.

[39] Nelson TE, Lewis BA. Separation and characterization of the soluble and insoluble components of insoluble laminaran. Carbohydr Res 1974;33:63–74. https://doi.org/10.1016/S0008-6215(00)82940-7.

[40] Food and Agriculture Organization of the United Nations n.d. http://www.fao.org/home/en/.

[41] Gani R. Chemical product design: Challenges and opportunities. Comput Chem Eng 2004;28:2441–57. https://doi.org/10.1016/j.compchemeng.2004.08.010.

[42] Seider WD, Seader J, Lewin DR. Process Design Principles: Synthesis, Analysis, and Evaluation. 3rd ed. New York: John Wiley & Sons; 2000.

[43] Dimian AC, Bildea CS, Kiss AA. Chemical Product Design. vol. 35. 2nd ed. Elsevier B.V.; 2014. https://doi.org/10.1016/B978-0-444-62700-1.00012-7.

[44] Takamatsu T. The nature and role of process systems engineering. Comput Chem Eng 1983;7:203–18. https://doi.org/10.1016/0098-1354(83)80012-X.

[45] Martin JN. Systems engineering guidebook: A process for developing systems and products. CRC; 1996.

[46] Biegler, Lorenz T., Ignacio E. Grossmann and AWW. Systematic methods for chemical process design. 1997.

[47] Klatt KU, Marquardt W. Perspectives for process systems engineering-Personal views from academia and industry. Comput Chem Eng 2009;33:536–50. https://doi.org/10.1016/j.compchemeng.2008.09.002.

[48] Yeomans H, Grossmann IE. A systematic modeling framework of superstructure optimization in process synthesis. Comput Chem Eng 1999;23:709–31. https://doi.org/10.1016/S0098-1354(99)00003-4.

[49] Grossmann IE. MINLP Optimization Strategies and Algorithms for Process Synthesis. 1989.

[50] Yuan Z, Chen B, Gani R. Applications of process synthesis: Moving from conventional chemical processes towards biorefinery processes. Comput Chem Eng 2013;49:217–29. https://doi.org/10.1016/j.compchemeng.2012.09.020.

[51] Karuppiah, R., Peschel, A., Grossmann, I. E., Martín, M., Martinson, W., & Zullo L. Energy optimization for the design of corn-based ethanol plants. AIChE J 2008;54:1499–525.

[52] Ahmetović E, Martín M, Grossmann IE. Optimization of Energy and Water Consumption in Corn – based Ethanol Plants. Ind Eng Chem Res 2010;49:1–37. https://doi.org/10.1021/ie1000955.

[53] Voll A, Marquardt W. Reaction Network Flux Analysis: Optimization-Based Evaluation of Reaction Pathways for Biorenewables Processing. AIChE J 2011;58:1788–801. https://doi.org/10.1002/aic.

[54] Zondervan E, Nawaz M, de Haan AB, Woodley JM, Gani R. Optimal design of a multi-product biorefinery system. Comput

Chem Eng 2011;35:1752–66. https://doi.org/10.1016/j.compchemeng.2011.01.042.

[55] Baliban RC, Elia JA, Floudas CA. Biomass to liquid transportation fuels (BTL) systems: Process synthesis and global optimization framework. Energy Environ Sci 2013;6:267–87. https://doi.org/10.1039/c2ee23369j.

[56] Kim J, Sen SM, Maravelias CT. An optimization-based assessment framework for biomass-to-fuel conversion strategies. Energy Environ Sci 2013;6:1093–104. https://doi.org/10.1039/c3ee24243a.

[57] Chen Y, Li X, II TAA, Barton PI. Decomposition Strategy for the Global Optimization of Flexible Energy Polygeneration Systems. AIChE J 2012;58:3080–95. https://doi.org/10.1002/aic.

[58] Rizwan M, Zaman M, Lee JH, Gani R. Optimal processing pathway selection for microalgae-based biorefinery under uncertainty. Comput Chem Eng 2015;82:362–73. https://doi.org/10.1016/j.compchemeng.2015.08.002.

[59] Gong J, You F. Optimal design and synthesis of algal biorefinery processes for biological carbon sequestration and utilization with

zero direct greenhouse gas emissions: MINLP model and global optimization algorithm. Ind Eng Chem Res 2014;53:1563–79. https://doi.org/10.1021/ie403459m.

[60] Posada JA, Patel AD, Roes A, Blok K, Faaij APC, Patel MK. Potential of bioethanol as a chemical building block for biorefineries: Preliminary sustainability assessment of 12 bioethanol-based products. Bioresour Technol 2013;135:490–9. https://doi.org/10.1016/j.biortech.2012.09.058.

[61] Gebreslassie BH, Slivinsky M, Wang B, You F. Life cycle optimization for sustainable design and operations of hydrocarbon biorefinery via fast pyrolysis, hydrotreating and hydrocracking. Comput Chem Eng 2013;50:71–91. https://doi.org/10.1016/j.compchemeng.2012.10.013.

[62] Zhang Q, Gong J, Skwarczek M, Yue D, You F. Sustainable Process Design and Synthesis of Hydrocarbon Biorefinery through Fast Pyrolysis and Hydroprocessing. AIChE J 2014;60:980–94.

[63] Kokossis AC, Yang A. On the use of systems technologies and a systematic approach for the synthesis and the design of future

biorefineries. Comput Chem Eng 2010;34:1397–405. https://doi.org/10.1016/j.compchemeng.2010.02.021.

[64] Ignacio E. Grossmann. Mixed-integer programming approach for the synthesis of integrated process flowsheets. Comput Chem Eng 1985;9:463–82.

[65] Grossmann IE, Santibanez J. Applications of mixed-integer linear programming in process synthesis. Comput Chem Eng 1980;4:205–14. https://doi.org/10.1016/0098-1354(80)85001-0.

[66] Sin G, Gernaey K V., Lantz AE. Good Modeling Practice for PAT Applications : Propagation of Input Uncertainty and Sensitivity Analysis. AIChE J 2009:1043–53. https://doi.org/10.1021/bp.166.

[67] Biegler LT, Varvarezos DK, Grossmann IE. A sensitivity analysis and based design approach of linear for flexibility. Comput Chem Eng 1995;19:1301–16.

[68] Brun R, Martin K, Siegrist H, Gujer W, Reichert P. Practical identifiability of ASM2d parameters — systematic selection and tuning of parameter subsets. Water Resour Res 2002;36:4113–27.

[69] Quaglia A, Sarup B, Sin G, Gani R, Carlo M. A systematic framework for enterprise-wide optimization : Synthesis and design of processing networks under uncertainty. Comput Chem Eng 2013;59:47–62. https://doi.org/10.1016/j.compchemeng.2013.03.018.

[70] Birge JR, Louveaux F. Introduction to stochastic programming. New York,: Springer; 2011.

[71] Cheali P, Quaglia A, Gernaey K V, Sin G. Effect of Market Price Uncertainties on the Design of Optimal Biorefinery Systems—A Systematic Approach. Ind Eng Chem Res 2014;53:6021−6032. https://doi.org/10.1021/ie4042164.

[72] Grossmann IE, Kravanja Z. Mixed-integer nonlinear programming techniques for process systems engineering. Comput Chem Eng 1995;19:189–204. https://doi.org/10.1016/0098-1354(95)87036-9.

[73] Iman R., Conover W. A distribution-free approach to inducing rank correlation among input variables. Commun Stat - Simul Comput 1982;11:311–44.

[74] Richard Turton, Richard C. Bailie, Wallace B. Whiting JAS.

Analysis, Synthesis and Design of Chemical Processes Third Edition. 3rd ed. Prentice Hall; 2013. https://doi.org/10.1017/CBO9781107415324.004.

[75] Davis R, Tao L, Scarlata C, Tan ECD, Ross J, Lukas J, et al. Process Design and Economics for the Conversion of Lignocellulosic Biomass to Hydrocarbons: Dilute-Acid and Enzymatic Deconstruction of Biomass to Sugars and Catalytic Conversion of Sugars to Hydrocarbons. Golden, CO (United States): 2015. https://doi.org/10.2172/1176746.

[76] Efe Ç, van der Wielen LAM, Straathof AJJ. Techno-economic analysis of succinic acid production using adsorption from fermentation medium. Biomass and Bioenergy 2013;56:479–92. https://doi.org/10.1016/j.biombioe.2013.06.002.

[77] Davis RE, Grundl NJ, Tao L, Biddy MJ, Tan EC, Beckham GT, et al. Process Design and Economics for the Conversion of Lignocellulosic Biomass to Hydrocarbon Fuels and Coproducts: 2018 Biochemical Design Case Update; Biochemical Deconstruction and Conversion of Biomass to Fuels and Products via Integrated Biorefinery Path. National Renewable Energy Lab

(NREL): 2018.

[78] Karen E. Thomas. Overview of Village Scale, Renewable Energy Powered Desalination. 1997.

[79] Equipment cost n.d. http://www.matche.com/equipcost.

[80] Amos WA. Report on Biomass Drying Technology Report on Biomass Drying Technology. 1998. https://doi.org/NREL/TP-570-25885.

[81] Davis R, Markham J, Kinchin C, Grundl N, Tan ECD, Humbird D. Process Design and Economics for the Production of Algal Biomass: Algal Biomass Production in Open Pond Systems and Processing Through Dewatering for Downstream Conversion. 2016. https://doi.org/10.2172/1239893.

[82] Biomass densification--cubing operations and costs for corn stover n.d. http://agris.fao.org/agris-search/search.do?recordID=US201300949683.

[83] Roesijadi G, Copping AEE, Huesemann MHH, Forster J, Benemann JR, Thom RM. Techno-Economic Feasibility Analysis

of Offshore Seaweed Farming for Bioenergy and Biobased Products. 2008.

[84] United States Department of Agriculture Economic Research Service n.d. https://www.ers.usda.gov/.

[85] Quispe CAG, Coronado CJR, Carvalho JA. Glycerol: Production, consumption, prices, characterization and new trends in combustion. Renew Sustain Energy Rev 2013;27:475–93. https://doi.org/10.1016/j.rser.2013.06.017.

[86] Independent Chemical Information Service n.d. https://www.icis.com/chemicals/channel-info-chemicals-a-z/.

[87] Giuliano A, Cerulli R, Poletto M, Raiconi G, Barletta D. Process Pathways Optimization for a Lignocellulosic Biorefinery Producing Levulinic Acid, Succinic Acid, and Ethanol. Ind Eng Chem Res 2016;55:10699–717. https://doi.org/10.1021/acs.iecr.6b01454.

[88] Garg N, Woodley JM, Gani R, Kontogeorgis GM. Sustainable solutions by integrating process synthesis-intensification. Comput Chem Eng 2019;126:499–519. https://doi.org/10.1016/j.compchemeng.2019.04.030.

[89] Xie H, Yue H, Zhu J, Liang B, Li C, Wang Y, et al. Scientific and Engineering Progress in CO2 Mineralization Using Industrial Waste and Natural Minerals. Engineering 2015;1:150–7. https://doi.org/10.15302/J-ENG-2015017.

[90] Mert SO. Application of electrodialysis for recovering sodium carbonate and sodium bicarbonate from Lake Van. Desalin Water Treat 2016;57:3940–6. https://doi.org/10.1080/19443994.2014.989417.

[91] Lane JM, Spath PL. Technoeconomic Analysis of the Thermocatalytic Decomposition of Natural Gas. 2001.

[92] Aden a, Ruth M, Ibsen K, Jechura J, Neeves K, Sheehan J, et al. Lignocellulosic Biomass to Ethanol Process Design and Economics Utilizing Co-Current Dilute Acid Prehydrolysis and Enzymatic Hydrolysis for Corn Stover. Natl Renew Energy Lab 2002:Medium: ED; Size: 154 pages. https://doi.org/NREL/TP-510-32438.

[93] Energy Information Administration n.d. https://www.eia.gov/.

[94] Chisti Y. Biodiesel from microalgae beats bioethanol. Trends Biotechnol 2008;26:126–31.

https://doi.org/10.1016/j.tibtech.2007.12.002.

[95] Energy Information Administration n.d. https://www.epa.gov/ghgemissions/sources-greenhouse-gas-emissions.

[96] Richard Turton; Richard C. Bailie;Wallace B. Whiting; Joseph A. Shaeiwitz; Analysis, Synthesis and Design of Chemical Processes. Third Edit. Prentice Hall International Series in the Physical and Chemical Engineering Sciences; 2009.

[97] Balat M. Production of bioethanol from lignocellulosic materials via the biochemical pathway: A review. Energy Convers Manag 2011;52:858–75. https://doi.org/10.1016/j.enconman.2010.08.013.

[98] Nigam PS, Singh A. Production of liquid biofuels from renewable resources. Prog Energy Combust Sci 2011;37:52–68. https://doi.org/10.1016/j.pecs.2010.01.003.

[99] Cherubini F. The biorefinery concept: Using biomass instead of oil for producing energy and chemicals. Energy Convers Manag 2010;51:1412–21. https://doi.org/10.1016/j.enconman.2010.01.015.

[100] Fannin KF, Srivastava VJ, Mensinger JD, Chynoweth DP. Marine Biomass Program: Anaerobic Digestion Systems Development and Stability Study 1982.

[101] Tompkins AN. Marine Biomass Program Annual Report 1982 1982.

[102] Bruton T, Lyons H, Lerat Y, Stanley M, Rasmussen MB. A Review of the Potential of Marine Algae as a Source of Biofuel in Ireland. 2009. https://doi.org/10.1016/j.envint.2003.08.001.

[103] Fleurence J. Seaweed proteins: Biochemical, nutritional aspects and potential uses. Trends Food Sci Technol 1999;10:25–8. https://doi.org/10.1016/S0924-2244(99)00015-1.

[104] Synytsya A, Kim WJ, Kim SM, Pohl R, Synytsya A, Kvasnička F, et al. Structure and antitumour activity of fucoidan isolated from sporophyll of Korean brown seaweed Undaria pinnatifida. Carbohydr Polym 2010;81:41–8. https://doi.org/10.1016/j.carbpol.2010.01.052.

[105] Hou X, Hansen JH, Bjerre AB. Integrated bioethanol and protein production from brown seaweed Laminaria digitata. Bioresour

Technol 2015;197:310–7. https://doi.org/10.1016/j.biortech.2015.08.091.

[106] Schultz-Jensen N, Thygesen A, Leipold F, Thomsen ST, Roslander C, Lilholt H, et al. Pretreatment of the macroalgae Chaetomorpha linum for the production of bioethanol - Comparison of five pretreatment technologies. Bioresour Technol 2013;140:36–42. https://doi.org/10.1016/j.biortech.2013.04.060.

[107] Floudas CA, Grossmann IE. Algorithmic approaches to process synthesis: logic and global optimization. Focapd'94 1995;91:198–221.

[108] van der Wal H, Sperber BLHM, Houweling-Tan B, Bakker RRC, Brandenburg W, López-Contreras AM. Production of acetone, butanol, and ethanol from biomass of the green seaweed Ulva lactuca. Bioresour Technol 2013;128:431–7. https://doi.org/10.1016/j.biortech.2012.10.094.

[109] Yanagisawa M, Nakamura K, Ariga O, Nakasaki K. Production of high concentrations of bioethanol from seaweeds that contain easily hydrolyzable polysaccharides. Process Biochem 2011;46:2111–6.

https://doi.org/10.1016/j.procbio.2011.08.001.

[110] Wargacki AJ, Leonard E, Win MN, Regitsky DD, Santos CNS, Kim PB, et al. An Engineered Microbial Platform for Direct Biofuel Production from Brown Macroalgae. Science (80-) 2012;230502:308–14. https://doi.org/10.1126/science.1214547.

[111] Lipnizki F, Field RW, Ten P-K. Pervaporation-based hybrid process: a review of process design, applications and economics. J Memb Sci 1999;153:183–210. https://doi.org/10.1016/S0376-7388(98)00253-1.

[112] Kwiatkowski JR, McAloon AJ, Taylor F, Johnston DB. Modeling the process and costs of fuel ethanol production by the corn dry-grind process. Ind Crops Prod 2006;23:288–96. https://doi.org/10.1016/j.indcrop.2005.08.004.

[113] Williams HP. Model building in mathematical programming. 2013. https://doi.org/10.1057/jors.1986.76.

[114] Bals B, Wedding C, Balan V, Sendich E, Dale B. Evaluating the impact of ammonia fiber expansion (AFEX) pretreatment conditions on the cost of ethanol production. Bioresour Technol

2011;102:1277–83. https://doi.org/10.1016/j.biortech.2010.08.058.

[115] index @ www.ers.usda.gov n.d. https://www.ers.usda.gov/.

[116] Fazlollahi S, Mandel P, Becker G, Maréchal F. Methods for multi-objective investment and operating optimization of complex energy systems. Energy 2012;45:12–22. https://doi.org/10.1016/j.energy.2012.02.046.

[117] Agriculture and Forestry n.d. http://www1.agric.gov.ab.ca/$department/deptdocs.nsf/all/agdex13760.

[118] Wang WC, Yung YL, Lacis AA, Mo T, Hansen JE. Greenhouse Effects due to Man-Mad Perturbations of Trace Gases. Science (80-) 1976;194. https://doi.org/10.1126/science.194.4266.685.

[119] Scott F, Quintero J, Morales M, Conejeros R, Cardona C, Aroca G. Process design and sustainability in the production of bioethanol from lignocellulosic materials. Electron J Biotechnol 2013;16. https://doi.org/10.2225/vol16-issue3-fulltext-7.

[120] Zhang Q, Cheng C, Nagarajan D, Chang J. Carbon capture and

utilization of fermentation CO2 : Integrated ethanol fermentation and succinic acid production as an efficient platform. Appl Energy 2017;206:364–71. https://doi.org/10.1016/j.apenergy.2017.08.193.

[121] Bonfim-Rocha L, Gimenes ML, Bernardo de Faria SH, Silva RO, Esteller LJ. Multi-objective design of a new sustainable scenario for bio-methanol production in Brazil. J Clean Prod 2018;187:1043–56. https://doi.org/10.1016/j.jclepro.2018.03.267.

[122] Willington IP, Marten GG. Options for handling stillage waste from sugar-based fuel ethanol production. Resour Conserv 1982;8:111–29. https://doi.org/10.1016/0166-3097(82)90036-0.

[123] Werpy T, Petersen G. Top Value Added Chemicals from Biomass Volume I — Results of Screening for Potential Candidates from Sugars and Synthesis Gas Top Value Added Chemicals From Biomass Volume I : Results of Screening for Potential Candidates 2004. https://doi.org/10.2172/15008859.

[124] Vlysidis A, Binns M, Webb C, Theodoropoulos C. A techno-economic analysis of biodiesel biorefineries: Assessment of integrated designs for the co-production of fuels and chemicals.

Energy 2011;36:4671–83. https://doi.org/10.1016/j.energy.2011.04.046.

[125] Bai B, Zhou J min, Yang M hua, Liu Y lan, Xu X hui, Xing J min. Efficient production of succinic acid from macroalgae hydrolysate by metabolically engineered Escherichia coli. Bioresour Technol 2015;185:56–61. https://doi.org/10.1016/j.biortech.2015.02.081.

[126] Ringsmuth AK, Landsberg MJ, Hankamer B. Can photosynthesis enable a global transition from fossil fuels to solar fuels, to mitigate climate change and fuel-supply limitations? Renew Sustain Energy Rev 2016;62:134–63. https://doi.org/10.1016/j.rser.2016.04.016.

[127] Song C, Xie M, Qiu Y, Liu Q, Sun L, Wang K, et al. Integration of CO2 absorption with biological transformation via using rich ammonia solution as a nutrient source for microalgae cultivation. Energy 2019;179:618–27. https://doi.org/10.1016/j.energy.2019.05.039.

[128] Demirbas A, Demirbas MF. Importance of algae oil as a source of biodiesel. Energy Convers Manag 2011;52:163–70. https://doi.org/10.1016/j.enconman.2010.06.055.

[129] Davis R, Aden A, Pienkos PT. Techno-economic analysis of autotrophic microalgae for fuel production. Appl Energy 2011;88:3524–31. https://doi.org/10.1016/j.apenergy.2011.04.018.

[130] Kadam KL. Microalgae Production from Power Plant Flue Gas: Environmental Implications on a Life Cycle Basis. 2001. https://doi.org/10.2172/783405.

[131] Maity JP, Hou CP, Majumder D, Bundschuh J, Kulp TR, Chen CY, et al. The production of biofuel and bioelectricity associated with wastewater treatment by green algae. Energy 2014;78:94–103. https://doi.org/10.1016/j.energy.2014.06.023.

[132] Picardo A, Soltero VM, Peralta ME, Chacartegui R. District heating based on biogas from wastewater treatment plant. Energy 2019;180:649–64. https://doi.org/10.1016/j.energy.2019.05.123.

[133] Enquist-Newman M, Faust AME, Bravo DD, Santos CNS, Raisner RM, Hanel A, et al. Efficient ethanol production from brown macroalgae sugars by a synthetic yeast platform. Nature 2014;505:239–43. https://doi.org/10.1038/nature12771.

[134] Davis R, Markham J, Kinchin C, Grundl N, Tan ECD, Humbird D.

Process Design and Economics for the Production of Algal Biomass: Algal Biomass Production in Open Pond Systems and Processing Through Dewatering for Downstream Conversion. 2016. https://doi.org/10.2172/1239893.

[135] Lundquist TJ, Woertz IC, Quinn NWT, Benemann JR. A Realistic Technology and Engineering Assessment of Algae Biofuel Production. 2010.

[136] Bhave R, Kuritz T, Powell L, Adcock D. Membrane-based energy efficient dewatering of microalgae in biofuels production and recovery of value added co-products. Environ Sci Technol 2012;46:5599–606. https://doi.org/10.1021/es204107d.

[137] Schlesinger A, Eisenstadt D, Bar-Gil A, Carmely H, Einbinder S, Gressel J. Inexpensive non-toxic flocculation of microalgae contradicts theories; overcoming a major hurdle to bulk algal production. Biotechnol Adv 2012;30:1023–30. https://doi.org/10.1016/j.biotechadv.2012.01.011.

[138] Vandamme D, Pontes SCV, Goiris K, Foubert I, Pinoy LJJ, Muylaert K. Evaluation of electro-coagulation-flocculation for

harvesting marine and freshwater microalgae. Biotechnol Bioeng 2011;108:2320–9. https://doi.org/10.1002/bit.23199.

[139] Dassey AJ, Theegala CS. Harvesting economics and strategies using centrifugation for cost effective separation of microalgae cells for biodiesel applications. Bioresour Technol 2013;128:241–5. https://doi.org/10.1016/j.biortech.2012.10.061.

[140] Huntley ME, Johnson ZI, Brown SL, Sills DL, Gerber L, Archibald I, et al. Demonstrated large-scale production of marine microalgae for fuels and feed. Algal Res 2015;10:249–65. https://doi.org/10.1016/j.algal.2015.04.016.

[141] Berglund, K. A., Yedur, S., & Dunuwila DD. Succinic acid production and purification. U.S. Patent 5,958,744, 1999. https://doi.org/U.S. Patent 5,958,744.

[142] Alexandri M, Vlysidis A, Papapostolou H, Tverezovskaya O, Tverezovskiy V, Kookos IK, et al. Downstream separation and purification of succinic acid from fermentation broths using spent sulphite liquor as feedstock. Sep Purif Technol 2019;209:666–75. https://doi.org/10.1016/j.seppur.2018.08.061.

[143] Yong SK, Sang WL, Un YK, Jyong SS. Pervaporation of water-ethanol mixtures through crosslinked and surface-modified poly(vinyl alcohol) membrane. J Memb Sci 1990;51:215–26. https://doi.org/10.1016/S0376-7388(00)80904-7.

[144] Kreis P, Górak A. Process analysis of hybrid separation processes: Combination of distillation and pervaporation. Chem Eng Res Des 2006;84:595–600. https://doi.org/10.1205/cherd.05211.

[145] IEA Bioenergy. Bio-based Chemicals - Value Added Products from Biorefineries. 2012. https://doi.org/10.1007/978-3-319-07593-8_30.

[146] Khan MA, Ngo HH, Guo WS, Liu Y, Nghiem LD, Hai FI, et al. Optimization of process parameters for production of volatile fatty acid, biohydrogen and methane from anaerobic digestion. Bioresour Technol 2016;219:738–48. https://doi.org/10.1016/j.biortech.2016.08.073.

[147] Pham TN, Nam WJ, Jeon YJ, Yoon HH. Volatile fatty acids production from marine macroalgae by anaerobic fermentation. Bioresour Technol 2012;124:500–3.

https://doi.org/10.1016/j.biortech.2012.08.081.

[148] Sato K, Sugimoto K, Kyotani T, Shimotsuma N, Kurata T. Synthesis , reproducibility , characterization , pervaporation and technical feasibility of preferentially b -oriented mordenite membranes for dehydration of acetic acid solution. J Memb Sci 2011;385:20–9. https://doi.org/10.1016/j.memsci.2011.09.001.

[149] Zhu Y, Jones S. Techno-economic Analysis for the Thermochemical Conversion of Lignocellulosic Biomass to Ethanol via Acetic Acid Synthesis. 2009.

[150] Bono A, Pin OP, Jiun CP. Simulation of Palm based Fatty Acids Distillation. J Appl Sci 2010;10:2508–15.

[151] Spath P, Aden A, Eggeman T, Ringer M, Wallace B, Jechura J. Biomass to Hydrogen Production Detailed Design and Economics Utilizing the Battelle Columbus Heated Gasifier Biomass to Hydrogen Production Detailed Design and Economics Utilizing the Battelle Columbus. 2005.

[152] Fasahati P, Liu JJ. Economic, energy, and environmental impacts of alcohol dehydration technology on biofuel production from brown

algae. Energy 2015;93:2321–36. https://doi.org/10.1016/j.energy.2015.10.123.

[153] Phillips S, Aden A, Jechura J, Dayton D. Thermochemical Ethanol via Indirect Gasification and Mixed Alcohol Synthesis of Lignocellulosic Biomass Thermochemical Ethanol via Indirect Gasification and Mixed Alcohol Synthesis of Lignocellulosic Biomass. 2007.

[154] Phillips S. Technoeconomic Analysis of a Lignocellulosic Biomass Indirect Gasification Process To Make Ethanol via Mixed Alcohols Synthesis. Ind Eng Chem Res 2007;46:8887–97. https://doi.org/10.1021/ie071224u.

[155] Dickson R, Liu J. Optimization of seaweed-based biorefinery with zero carbon emissions potential. 29th Eur. Symp. Comput. Aided Process Eng., vol. 46, Elsevier Masson SAS; 2019, p. 247–52. https://doi.org/10.1016/B978-0-12-818634-3.50042-4.

[156] Chang HN, Kim N, Kang J, Jeong CM. Biomass-derived Volatile Fatty Acid Platform for Fuels and Chemicals. Biotechnol Bioprocess Eng 2010;15:1–10. https://doi.org/10.1007/s12257-

009-3070-8.

[157] Delhomme C, Weuster-Botz D, Kühn FE. Succinic acid from renewable resources as a C4building-block chemical - A review of the catalytic possibilities in aqueous media. Green Chem 2009;11:13–26. https://doi.org/10.1039/b810684c.

[158] Mancini E, Mansouri SS, Gernaey K V, Pinelo M, Luo J. From second generation feed-stocks to innovative fermentation and downstream techniques for succinic acid production. Crit Rev Environ Sci Technol 2019;0:1–45. https://doi.org/10.1080/10643389.2019.1670530.

[159] EC-DGE. From the Sugar Platform to biofuels and biochemicals. 2015. https://doi.org/contract No. ENER/C2/423-2012/SI2.673791.

[160] Hermann BG, Blok K, Patel MK. Producing Bio-Based Bulk Chemicals Using Industrial Biotechnology Saves Energy and Combats Climate Change. Environ Sci Technol 2007:7915–21. https://doi.org/10.1021/es062559q.

[161] Morales M, Ataman M, Badr S, Linster S, Kourlimpinis I, Papadokonstantakis S, et al. Sustainability assessment of succinic

acid production technologies from biomass using metabolic engineering. Energy Environ Sci 2016;9:2794–805. https://doi.org/10.1039/c6ee00634e.

[162] Lin CSK, Pfaltzgraff LA, Herrero-Davila L, Mubofu EB, Abderrahim S, Clark JH, et al. Food waste as a valuable resource for the production of chemicals, materials and fuels. Current situation and global perspective. Energy Environ Sci 2013;6:426–64. https://doi.org/10.1039/c2ee23440h.

[163] Alvarado-Morales M, Gunnarsson IB, Fotidis IA, Vasilakou E, Lyberatos G, Angelidaki I. Laminaria digitata as a potential carbon source for succinic acid and bioenergy production in a biorefinery perspective. Algal Res 2015;9:126–32. https://doi.org/10.1016/j.algal.2015.03.008.

[164] Dickson R, Mancini E, Garg N, Liu J, Pinelo M. Sustainable process synthesis , design and innovation of bio-succinic acid production. 30th Eur. Symp. Comput. Aided Process Eng., 2020.

[165] Thuy NTH, Boontawan A. Production of very-high purity succinic acid from fermentation broth using microfiltration and

nanofiltration-assisted crystallization. J Memb Sci 2017;524:470–81. https://doi.org/10.1016/j.memsci.2016.11.073.

[166] Garde A. Production of lactic acid from renewable resources using electrodialysis for product recovery. Technical University of Denmark, 2002.

[167] Hong WH, Lee SY, Hong YK, Won HJ, Huh YS, Song H, et al. Method for purifying succinic acid by crystallization of culture broth. WO 2009/082050, 2009.

[168] Kurzrock T, Schallinger S, Weuster-Botz D. Integrated separation process for isolation and purification of biosuccinic acid. Biotechnol Prog 2011;27:1623–8. https://doi.org/10.1002/btpr.673.

[169] Datta R, Glassner DA, Jain MK, Roy JRV. Fermentation and purification process for succinic acid. U.S. Patent No. 5,168,055, 1992.

[170] Yedur S, Berglund KA, Dunuwila DD. Succinic acid production and purification. US patent No. US 6,265,190 B1, 2001.

[171] Li J, Zheng XY, Fang XJ, Liu SW, Chen KQ, Jiang M, et al. A

complete industrial system for economical succinic acid production by Actinobacillus succinogenes. Bioresour Technol 2011;102:6147–52. https://doi.org/10.1016/j.biortech.2011.02.093.

[172] Salvachúa D, Mohagheghi A, Smith H, Bradfield MFA, Nicol W, Black BA, et al. Succinic acid production on xylose-enriched biorefinery streams by Actinobacillus succinogenes in batch fermentation. Biotechnol Biofuels 2016;9:1–15. https://doi.org/10.1186/s13068-016-0425-1.

[173] Chen X, Shekiro J, Pschorn T, Sabourin M, Tucker MP, Tao L. Techno-economic analysis of the deacetylation and disk refining process: Characterizing the effect of refining energy and enzyme usage on minimum sugar selling price and minimum ethanol selling price. Biotechnol Biofuels 2015;8:1–13. https://doi.org/10.1186/s13068-015-0358-0.

[174] Kuhn EM, O'Brien MH, Ciesielski PN, Schell DJ. Pilot-Scale Batch Alkaline Pretreatment of Corn Stover. ACS Sustain Chem Eng 2016;4:944–56. https://doi.org/10.1021/acssuschemeng.5b01041.

[175] cost-effective membrane technologies for minising wastes and

effluents. 1997.

[176] Gargalo CL, Carvalho A, Gernaey K V., Sin G. A framework for techno-economic & environmental sustainability analysis by risk assessment for conceptual process evaluation. Biochem Eng J 2016;116:146–56. https://doi.org/10.1016/j.bej.2016.06.007.

ACKNOWLEDGEMENTS

All my heartiest praises and thanks to Almighty God for giving me good health and peace of mind during my stay abroad.

I express my sincere gratitude to my advisor Prof. Jay Liu for the continuous support of my PhD study and his patience, motivation, enthusiasm, and immense knowledge. I have been extremely lucky to have a supervisor and mentor like you. I am also grateful to you for giving me all the necessary pieces of training. Once, again thank you for everything, Sir!

Besides my advisor, I would like to thank my thesis committee: Prof. Gyeongbeom Yi, Prof. Min-Kyu Lee, Prof. Jun-Hyung Ryu, Prof. Seyed Soheil Mansouri, for their valuable time, insightful comments, and stimulating discussion.

I would also like to thank the National Research Foundation of Korea (NRF) grants funded by the Ministry of Science and ICT (2019R1A2C2084709, 2019M3E6A1064422) for supporting my research.

My sincere thanks are also extended to Prof. Seyed Soheil Mansouri and Prof. Manuel Pinelo for giving me the opportunity to work at the Technical University of Demark. Your valuable advice, discussion, and supervision have refined my research expertise. Thank you, sirs!

I respectfully give my thanks to the administration staff of both Pukyong National University and the Technical University of Denmark for your patience, co-operation, and help.

I wish to record here with great pleasure my sincere thanks to my colleagues: Petar, Ivannie, Haider, Alham, Amin, and Sajawal for their moral support, kind co-operation, and encouragement, and for all the fun we have had in the last three and half years.

I am grateful to Boris Brigljević—a good colleague and a very sincere friend of mine—for his time, fruitful discussion, useful critiques, and pleasant company. Thank you, Boris!

I also feel grateful for all the beautiful things I received within these three and a half years from wonderful people whom I called my Korean & Danish family.

Finally, I must express my very profound gratitude to my family for their continuous and unparalleled love, support, and encouragement throughout my study. This accomplishment would not have been possible without them. Thank you all!